No. 460 is missing

Theoretical and Experimental Analyses of Members Made of Materials That Creep

by

O. M. Sidebottom

PROFESSOR OF THEORETICAL AND APPLIED MECHANICS

G. A. Costello

ASSISTANT PROFESSOR OF THEORETICAL AND APPLIED MECHANICS

S. Dharmarajan

FORMERLY RESEARCH ASSOCIATE IN THEORETICAL AND APPLIED MECHANICS

(Assistant Professor of Engineering Mechanics, San Diego State College)

ENGINEERING EXPERIMENT STATION BULLETIN NO. 460

(73420)

UNIVERSITY
OF ILLINOIS
:: PRESS ::

ACKNOWLEDGMENT

This investigation was conducted as a part of the work of the Engineering Experiment Station of the University of Illinois, of which Professor Ross J. Martin is the Director, in the Department of Theoretical and Applied Mechanics, of which Professor T. J. Dolan is the Head. The part of the investigation dealing with test members made of 17-7PH stainless steel and Ti 155A titanium alloy was sponsored by the Materials Laboratory of the Wright Air Development Center, Dayton, Ohio [Contract No. AF 33(616) — 5658 with R. F. Klinger acting as project engineer]. The part of the investigation dealing with plastics was initiated by a grant in aid donated by the Polychemical Department of E. I. duPont de Nemours & Co., Inc., who also donated the nylon plastic.

Part of the work described herein was performed by George A. Costello while satisfying the thesis requirements for the degree of Doctor of Philosophy in Theoretical and Applied Mechanics at the University of Illinois. Other parts were performed by S. Dharmarajan, John L. Gubser, and Robert E. Carlson while satisfying the thesis requirements for the degree of Master of Science in Theoretical and Applied Mechanics at the University of Illinois. Acknowledgment is also due to Professor J. O. Smith for his initiation of the contract with Wright Air Development Center.

This page is intentionally blank.

CONTENTS

FIGURES

FIGURES (Cont'd)

TABLES

This page is intentionally blank.

I. INTRODUCTION

A. PRELIMINARY STATEMENT

Progress in technology requires more efficient utilization of materials by the engineer. Hence the engineer in designing a load-carrying member must be informed as to the various properties of the materials and also as to the design procedures for making use of these properties. One property which has become increasingly important in design is creep. The design procedures, as well as the experimental data, presented in this bulletin should aid in alleviating some of the difficulties in the problem of design for creep.

As the authors see it, the problem of design for creep is that of predicting the load and resulting deformation of a load-carrying member necessary to produce a specified strain in the most strained fibers of the member in a specified time. An exact analysis requires that the stress-strain-time-temperature relation be known for the material. Usually the problem is simplified by assuming constant temperature; however, even then the stress-strain-time relation is not known for real materials. This means that the design procedure must be based on certain approximations. In general, investigators in this field have made 1 or 2 types of approximations. One is to idealize the material so that the stress-strain-time relation is known, and the other is to assume that the stress-strain-time relation for the material is given by the constant stress-creep curves.

In idealizing the material, some investigators[1, 2, 3]* have assumed that the material was viscoelastic and could be represented by various models composed of springs and dashpots. In deriving load-deflection relations for beams and eccentrically loaded columns, Kempner in one paper[1] assumed that the material could be represented by linear springs and dashpots, and, in another paper,[2] by a linear spring and nonlinear dashpot. In treating the column problem, Hilton[3] assumed that the column was made of a generalized viscoelastic material. One of the difficulties in idealizing the material lies in the fact that a model which approximates closely the material behavior is too complex to be easily analyzed.

Based on the assumption that the stress-strain-time relation for the material is given by the constant stress-creep curves, two different approaches have been used in deriving theoretical load-deflection relations for beams and eccentrically loaded members for which the action line of the loads is parallel to the axis of the member. In one approach an equation is sought which will represent a family of creep curves such as those shown in Figure 1. The other approach considers design for a specified time t_1. From the intersection of a vertical line AB (Fig. 1) with the creep curves for time t_1 a plot may be obtained for corresponding values of stress and strain as shown in Figure 2. This plot is called the isochronous stress-strain diagram for time t_1 and is used in the derivation of the theoretical relations for time t_1.

In attempting to find a relation which would represent a family of creep curves, many investigators[4, 5, 6, 7] have neglected the nonlinear first

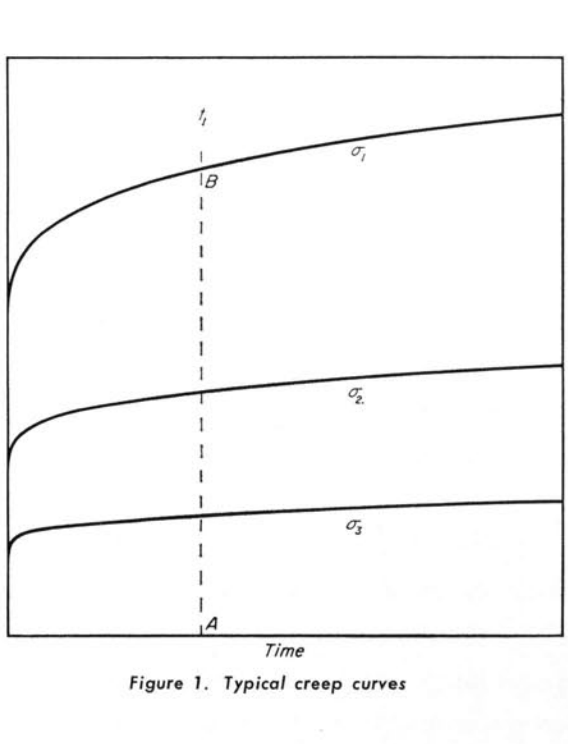

Figure 1. Typical creep curves

* Superscript numbers in parentheses refer to corresponding entries in the bibliography.

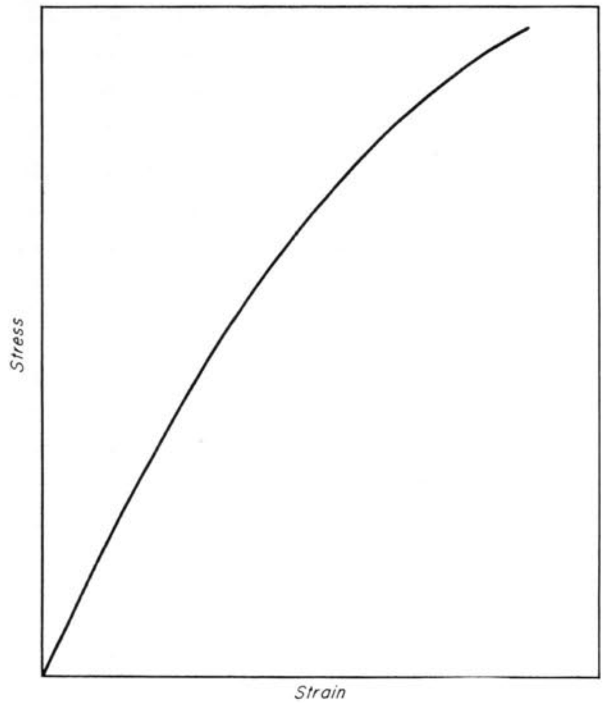

Figure 2. Typical isochronous stress-strain diagram

stage of the creep curve and have assumed the time dependence of creep to be a linear function of time. Theories based on this analysis cannot be used to predict behavior of members loaded for only a short time. Other investigators[7, 8, 9, 10] have considered the fact that creep is a nonlinear function of time. Pao and Marin[8] assumed that the stress-strain-time relations in tension and compression are identical and are defined by the relation

$$\epsilon = \frac{\sigma}{E} + K\,\sigma^{\alpha}\,(1 - e^{-qt}) + \beta\,\sigma^{n}\,t \tag{1}$$

where ϵ is total strain, σ is stress, t is time, and E, K, α, q, n, and β are experimental constants. Findley, Poczatek, and Mathur[9,10] assumed that the stress-strain-time relation in tension and compression could be represented by an equation of the form

$$\sigma = \sigma_0 \sinh^{-1} \frac{\epsilon}{\epsilon_0' + m'\,t^{n}} \tag{2}$$

in which ϵ_0', m', n, and σ_0 are experimental constants which may be different for tension and compression. This expression was found to give an excellent representation of creep data for several plastics. It should be noted that the stress dependence in Equation 2 is of the same form as that in the activation energy theory advanced by Kauzmann.[11] In a recent book by Finnie and Heller,[7] several of the relations, which have been proposed to represent the creep curves, are discussed relative to their use in the design of load-carrying members.

If the time variable is assumed constant, Equation 2 becomes

$$\sigma = \sigma_0 \sinh^{-1} \frac{\epsilon}{\epsilon_0}. \tag{3}$$

Equation 3 represents the isochronous stress-strain diagram in Figure 2 if Equation 2 represents the creep curves in Figure 1. It will be noted that Equation 3 has 2 variables instead of 3 and only 2 experimental constants must be determined instead of 4. Experimental constants σ_0 and ϵ_0 in Equation 3 may be different for different values of time; however, σ_0 will have to remain constant if Equation 2 is used. Hence, Equation 3 will in general give a better approximation of the isochronous stress-strain diagram than either Equation 1 or 2 will approximate the creep curves.

Carlson and Manning[12] used the isochronous stress-strain diagrams of the material to derive theoretical buckling loads for eccentrically loaded columns; however, they did not represent the diagrams by an arc hyperbolic sine curve (Eq. 3). They found the theory to be conservative by 20% to 60%. This great difference between the theoretical and experimental collapse loads is believed to result from the fact that the isochronous stress-strain diagrams obtained from compression creep specimens were probably in error. The authors have undertaken many investigations in recent years[13, 14, 15, 16, 17, 18, 19, 20, 21] and have found that theories based on Equation 3 adequately predicted the experimental results.

B. PURPOSE AND SCOPE

The purpose of this investigation may be summarized as follows:

1. To present a theory for predicting the load-deflection curves for beams, centrally loaded columns, and eccentrically loaded tension members and columns, based on the arc hyperbolic sine curve representation of the isochronous stress-strain diagram.

2. To bring together the results of several experimental investigations comparing theoretical and experimental load-deflection curves for metal members at elevated temperatures and for plastic members in a controlled atmosphere room.

3. To consider the suitability of using a modi-

fied secant formula for predicting the collapse loads and the maximum deflections of eccentrically loaded columns made of materials that creep.

In the development of the theory referred to as the arc hyperbolic sine theory, simplifying approximations were used. A qualitative analysis of the effect of these approximations is presented to determine whether they will make the theory conservative or nonconservative. A theoretical analysis is presented for a general I-section member made of a material whose isochronous stress-strain diagrams in tension and compression are identical and can be represented by Equation 3. Using the theory, dimensionless moment vs. angle-change curves were constructed for beams to be used in the design of beams for either strength or deflection. Also, 2 families of dimensionless curves were constructed for eccentrically loaded members (tension members or columns for which the action line of the loads is parallel to the axis of the member). One family of curves is used to locate the neutral axis of the eccentrically loaded member and to determine the deflection. The other family of curves is used to calculate the load once the neutral axis has been located. Except for the rectangular section, these families of curves have to be constructed for each cross-section having different relative dimensions. If the initial eccentricity is less than 5%, a modified secant formula may be used to compute the collapse load and column deflection without the use of these families of curves.

The experimental part of the investigation included tests of members made of two plastics and two metals. High pressure canvas laminate and Zytel 101 nylon members were tested in a controlled-atmosphere room, 17-7PH stainless steel members were tested at 972° F. and Ti 155A titanium alloy members were tested at 772° F. Tension and compression creep specimens were subjected to constant loads in order to obtain the experimental constants for Equation 3. The beams and eccentrically loaded members had either a rectangular section or a T-section in order to check the validity of the theory for various cross-sections.

The duration of each test for test members made of plastics was 1,000 hours or until collapse in the case of the columns. In the investigations of members made of canvas laminate, constant load tests were made on 4 beams subjected to pure bending, 8 statically indeterminate beams, 4 eccentrically loaded tension members, and 27 eccentrically loaded columns with slenderness ratios of 30, 50, and 70 and initial eccentricities of 2%, 5%, and 25% of their depths. Nylon test members were limited to 4 straight beams and 4 eccentrically loaded tension members. In all cases good agreement was found between the experimental data and the arc hyperbolic sine theory.

Only short-time tests were considered for the metal members. Except for the columns which buckled at various intervals of time, the test duration was 30 minutes for all test members. Constant load tests were made on 11 eccentrically loaded tension members and 29 eccentrically loaded columns made of 17-7 PH stainless steel. The columns had slenderness ratios of 50, 60, 75, and 100 and were subjected to initial eccentricities of 5% and 25% of their depths. Good agreement was found between the arc hyperbolic sine theory and the experimental data.

The test members made of Ti 155A titanium alloy were subjected to 2 different aging temperatures in their heat treatment. Three eccentrically loaded tension members and 20 eccentrically loaded columns were aged at 1085° F.; the columns had slenderness ratios of 50, 60, 75, and 100 and were subjected to initial eccentricities of 5% and 25% of their depths. Four columns were aged at 972° F.; they had a slenderness ratio of 75 and were subjected to initial eccentricities of 5% and 25% of their depths. In the case of the titanium alloy, the inelastic deformation was primarily time independent, and the isochronous stress-strain diagram could best be approximated by 2 straight lines. Consequently, the experimental data were analyzed using the interaction curve — moment-load curve theory presented in a previous bulletin.[22] Good agreement was found between theory and experiment.

II. THEORY

This section presents the theoretical relations necessary to construct theoretical load-deformation curves for beams and eccentrically loaded members for which the action line of the loads is parallel to the axis of the member. Two different theories are considered.

If the inelastic deformation of the material is time-dependent creep, the isochronous stress-strain diagram of the material is represented by an arc hyperbolic sine curve, Equation 3. The theory based on this stress-strain diagram is called the arc hyperbolic sine theory. A discussion of the assumptions necessary to develop this theory will be presented, followed by the derivations of the necessary theoretical relations.

If the deformation of the material is predominantly time independent, the isochronous stress-strain diagram of the material can be more accurately approximated by 2 straight lines. The theory for this stress-strain representation is called the interaction curve — moment-load curve theory. Since this theory was presented in a previous bulletin,[22] only the derived relations will be presented herein.

A. ASSUMPTIONS

Theoretical relations will be derived to predict the load-deflection curves of beams and eccentrically loaded members made of materials that creep. The assumptions made in this theory for time-dependent inelastic deformation will be the same as that made in a previous bulletin[22] for time independent inelastic deformation. In deriving the theoretical relations, 3 assumptions were made:

1. Plane sections remain plane.
2. The stress-strain relation for each fiber of a beam or eccentrically loaded member is the same as that obtained from tension and compression specimens.
3. The deflected configuration of the eccentrically loaded member is either a segment of a circle or a cosine curve.

The first assumption is usually made by all investigators. The second assumption is also generally accepted by all investigators as long as the inelastic deformation is time independent.

In case the inelastic deformation is time dependent creep, an isochronous stress-strain diagram for a specified time can be obtained from constant-stress tension or compression creep curves. For a theory based on this stress-strain diagram it is assumed that the stress in any fiber of a member does not change with time. Since the stress distribution in beams and eccentrically loaded members changes with time as the result of creep, the second assumption, listed above, introduces an error into the theory. In the most strained fibers of beams and eccentrically loaded tension members subjected to constant load, the stress decreases with time from some value σ_1 to the final value σ (corresponding to the specified time) so that the strain in the most strained fibers of the beam corresponding to stress σ is greater than that obtained from tension or compression specimens subjected to constant stress σ for the same duration of time. Thus, the deflection in these members is greater than that predicted by the theory. In contrast to the beams and eccentrically loaded tension member, the assumption results in a conservative estimate of the deflection for eccentrically loaded columns.

The load and moment at various sections of the eccentrically loaded member are related through the configuration of the deformed member, since the moment at a given section is equal to the product of the load and the distance from the action line of the load to the centroid of the section. The exact configuration of the member is difficult if not impossible to obtain; therefore, 2 different approximations of the configuration of the member are considered as indicated by the third assumption. The assumption that the member deforms into a segment of a circle requires that every section of the eccentrically loaded member be subjected to the same moment as the central section. For an eccentrically loaded tension member, the central section has the smallest eccentricity. Since every other section has a greater moment than that assumed

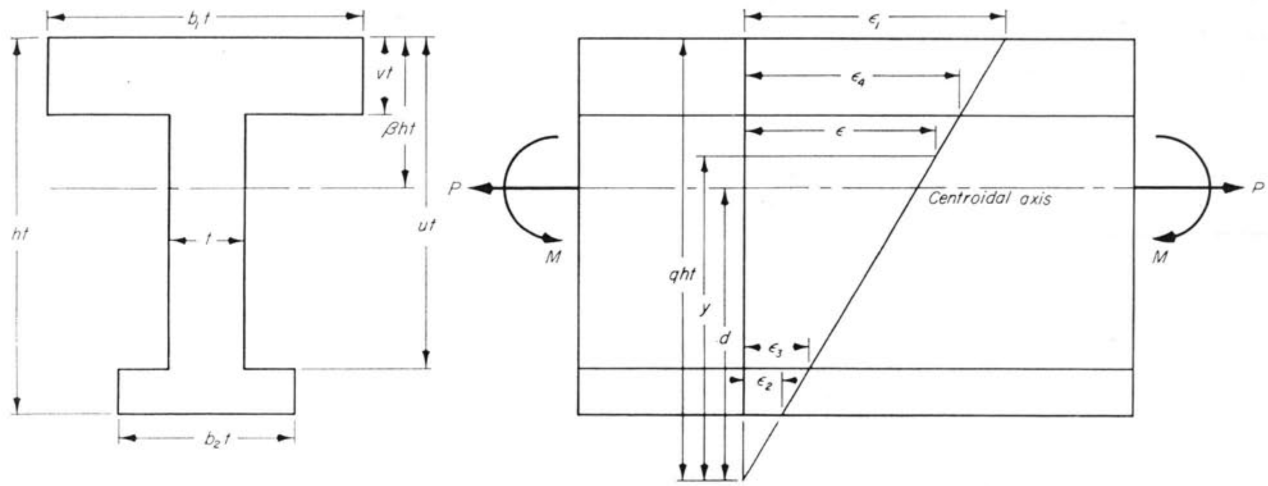

Figure 3. I-section member showing dimensions of cross-section loading arrangement and strain distribution

by the theory, the theoretical deflection will be nonconservative (i.e. less than actual). In the case of eccentrically loaded columns, the central section has the largest moment; therefore, the theoretical moment at all other sections will be greater than actual, and the theoretical deflection will be conservative (i.e. greater than actual). The segment of circle assumption is exact if the initial eccentricity approaches infinity; conversely, the error becomes large for small initial eccentricities.

In many cases, the initial eccentricity of columns is small and so the error introduced by the segment of circle assumption is too large although conservative. If the column is assumed to deform into a cosine curve, the theoretical moment at the end is assumed to be zero while the actual moment at the end is equal to the product of the load and the initial eccentricity. For this assumption the theoretical moment at every section except the central section is less than actual, and the theoretical deflection will be nonconservative (i.e. less than actual). If the initial eccentricity of the column is small, the cosine curve assumption gives an accurate estimate of the column deflection.

The second assumption introduces an error into the theory for beams, while the second and third assumptions introduce errors into the theory for eccentrically loaded members. The beam test data indicate that the error is not large and that the theory can be made conservative in most cases by reducing the theoretical load by 5%. The test data for the eccentrically loaded members indicate that good agreement will be found between theory and experiment if the theoretical load is decreased by 10% for eccentrically loaded tension members assumed to deflect into a segment of a circle and increased by 10% for eccentrically loaded columns assumed to deflect into a cosine curve.

B. ARC HYPERBOLIC SINE THEORY

If the inelastic deformation of a member is completely time dependent, i.e., due to creep, the isochronous stress-strain diagram of the material can be accurately approximated in most cases by an arc hyperbolic sine curve relation represented by Equation 3. Using this relation between stress and strain, theoretical relations will be derived in this article for constructing load-deflection curves for beams and eccentrically loaded members.

It is assumed that the problem in design for creep is to determine the load and resulting deflection necessary to produce a specified strain in the most strained fibers of a member in a given time. Consider the general I-section member shown in Figure 3. The member is subjected to a load P and moment M necessary to produce a strain ϵ_1 in the most strained fibers and to locate the neutral axis at a distance qht from the most strained fibers. With the strain distribution known, the stress distribution is obtained using Equation 3, and the magnitude of P and M can be determined from the equations of equilibrium.

$$P = \int \sigma \, da \qquad \textbf{(4)}$$

$$M = \int (y - d) \, \sigma \, da \qquad \textbf{(5)}$$

In integrating these equations, it is convenient to

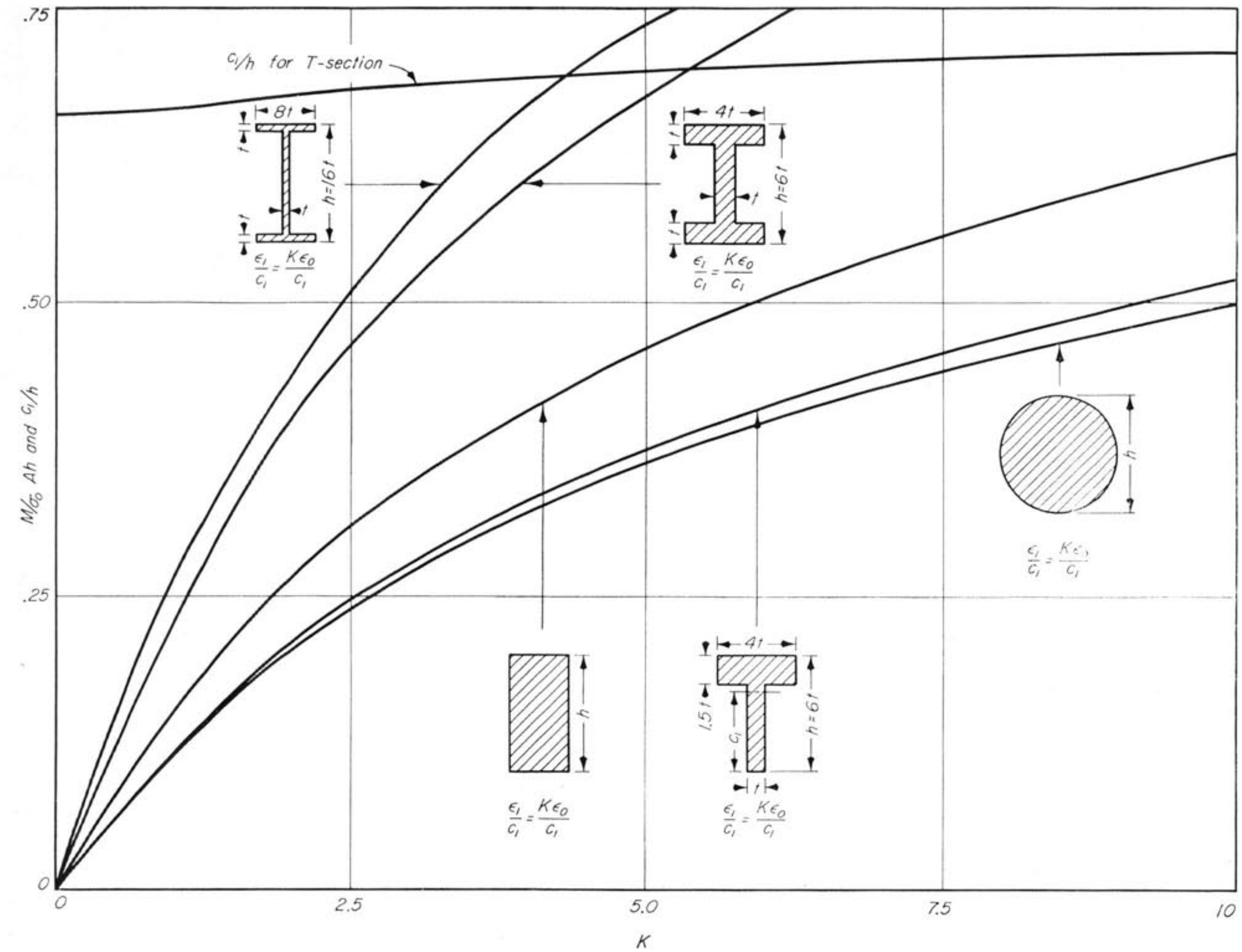

Figure 4. Dimensionless curves for obtaining bending moment and angle change in beams

make ϵ the variable instead of y by using geometrical relations. Equations 4 and 5 integrate into the following equations:

$$P = \frac{\sigma_0\, qht^2}{K}\left[b_1\, B_K - (b_1 - 1)\, B_{\frac{qh-v}{qh}K} + (b_2 - 1)\, B_{\frac{qh-u}{qh}K} - b_2\, B_{\frac{q-1}{q}K}\right] \qquad (6)$$

$$M = \frac{\sigma_0\, q^2h^2t^3}{K^2}\left[b_1\, C_K - (b_1 - 1)\, C_{\frac{qh-v}{qh}K} + (b_2 - 1)\, C_{\frac{qh-u}{qh}K} - b_2\, C_{\frac{q-1}{q}K}\right] - (q - \beta)\, P\, h\, t \qquad (7)$$

in which $K = \epsilon_1/\epsilon_0$. In these equations the functions B_N and C_N are defined as follows:

$$B_N = N\, log_e\,(N + \sqrt{N^2 + 1}) - \sqrt{N^2 + 1} \qquad (8)$$

$$C_N = \frac{1}{4}\left[(1 + 2N^2)\, log_e\,(N + \sqrt{N^2 + 1}) - N\sqrt{N^2 + 1}\right] \qquad (9)$$

in which N represents the various subscripts for B and C in Equations 6 and 7. Four-place tables of B_N and C_N are given in appendix A. The values in these tables are for positive values of N; in case N is negative, $B_{(-N)} = B_{(+N)}$ and $C_{(-N)} = -C_{(+N)}$.

Equations 6 and 7 are sufficient to analyze beams made of materials that creep. If the load P is assumed zero for a specified strain ϵ_1, Equation 6 is used to locate the neutral axis, and the moment is determined by using Equation 7. Additional relations are needed for the eccentrically loaded members, since the load and moment are related through the initial eccentricity and the deflection.

Equations 6 and 7 are based on the assumption that the properties of the material are the same for

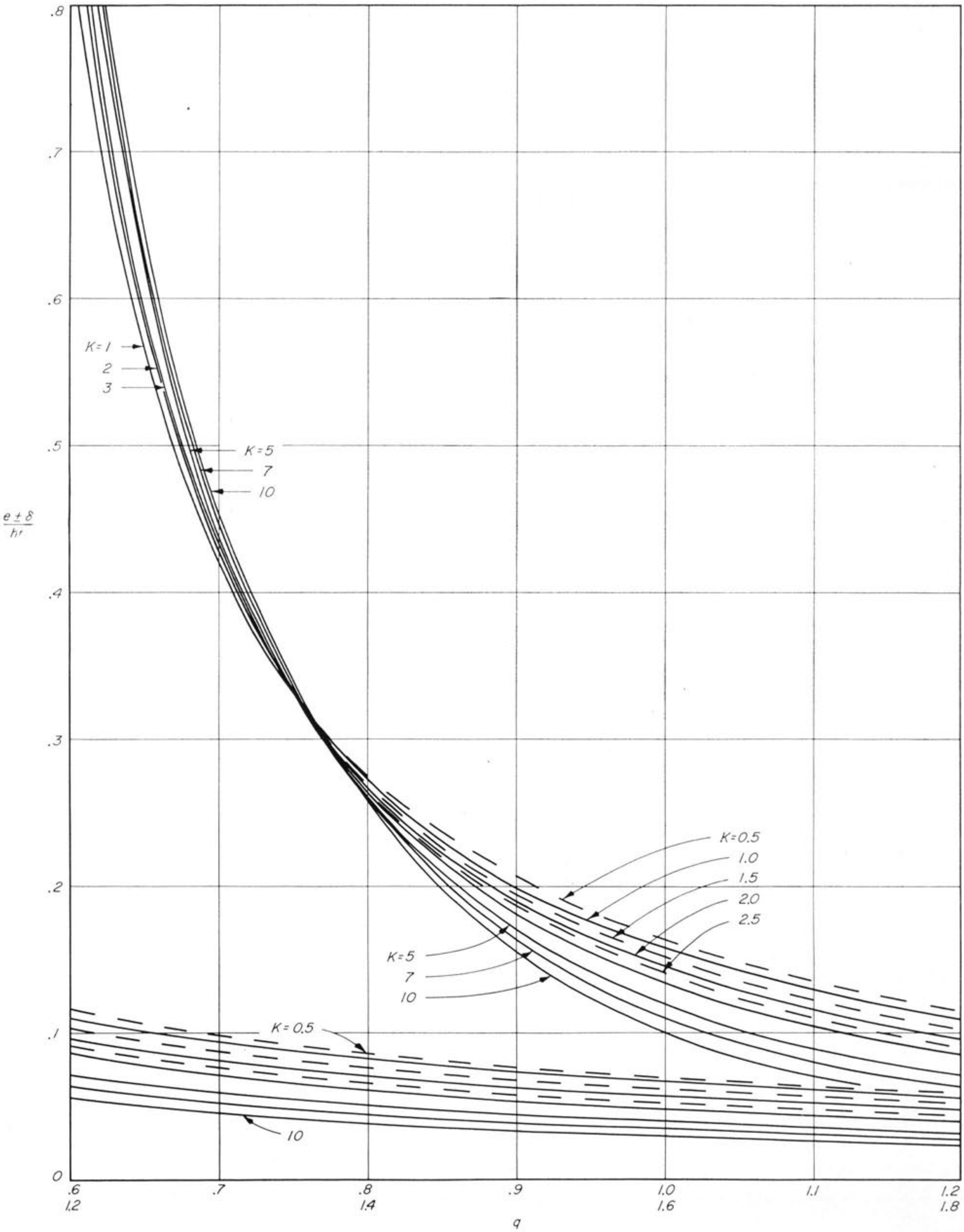

Figure 5. Family of curves for a rectangular-section member used in determining the value of q

tension and compression. More general equations are available in the literature[14]; however, it is recommended that the average isochronous stress-strain diagram be used in predicting the load and deflection for beams. Calculations have been made which indicate that the load-deflection diagram for a beam, made of a material whose tension and compression isochronous stress-strain diagrams are 10% on either side of the average, lies within 2% of that obtained by using the average isochronous stress-strain diagram. It is recommended that either the tension or the compression isochronous stress-strain diagrams be used to analyze eccentrically loaded tension members and columns, respectively. Except for large initial eccentricities, the stress in most fibers of the eccentrically loaded members is of one sign.

Using Equations 6 and 7, dimensionless moment versus K design curves were constructed for beams having a rectangular section and the I- and T-sections shown in Figure 4. A design curve is also shown for a circular cross section in Figure 4. Since it is assumed that $\epsilon_1 = K\epsilon_0$ (ϵ_0 is an experimental constant, see Equation 3) is specified for a given design, the design of a beam for strength is readily obtained from the appropriate curve in Figure 4. Once the moment diagram is known, the angle change diagram for the beam can be readily constructed using the appropriate curve in Figure 4 and the relation shown directly below the beam cross section. The beam deflection can be obtained from the angle change diagram using the numerical integration procedure given by Newmark.[23]

The load-deflection curve for an eccentrically loaded member can be obtained using Equations 6 and 7 and the following relation:

$$M = P\,(e \pm \delta) \tag{10}$$

in which e is the initial eccentricity and δ is the deflection of the center section of the member. The plus and minus signs in Equation 10 are for compression and tension, respectively. Using Equations 6, 7, and 10, an expression relating the variables q, δ, and K can be obtained as follows:

$$\frac{e \pm \delta}{ht} = \frac{\frac{q}{K}\left[b_1\, C_K - (b_1 - 1)\, C_{\frac{qh-v}{qh}K} + (b_2 - 1)\, C_{\frac{qh-u}{qh}K} - b_2\, C_{\frac{q-1}{q}K}\right]}{b_1\, B_K - (b_1 - 1)\, B_{\frac{qh-v}{qh}K} + (b_2 - 1)\, B_{\frac{qh-u}{qh}K} - b_2\, B_{\frac{q-1}{q}K}} - q + \beta \tag{11}$$

Equation 11 is difficult to work with, unless available in graphic form. The families of curves shown in Figures 5 and 6 were constructed using Equation 11 for a rectangular section ($b_1 = b_2 = 1$) and for a T-section ($h = 6$, $b_1 = 4$, $b_2 = 1$, and $v = 1.5$), respectively.

In the design of a given eccentrically loaded member, it is assumed that K is known. However, the appropriate curve in either Figures 5 or 6 cannot be used unless either q or δ is known. Another relation between q, δ, and K can be obtained if the configuration of the deflected member is known. If the deflected axis is assumed to take the shape of a segment of a circle or a cosine curve, the deflections[22] of the members are given by the relations

$$\delta = \frac{l^2 K\, \epsilon_0}{8\, q\, ht} \text{ and} \tag{12}$$

$$\delta = \frac{l^2 K\, \epsilon_0}{\pi^2\, q\, ht}, \text{ respectively.} \tag{13}$$

By adding and subtracting the initial eccentricity to each side of Equations 12 and 13, the following relations may be obtained:

$$q = \frac{\dfrac{l^2 K\, \epsilon_0}{8 h^2\, t^2}}{\mp \dfrac{e}{ht} \pm \dfrac{e \pm \delta}{ht}} \tag{14}$$

$$q = \frac{\dfrac{l^2 K\, \epsilon_0}{\pi^2\, h^2\, t^2}}{\mp \dfrac{e}{ht} \pm \dfrac{e + \delta}{ht}} \tag{15}$$

For a given value of K, assume a value of q and read off the value of $\frac{e \pm \delta}{ht}$ from the appropriate curve in Figures 5 or 6, and calculate q by Equations 14 or 15. If the calculated value of q does not equal the assumed value, assume a new value of q and repeat the process. The trial and error solution does not require much time. Once q is known, the magnitude of the load P is obtained from Equation 6. As an aid to solving Equation 6, the families of curves in Figures 7 and 8 were constructed for rectangular and T-section members, respectively.

Typical theoretical load-deflection curves for columns having an initial eccentricity of 5% and 25% of their depths are shown in Figure 9 for both the cosine-curve and segment-of-circle assumption of the configuration of the column. It will be noted

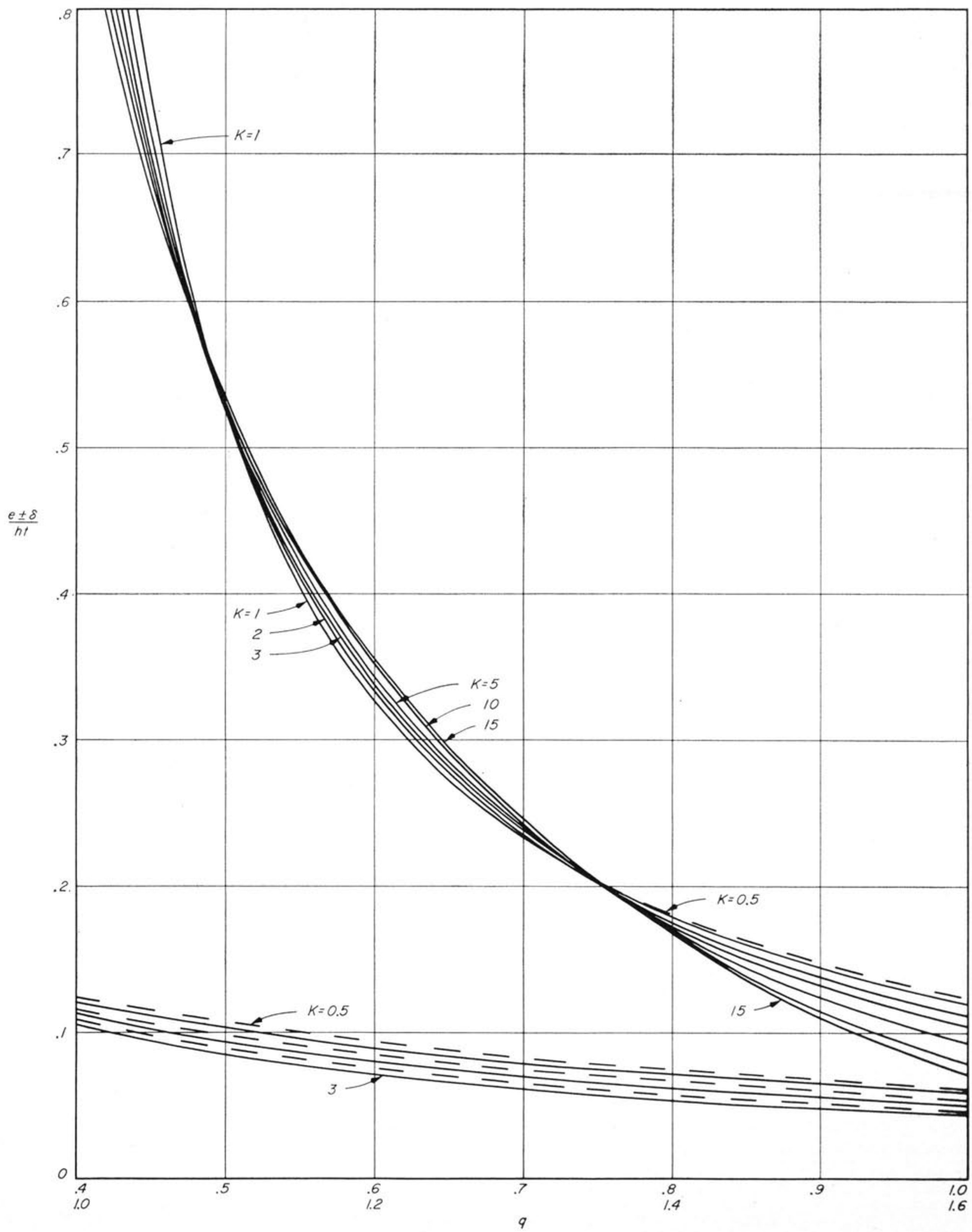

Figure 6. Family of curves for a T-section member used in determining the value of q

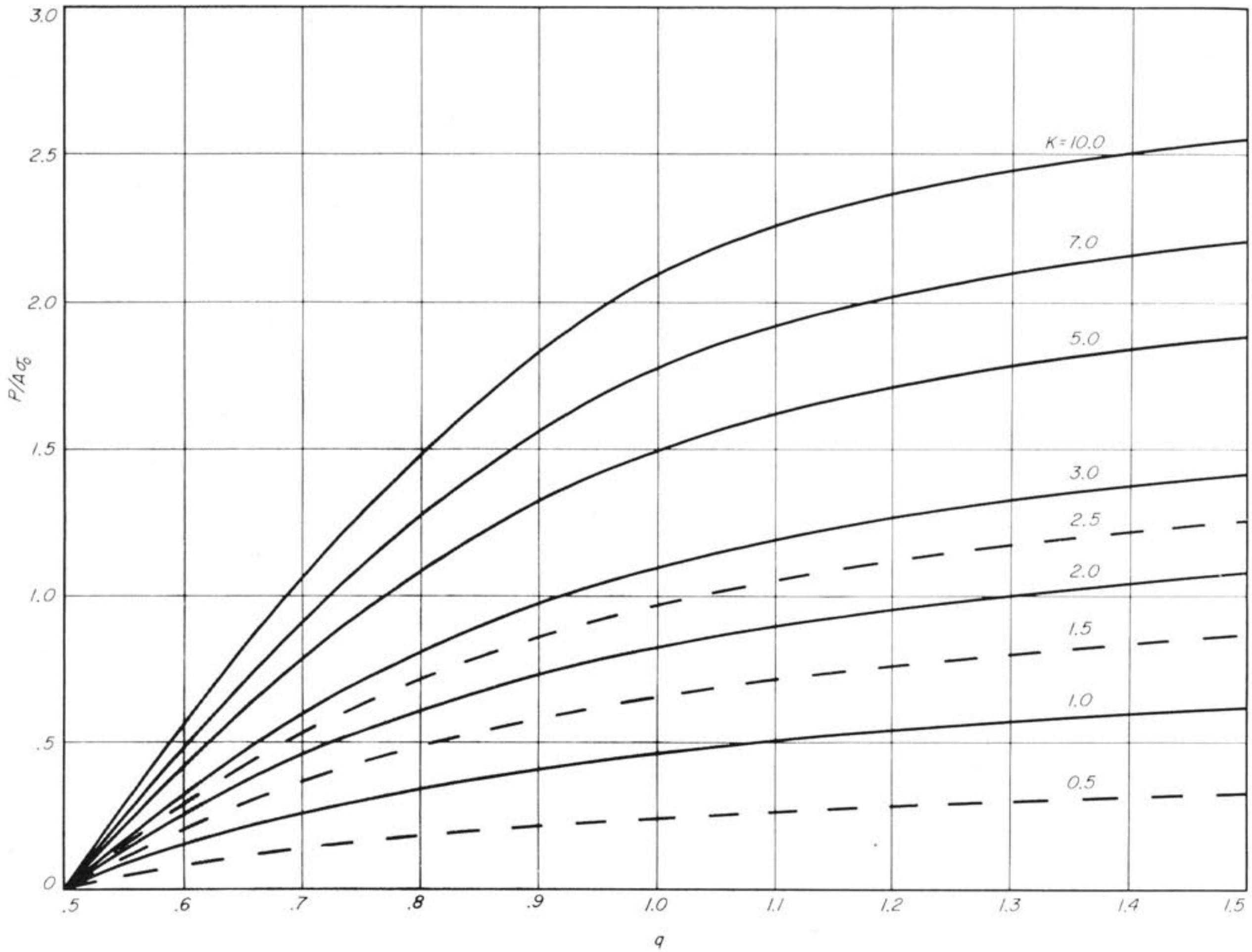

Figure 7. Family of curves for a rectangular-section member used in determining P

that the load-deflection curves based on the cosine-curve assumption lie appreciably above those based on the segment-of-circle assumption.

C. ELASTIC LOAD-DEFLECTION RELATIONS

In designing for creep it may be desirable to know the load-deflection curve for an eccentrically loaded member for zero time. If the material is elastic for zero time, the load-deflection curve cannot be obtained from the theory presented in Article IIA since Equation 3 is nonlinear except for extremely small values of K, and the design curves shown in Figures 5 through 8 were not constructed for small values of K. For elastic conditions, the secant formula,

$$e + \delta = e \sec \sqrt{\frac{P\left(\frac{l}{r}\right)^2}{4AE}}\,, \tag{16}$$

gives an exact load-deflection curve for eccentrically loaded columns.

In case of an eccentrically loaded tension member, an approximate load-deflection relation can be derived based on the assumption that the member deflects into a segment of a circle. If the member is elastic, the radius of curvature can be written in terms of the moment,

$$\frac{1}{R} = \frac{M}{EI} \tag{17}$$

The radius of curvature can also be written in terms of the strain distribution shown in Figure 3 to give

$$\frac{1}{R} = \frac{\epsilon_1}{q\,h\,t} \tag{18}$$

Using Equations 10, 12, 17, and 18, the load P can be written in terms of the deflection δ as follows:

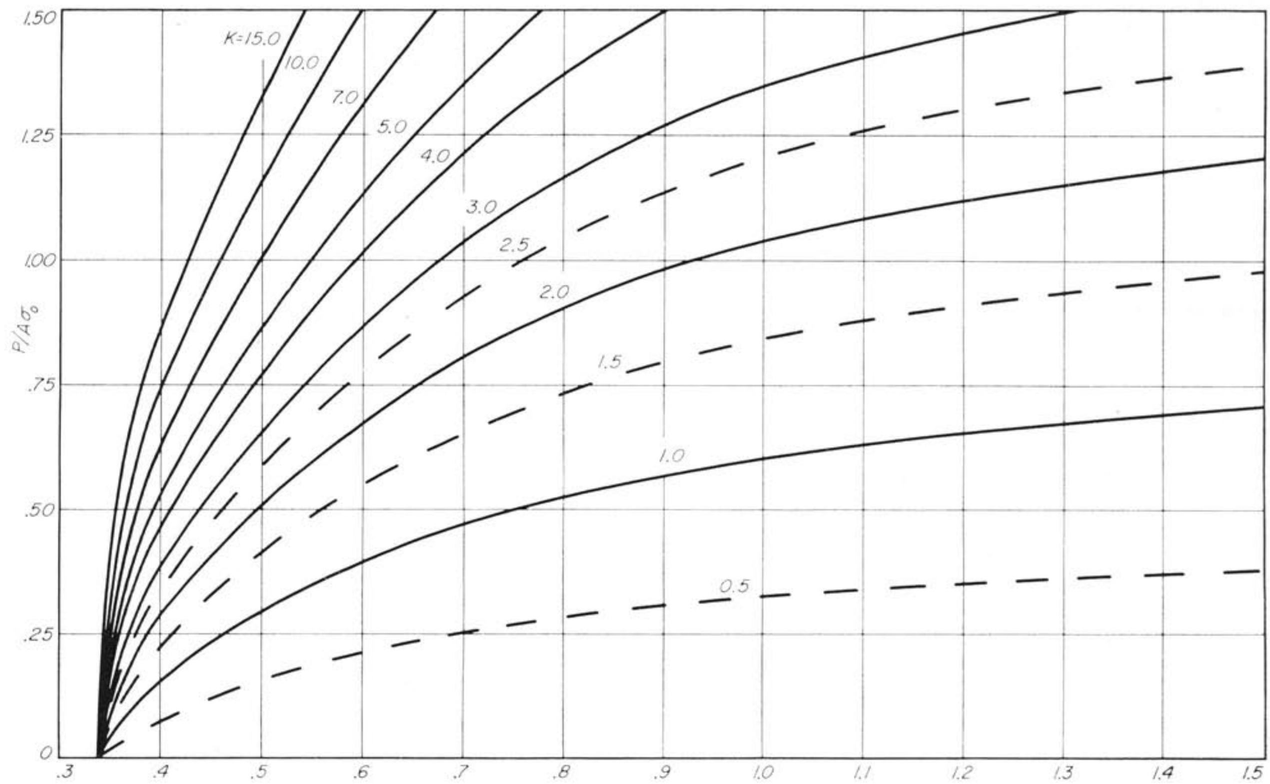

Figure 8. Family of curves for a T-section member used in determining P

$$P\ (e - \delta) = \frac{8\ \delta\ E\ I}{l^2} \tag{19}$$

D. MODIFIED SECANT FORMULA

If the initial eccentricity and the deflection are small, the resisting moment is small; consequently, the difference in stress between the outside and inside fibers of the column is small. Under these conditions an assumption of linear stress distribution is reasonable. The secant formula is valid for a linear stress distribution so that the column formula for a material whose stress-strain properties are given by Equation 3 is represented by the following equation:

$$\delta = e\left[\sec\sqrt{\frac{\epsilon_0\left(\frac{P}{A}\right)\left(\frac{l}{r}\right)^2\sqrt{1+K^2}}{4\sigma_0}} - 1\right] \tag{20}$$

in which the ratio $\dfrac{\sigma_0}{\epsilon_0\sqrt{1+K^2}}$ is the tangent modulus obtained from Equation 3 and the average stress P/A is also obtained from Equation 3.

The load-deflection curves represented by Equa-

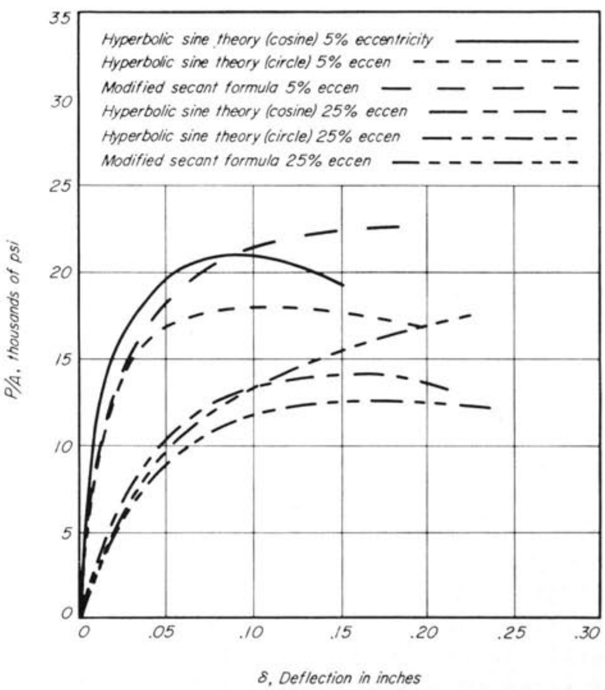

Figure 9. Comparison of theoretical P/A-deflection curves for rectangular-section columns

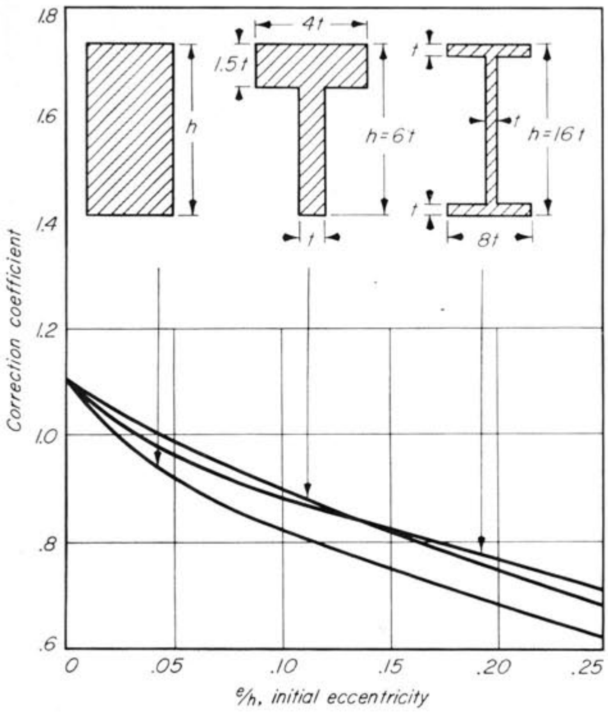

Figure 10. Coefficients to be used in connection with collapse loads obtained by modified secant formula

tion 20 are shown in Figure 9 for columns having initial eccentricities of 5% and 25% of their depths. It will be noted that the modified secant formula (Eq. 20) lies between the 2 theoretical load-deflection curves based on segment-of-circle and cosine-curve approximations of the deflected axis of the column. Since the assumption based on the segment of circle gives a conservative deflection, and the assumption based on a cosine curve gives a nonconservative deflection, Equation 20 might be expected to give a reasonably accurate prediction of the column deflection within its range of applicability. For eccentricities up to 5% of the column depth, Equation 20 was found to give a good estimate of the column deflection for any load up to the collapse load. As the initial eccentricity increases, Equation 20 becomes less reliable, since the stress distribution can no longer be assumed linear. At an eccentricity of 25% of the depth, Equation 20 was found to give a reliable value of the deflection only up to a load of one half the collapse load.

Since Equation 20 gives a reasonably good approximation of the deflection for columns having small eccentricities, a question arises as to its applicability for predicting the collapse load. If the radical in Equation 20 is equal to $\pi/2$, the deflection becomes infinite. The resulting load is equal to the tangent modulus load for the column having an initial eccentricity equal to zero. Since the experimental collapse load is approximately 10% larger than that predicted by the arc hyperbolic sine theory, there will be an eccentricity for which Equation 20 will agree with the experimental results. Based on the 10% difference between theory and experiment, correction coefficients were computed for the tangent moduli loads for columns having a rectangular section and the T- and I-sections shown in Figure 10. The T-section shown in Figure 10 is the one used in the experimental investigation. The experimental data for the eccentrically loaded columns will be analyzed in Article VA using both the arc hyperbolic sine theory and the corrections shown in Figure 10.

E. INTERACTION CURVE — MOMENT-LOAD CURVE THEORY

For some metals at an elevated temperature, the inelastic deformation may be mostly time independent. In this case, the isochronous stress-strain diagram cannot be represented by Equation 3 but can be approximated by 2 straight lines (Fig. 24). The theoretical load-deflection curves for eccentrically loaded members made of this material can best be constructed using the interaction curve — moment-load curve theory which was developed in a previous bulletin.[22] The derivations of the relations required for this theory will not be repeated; however, the desired relations will be listed.

Theoretical moment-load and load-deflection curves for eccentrically loaded members are constructed using constant depth of yielding moment and load interaction curves. Consider a T-section member whose cross-sectional dimensions are depth h, flange width b, flange thickness t_2 and web thickness t. Let a short length of this member be subjected to a load P acting along the centroidal axis and to a moment M of sufficient magnitudes to initiate yielding to a depth a_1 on the flange side and to a depth a_2 on the web side. For conditions that a_1 is less than or equal to t_2, the magnitude of P and M are given by the following relations:

$$P = P_e - \frac{2A\sigma_e}{a}(c_1 - a_1) - (1 - \alpha)\frac{\sigma_e}{a}(a_1^2 b - a_2^2 t) \quad (21)$$

$$M = \frac{2\sigma_e I}{a} - (1-\alpha)\frac{\sigma_e}{a}\left[a_1^2\, b\left(c_1 - \frac{a_1}{3}\right)\right.$$
$$\left. + a_2^2\, t\left(c_2 - \frac{a_2}{3}\right)\right] \tag{22}$$

in which A is the cross-sectional area, σ_e is the yield stress in compression and αE is the slope of the stress-strain diagram for post-yielding conditions (Fig. 24a).

For conditions in which yielding has progressed through the tension flange into the web, the load and moment expression are

$$P = P_e - \frac{2A\sigma_e}{a}(c_1 - a_1) - (1-\alpha)\frac{\sigma_e}{a}\left[ba_1^2\right.$$
$$\left. - (b-t)(a_1 - t_2)^2 - a_2^2\, t\right] \tag{23}$$

$$M = \frac{2\sigma_e I}{a} - (1-\alpha)\frac{\sigma_e t}{a}\left[\frac{2I}{t}\right.$$
$$- (a + a_2)^2\left(c_2 - \frac{a + a_2}{3}\right)$$
$$\left. + a_2^2\left(c_2 - \frac{a_2}{3}\right)\right] \tag{24}$$

Interaction curves for a rectangular-section member can be constructed using Equations **21** and **22** (let $b = t$) while Equations **21** through **24** are used for a T-section member. It should be noted that Equations **21** and **22** are valid if either a_1 or a_2 is zero and Equations **23** and **24** are valid if a_2 is zero. In this report the interaction curves are made dimensionless by dividing the load P by $P_e = \sigma_e A$ and the moment M by $M_e = \sigma_e I/c_2$.

The theoretical moment-load curves for the eccentrically loaded members were constructed by finding their intersection with each of a family of interaction curves. The slope of a straight line drawn from the origin of the interaction curve to the intersection of the moment-load curve with a given interaction curve is given by the relation

$$\tan\theta = \frac{c_2 e}{r^2} - \frac{c_2\left(\frac{l}{r}\right)^2 \epsilon_e}{4\,k\,h}\,\frac{M_L}{M_U} \tag{25}$$

if the deflected shape of the member is a segment of circle and

$$\tan\theta = \frac{c_2 e}{r^2} - \frac{2c_2\left(\frac{l}{r}\right)^2 \epsilon_e}{\pi^2\,k\,h}\,\frac{M_L}{M_U} \tag{26}$$

if the deflected shape of the member is a cosine curve. In Equations **25** and **26** e is the initial eccentricity, $r^2 = I/A$, $\epsilon_e = \sigma_e/E$, and $k = (h - a_1 - a_2)/h$. If the line intersects the interaction curve in the curved portion (see Figure 37) the ratio M_L/M_U is taken to be unity. If the intersection is in the straight line portion of the interaction curve, the solution is by trial and error since M_L is the moment at the unknown intersection and M_U is the moment for the upper end of the straight line portion of the interaction curve. After the moment-load curve has been determined, the deflection δ for assumed configurations of segment of circle and cosine curve are

$$\delta = \frac{l^2\,\epsilon_e}{4\,k\,h}\,\frac{M_L}{M_U}\ \text{and} \tag{27}$$

$$\delta = \frac{2l^2\,\epsilon_e}{\pi^2\,k\,h}\,\frac{M_L}{M_U}\ \text{respectively.} \tag{28}$$

III. MATERIALS AND METHOD OF TESTING

A. MATERIALS AND TEST MEMBERS

Four different materials were considered in the experimental investigations. Two of the materials were plastics, high pressure canvas laminate and Zytel 101 nylon, and the others were metals, 17-7PH stainless steel and Ti 155A titanium alloy. The canvas laminate test members were all machined from a 3 ft. by 4 ft. plate having a thickness of ½ in. The nylon test members were all machined from a 10 in. by 20 in. plate having a thickness of ¾ in. All of the test members for each metal were machined from one ½ in. by 2 in. bar of that material. The chemical analysis of the 2 metals are as follows:

	C	Mn	P	S
17-7PH	0.066	0.59	0.030	0.010
	Si	Cr	Ni	Al
	0.30	17.09	7.25	1.06
	C	Fe	N_2	Va
Ti-155A	0.015	1.4	0.009	1.5
	Mo	H_2	Al	
	1.1	0.009	5.4	

To obtain the theoretical curves for the beams and eccentrically loaded members, tension and compression creep properties of the materials were required. These properties were obtained from tension and compression specimens having the dimensions shown in Figures 11, 12, and 13. A hollow compression specimen was chosen for the nylon since the minimum thickness for this material had to be less than ¼ in. to moisture-condition the plastic. Sketches of the nylon beams and eccentrically loaded tension members are shown in Figure 11. In Figure 12 are shown sketches of the canvas laminate simply supported, and statically indeterminate beams and the eccentrically loaded tension members and columns. In the case of the 17-7PH stainless steel and Ti 155A titanium alloy, only eccentrically loaded tension members and columns were considered in the investigation. Sketches of these members are shown in Figure 13. The test lengths of the columns shown in Figures 12 and 13 were 1.20 in. longer than the values shown, since knife-edge fixtures were added to each end of the column.

The 17-7PH stainless steel test members were precipitation hardened after machining. They were heated to 1400° F. for 90 minutes, cooled to 60° F. in 60 minutes, held at 60° F. for 30 minutes, heated to 1050° F. for 90 minutes, and air cooled. Most of the Ti 155A titanium alloy specimens were tested in the "as received" condition; the manufacturer reported that the bars were heated to 1650° F. for 1 hour, water quenched, heated to 1085° F. for 12 hours, and air cooled. This heat treatment resulted in properties lower than those usually reported for

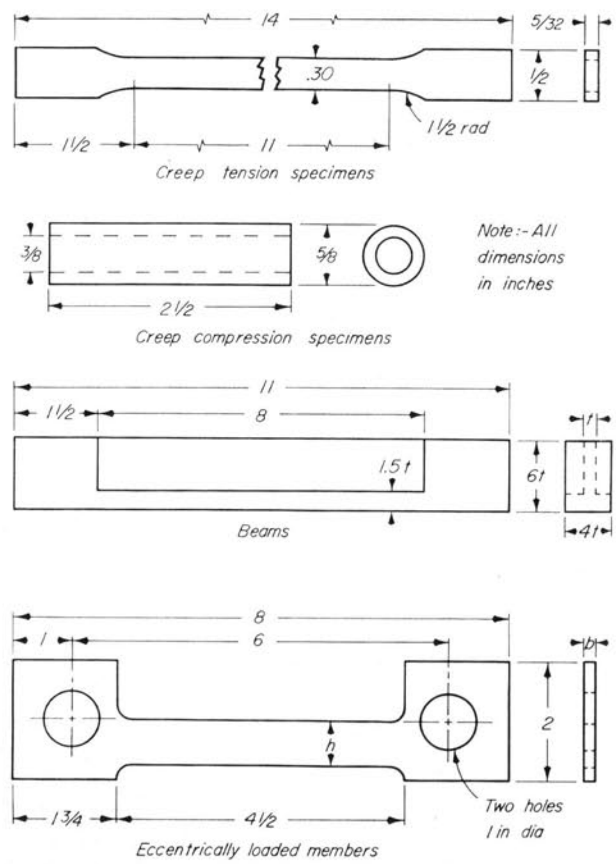

Figure 11. Nylon test members

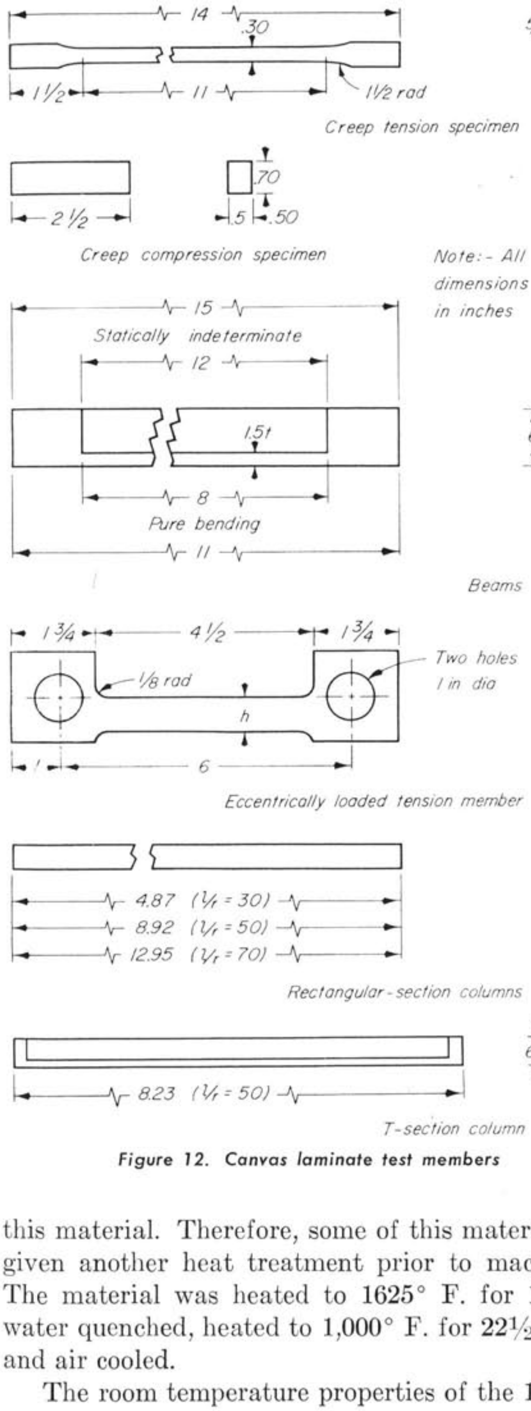

Figure 12. Canvas laminate test members

this material. Therefore, some of this material was given another heat treatment prior to machining. The material was heated to 1625° F. for 1 hour, water quenched, heated to 1,000° F. for 22½ hours, and air cooled.

The room temperature properties of the 17-7PH stainless steel material were modulus of elasticity of 28,400,000 psi, yield stress at 0.2% offset of 181,000 psi, and elongation in 2 in. gage length of 9.5%. The modulus of elasticity of the Ti 155A titanium alloy at room temperature was 16,600,000 psi. When the titanium alloy was aged at 1,000° F. following the water quench, the yield stress at 0.2% offset was 165,000 psi and the elongation in 2 in. gage length was 11.7%. When the titanium alloy was aged at 1085° F., the yield stress at 0.2% offset was 130,000 psi and the elongation was 19.0%.

B. METHOD OF TESTING

Since the strength properties of the plastics are known to be affected by the moisture content of the atmosphere, the tests were performed in a controlled-atmosphere room maintained at 77 ± 1° F. and 50 ± 2% relative humidity. In the case of the statically indeterminate beams made of canvas laminate, the temperature was changed to 72 ± 1° F. The canvas laminate test members were placed in this room at least 3 weeks prior to testing. Since the nylon test members would require several months to become moisture conditioned at room temperature, they were moisture conditioned by boiling in a potassium acetate solution (specific gravity = 1.305 at room temperature). Even at the boiling temperature of 119° C., the ¼ in. thickness required 70 to 80 hours for conditioning; this time

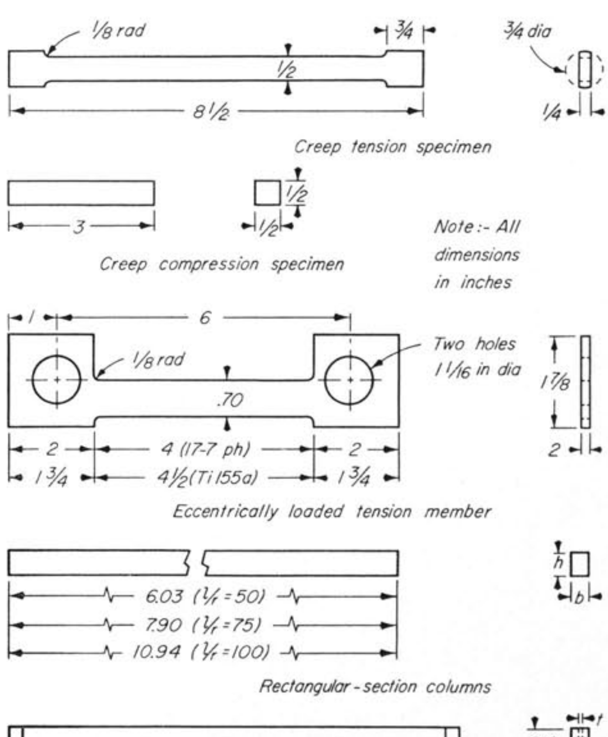

Figure 13. 17-7PH stainless steel and Ti 155A titanium alloy test members

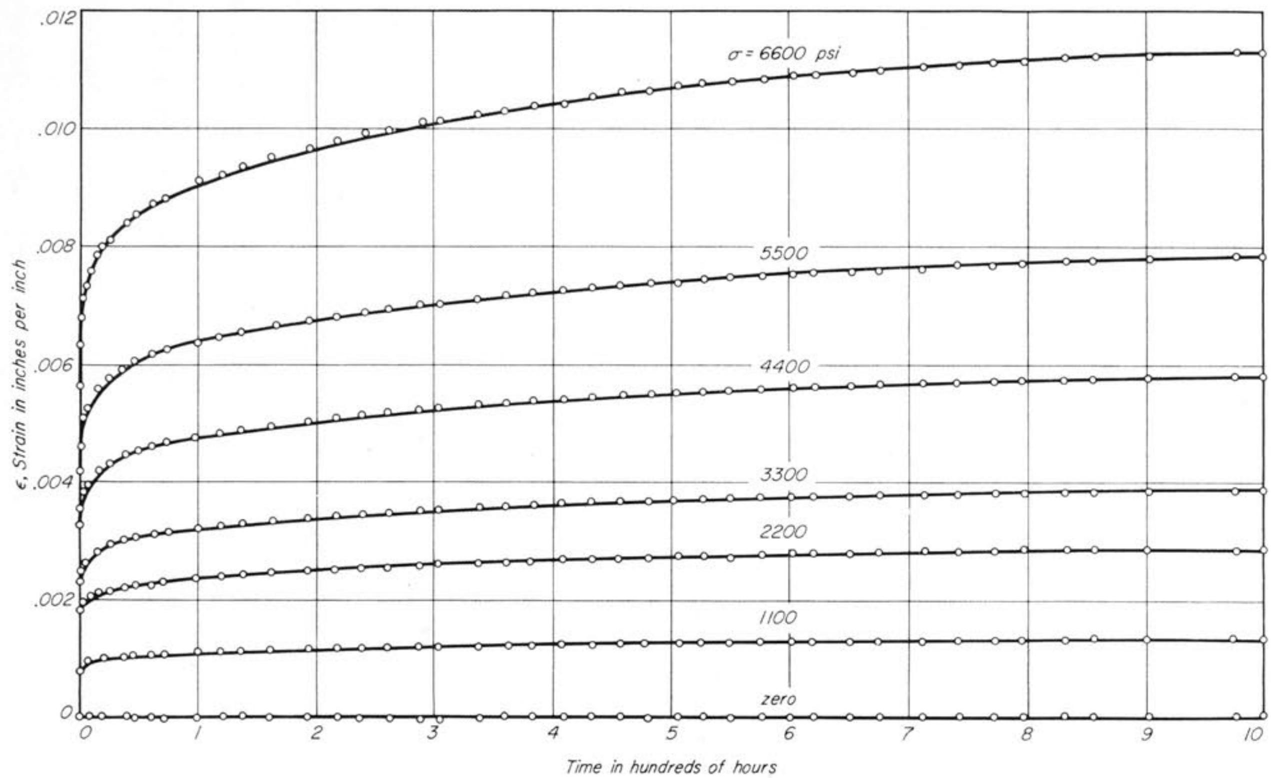

Figure 14. Tension creep curves for canvas laminate

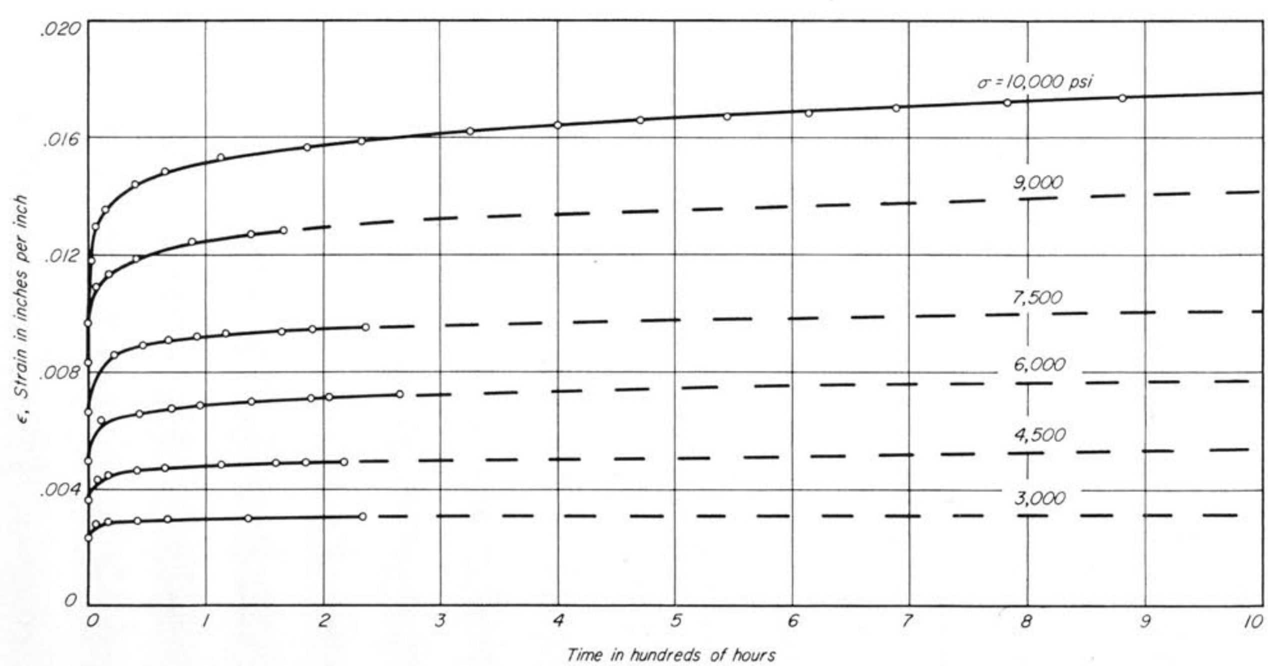

Figure 15. Compression creep curves for canvas laminate

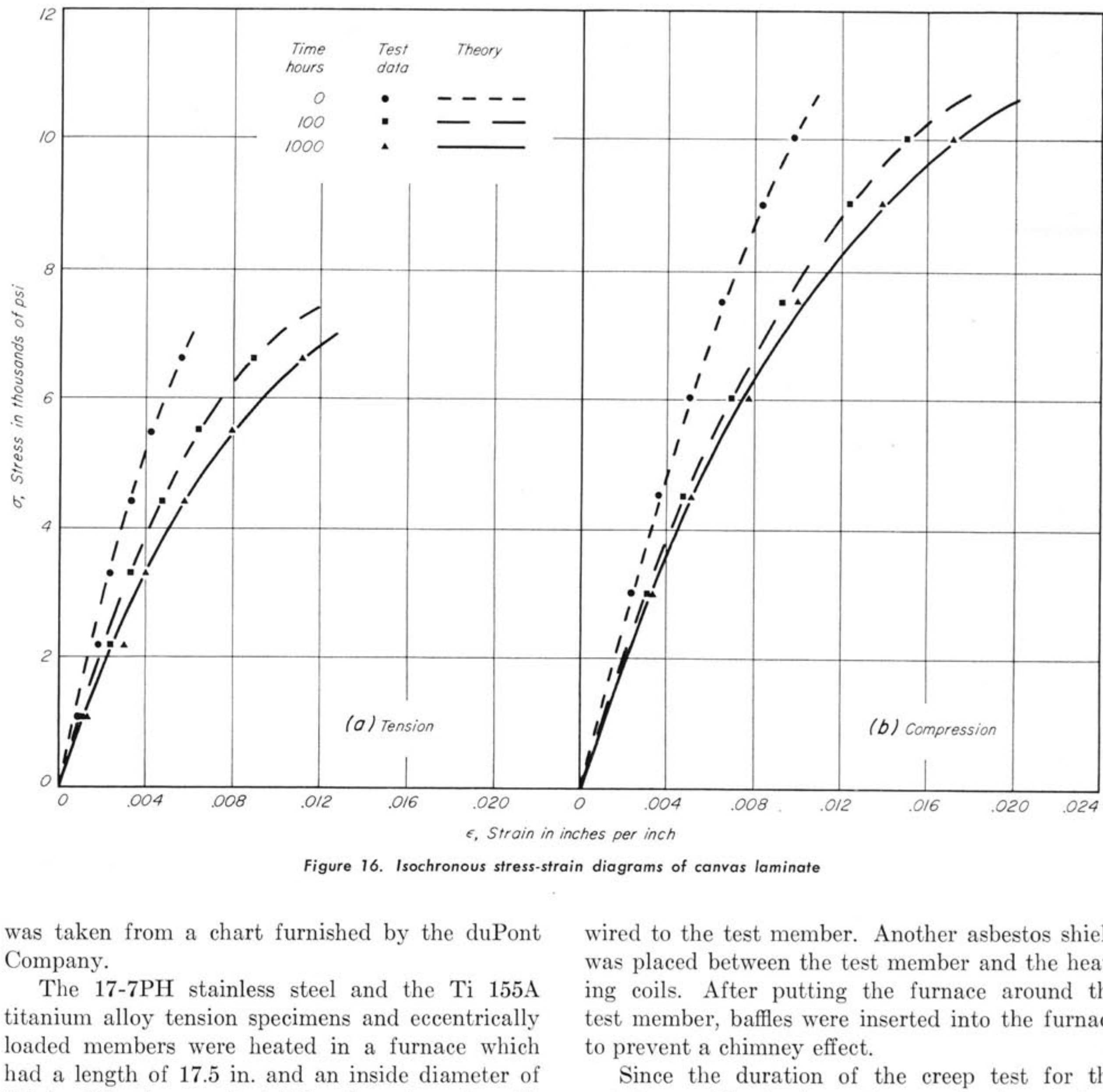

Figure 16. Isochronous stress-strain diagrams of canvas laminate

was taken from a chart furnished by the duPont Company.

The 17-7PH stainless steel and the Ti 155A titanium alloy tension specimens and eccentrically loaded members were heated in a furnace which had a length of 17.5 in. and an inside diameter of 2.5 in. The furnace had 3 heating elements with separate controls. It was made in 2 parts with hinges so that it could be opened. The compression specimens were tested in a furnace which had a length of 12.5 in. and an inside diameter of 2 in. It had 2 heating elements with separate controls and could not be opened.

Two thermocouples were used in measuring the temperature of the tension and compression specimens having a 2 in. gage length. In all other cases the temperature was measured in the center and near each end of the test section. A piece of asbestos was placed over each thermocouple as it was wired to the test member. Another asbestos shield was placed between the test member and the heating coils. After putting the furnace around the test member, baffles were inserted into the furnace to prevent a chimney effect.

Since the duration of the creep test for the metals was 30 min. in most cases, the temperature was manually controlled during the test. The temperature at each thermocouple was maintained at $972 \pm 2°$ F. for the 17-7PH stainless steel test members; each test was started $1\frac{1}{2}$ hours after starting the furnace. For the Ti 155A titanium alloy test members, the temperature was maintained at $772 \pm 2°$ F., and each test began 1 hour after starting the furnace.

Dead loads were applied to the plastic test members either by having the load applied directly to the test member or by having the load applied through a lever having a 14 to 1 or 20 to 1 ratio.

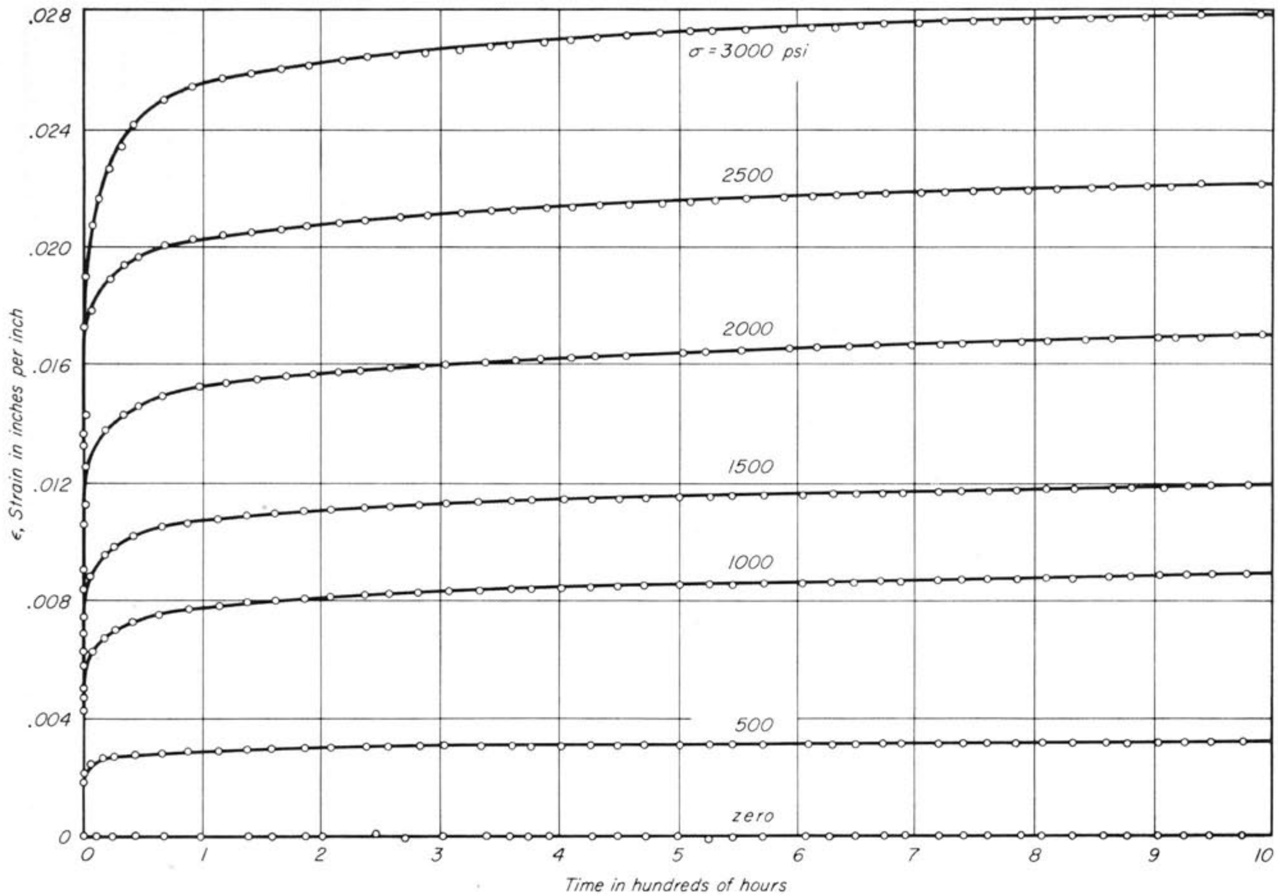

Figure 17. Tension creep curves for Zytel 101 nylon

These loads were first carried by a hydraulic jack and were applied by slowly reducing the oil pressure in the jack. In this way, the load could be applied in a short time without inertia effects. The time for each test was started when the load pan was free of the jack. Several deformation readings were taken the first day and one each day thereafter.

Constant loads were applied to the metal members either by applying dead loads through a 20 to 1 lever or by a Riehle testing machine which was equipped with a load holder to maintain any desired load. Deformation readings were started as soon as the load was applied and were taken every minute thereafter.

C. PROPERTIES OF MATERIALS

1. Properties of the Plastics

As indicated in Figures 11 and 12, the tension specimens were sufficiently long to accommodate an extensometer with a 10 in. gage length. This gage length was used in all cases in which the strain in the first few minutes was less than 1%. For larger strains, an extensometer with a 4 in. gage length was used. In either case, the extensometer had a multiplying lever with a ratio of 10 to 1. The strains were measured by a traveling microscope using a 1/1,000 in. dial. For the compression tests, a 1 in. extensometer with a 1/10,000 in. dial was used in most cases. A 2 in. extensometer was used in a few cases, and the results obtained from the two extensometers were identical.

The strength properties of the canvas laminate were influenced by its environment prior to being placed in the controlled-atmosphere room. It was necessary to put all of the test members for a given investigation into the controlled-atmosphere room at the same time. Compression specimens put in the controlled-atmosphere room at different times were found to have strengths which varied by as much as 8%. After attaining equilibrium condi-

Table 1

Isochronous Stress-Strain Properties of Canvas Laminate and Zytel 101 Nylon

Time	Tension		Compression		Average	
	σ_0	ϵ_0	σ_0	ϵ_0	σ_0	ϵ_0
Canvas Laminate for Straight Beams and Eccentrically Loaded Tension Members						
Zero	5330	0.00355	5170	0.00355	5250	0.00355
100 hr.	3750	0.00320	3560	0.00320	3660	0.00320
1000 hr.	3750	0.00399	3450	0.00399	3600	0.00399
Canvas Laminate for Statically Indeterminate Beams						
Zero	5340	0.00381	5180	0.00381	5260	0.00381
100 hr.	3800	0.00312	3570	0.00312	3570	0.00312
1000 hr.	3700	0.00338	3340	0.00338	3520	0.00338
Canvas Laminate for Columns						
Zero	....	....	8260	0.00636	....	....
100 hr.	....	....	5785	0.00551	....	....
1000 hr.	....	....	5240	0.00524	....	....
Nylon for Straight Beams and Eccentrically Loaded Tension Members						
Zero	3125	0.01157	3125	0.01157	3125	0.01150
100 hr.	2790	0.01990	2790	0.01990	2790	0.01990
1000 hr.	2650	0.02040	2650	0.02040	2650	0.02047

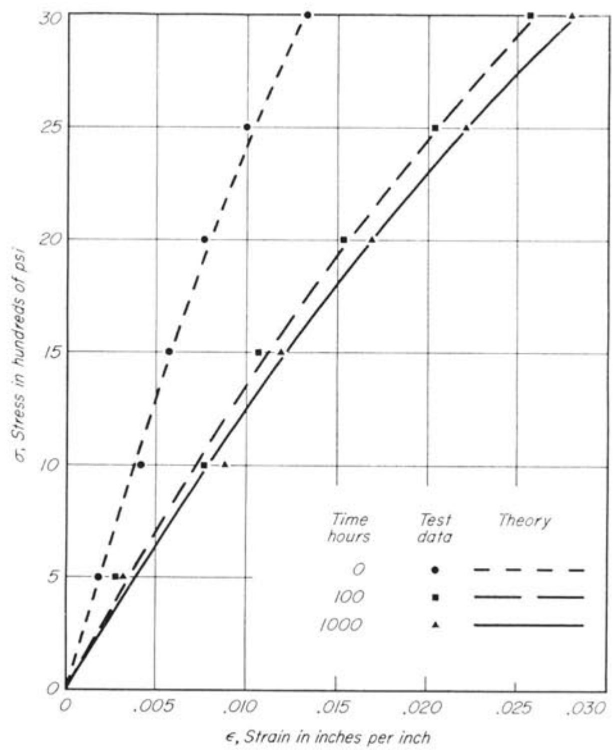

Figure 18. Tension isochronous stress-strain diagrams for Zytel 101 nylon

tions in the controlled-atmosphere room, the properties were found to remain constant, since identical results were obtained from specimens subjected to identical loading conditions but tested several months apart.

Canvas laminate was used in 3 different investigations. The most extensive tension and compression creep data from these investigations are shown in Figures 14 and 15*; however, those specimens were not put in the controlled-atmosphere room at the same time and do not represent the material under identical conditions. Test data obtained from tension and compression specimens tested under identical conditions indicated that the stress in compression had to be 10% greater than that in tension in order to produce the same strain at 1,000 hr.

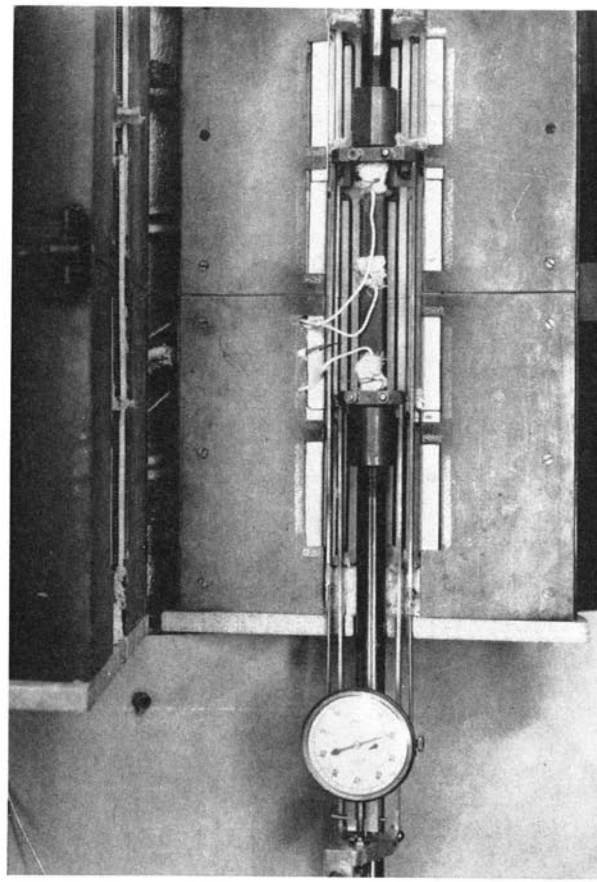

Figure 19. Creep furnace showing 6-in. creep specimen and extensometer

* Only one compression creep machine was available; therefore, most of the compression creep tests were stopped before 1,000 hours. Since the creep data plotted as a straight line on log-log graph paper, the data for 1,000 hours were taken from this plot.

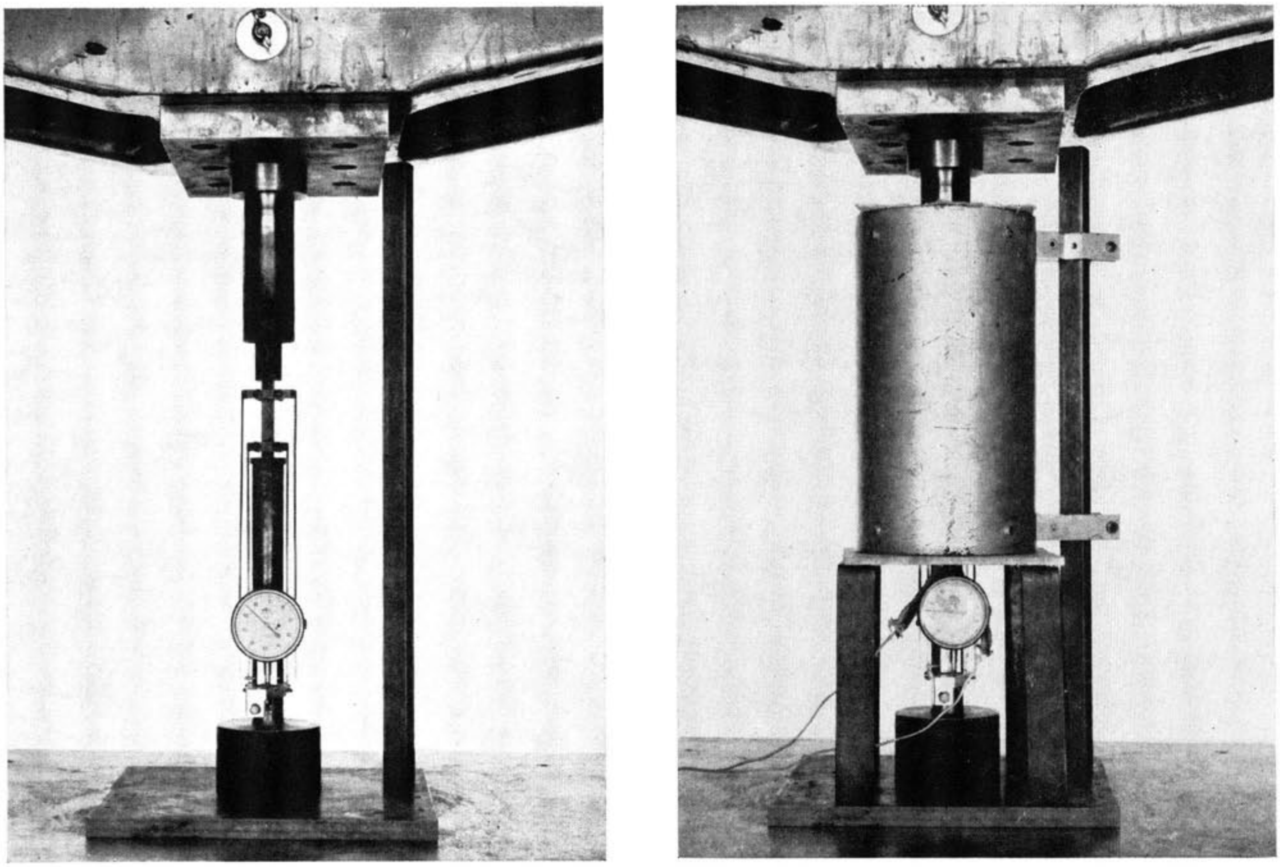

Figure 20. Fixture for testing creep compression specimens at elevated temperatures

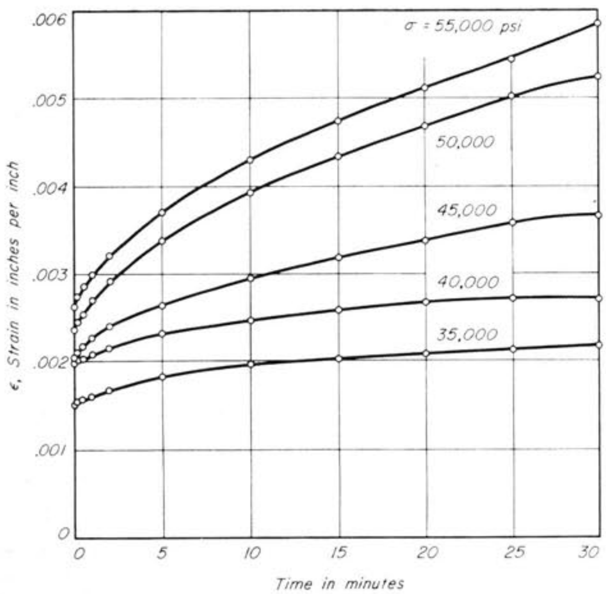

Figure 21. Tension creep curves for 17-7PH stainless steel at 972° F.

Experimental data for isochronous stress-strain diagrams were taken from Figures 14 and 15 for zero time (approximately 30 seconds), 100 hours, and 1,000 hours and are shown in Figure 16. It will be noted that these isochronous stress-strain diagrams have been represented by arc hyperbolic sine curves as given by Equation 3. The correlation between the theoretical curves and the test data is shown to be excellent. The magnitudes of the experimental constants σ_0 and ϵ_0 are shown in Table 1. Only the compression isochronous stress-strain diagrams were used in the column investigation, since the stresses in the columns were predominately compression.

The creep data for the Zytel 101 nylon are shown in Figure 17. From these curves the isochronous stress-strain diagrams for zero time, 100 hours, and 1,000 hours were obtained and are shown in Figure 18. These data were approximated by Equation 3, and the magnitudes of the experimental

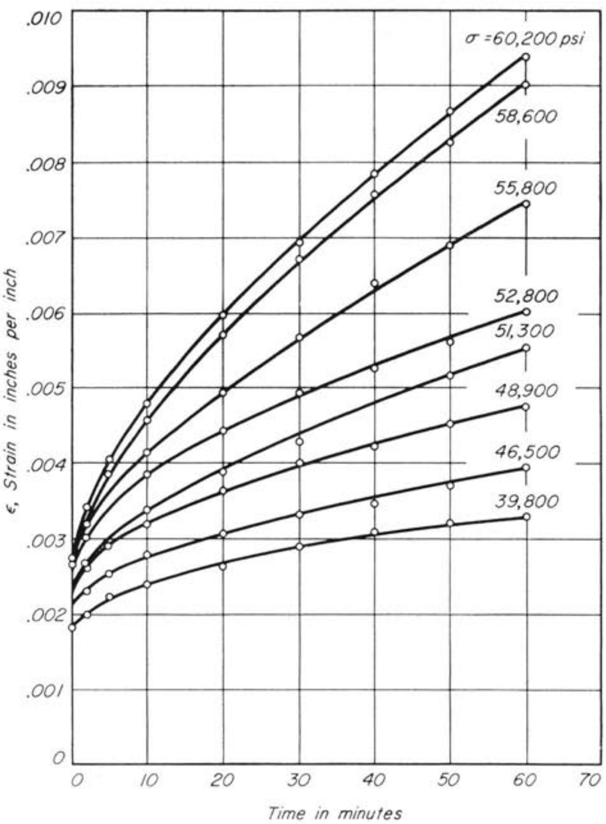

Figure 22. Compression creep curves for 17-7PH stainless steel at 972° F.

constants are shown in Table 1. The constants were assumed to be the same in tension and compression since the creep data from 3 compression specimens were nearly identical with the tension data.

2. Elevated Temperature Properties of Metals

The deformations of tension and compression specimens of 17-7PH stainless steel and Ti 155A titanium alloy were measured with a Riehle dial-type high-temperature creep extensometer with a 2 in. gage length. The extensometer was made to accommodate a flat specimen. The extensometer is shown on a tension specimen in Figure 19 and on a compression specimen in Figure 20. The strains were measured by a 1/10,000 in. dial.

A gage length of 2 in. is not long enough to determine a reliable value of the modulus of elasticity, E. Since this property has a decided influence on the theory, a more accurate value of the modulus of elasticity was needed. The accuracy was obtained in tension by using a 6 in. gage length specimen. In Figure 19 the extensometer is shown adapted to this gage length. The compressive modulus of elasticity was obtained from the eccentrically loaded column tests. All of the 17-7PH stainless steel test members were elastic at zero time and the Ti 155A titanium alloy was elastic at sufficiently high stress levels to obtain reproducible values of the modulus of elasticity.

The tension and compression creep curves for the 17-7PH stainless steel at 972° F. are shown in Figures 21 and 22, respectively. Using data from those curves, the tension and compression isochronous stress-strain diagrams shown in Figure 23 were constructed for zero time, 30 minutes, and for compression, 60 minutes. Since the material was elastic at zero time, all of the data in each case were adjusted to fall on the straight line of slope E. The data for 30 minutes and 60 minutes were closely approximated by an arc hyperbolic sine curve (Eq. 3). The properties which were used in the theory are listed on Figure 23.

Creep curves for the Ti 155A titanium alloy are not shown since the inelastic deformation at 772° F. was mostly time independent, at least for a test duration of 1 hour or less. The tension and compression isochronous stress-strain diagrams for zero time and for 30 minutes are shown in Figure 24. Since most of the inelastic deformation was time independent, the stress-strain diagrams were more accurately approximated by 2 straight lines than by Equation 3. The yield stress was taken as the intersection of the straight lines. Both the modulus of elasticity and the yield stress were lowered a few percent as the result of creep. The pertinent properties are listed in Figure 24. The comparison between the stress-strain data for the material aged at 1,000° F. and 1,085° F. indicates that the lower aging temperature greatly increases the strength.

D. LOADING FIXTURES FOR BEAMS AND ECCENTRICALLY LOADED MEMBERS

Schematic diagrams of the fixtures used in testing the beams subjected to pure bending and the statically indeterminate beams are shown in Figure 25. As indicated in Figure 25a, the load arms were extended so that counterweights could be added to balance the weight of the fixtures and the load pan. The deflection measuring fixture was supported by a spring so that it would not apply a load to the test beam. The deflection was measured over a

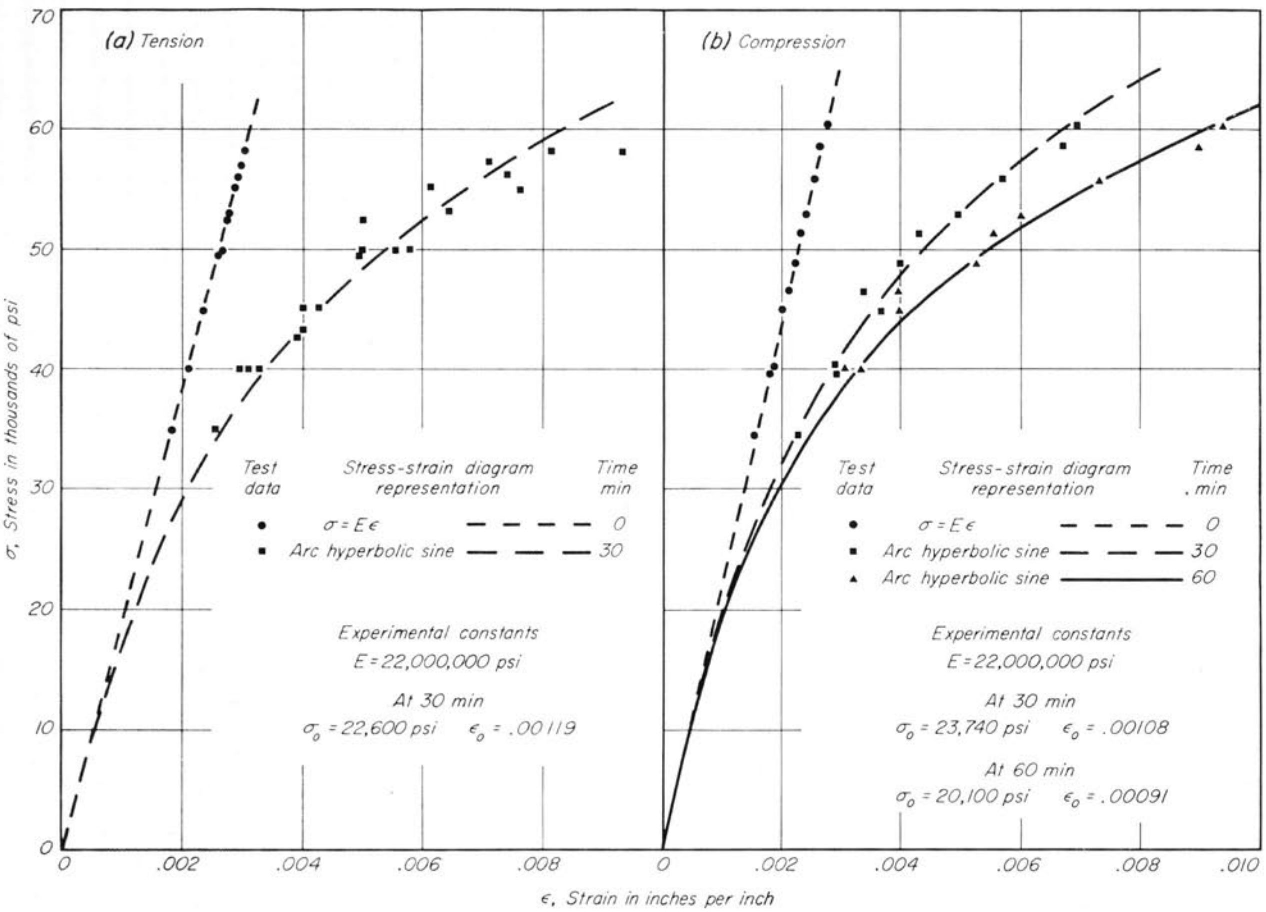

Figure 23. Tension and compression isochronous stress-strain diagrams for 17-7PH stainless steel at 972° F.

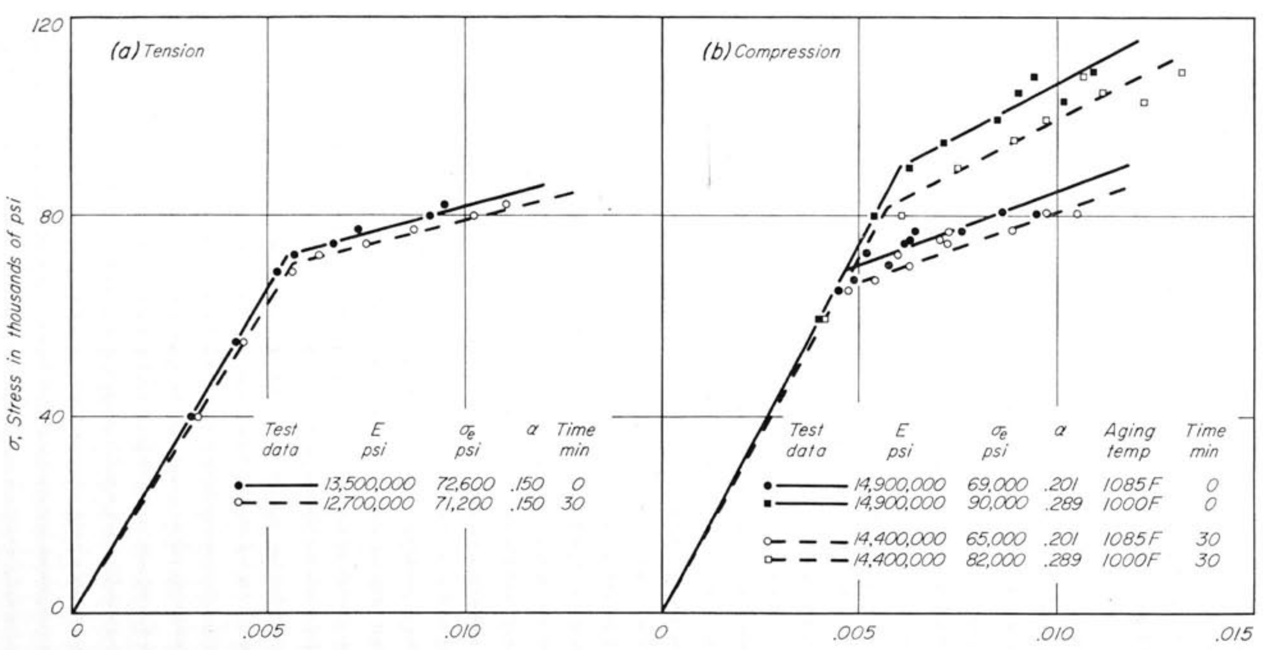

Figure 24. Tension and compression isochronous stress-strain diagrams of Ti 155A titanium alloy at 772° F.

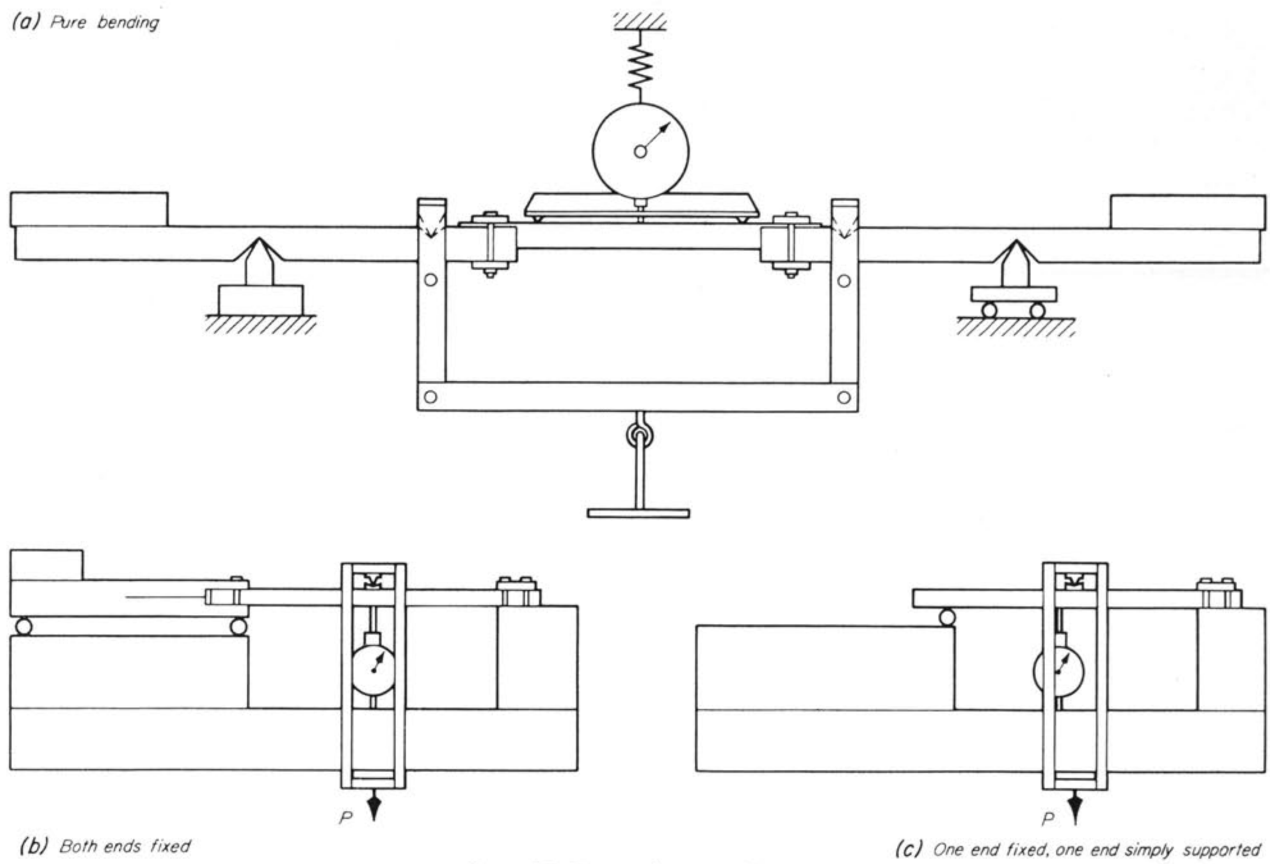

Figure 25. Fixtures for testing beams

6 in. length of the constant moment section of the beam by a 1/1,000 in. dial. The fixed-ended beams were loaded in the fixture shown in Figure 25b; the deflection was measured in the center of the beam by a 1/1,000 in. dial. In Figure 25c is shown the fixture for loading the beams which were fixed at one end and simply supported at the other. The deflection was measured at a distance $l/16$ from the center of the beam by a 1/1,000 in. dial.

The same type of loading fixture was used in loading the plastic and metal eccentrically loaded tension members. The only difference was in the materials used in making the fixtures. A schematic diagram of the fixtures used in the elevated temperature tests is shown in Figure 26. The load, obtained from dead weights, was transmitted to the test member through the yoke, knife edges, and pin arrangement shown. The pin had a 90° groove machined to its center to receive 60° knife edges. The yokes were made of 18 chromium — 8 nickel stainless steel. The knife edges were made of Stellite. A typical setup of the test member in the elevated temperature creep machine is shown in Figure 27.

The method of measuring the central deflection of the eccentrically loaded member is illustrated in Figure 26 and shown in Figure 27. Three ⅛ in. diameter ceramic rods extended through the side of the furnace and contacted each of the yokes and the center of the specimen. After closing the furnace, rubber bands were used to hold the vertical bar against the top and bottom rods, and a 1/1,000 in. dial measured the relative movement of the center rod.

The same type of loading fixture was used in

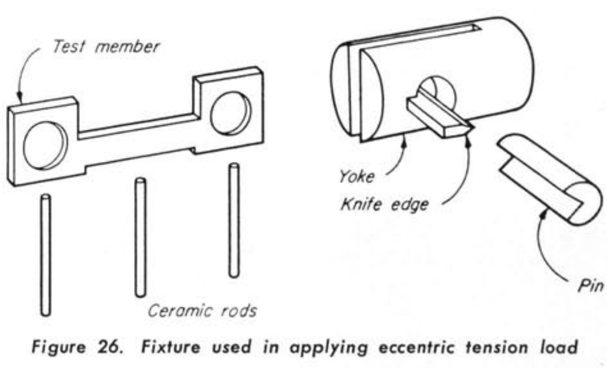

Figure 26. Fixture used in applying eccentric tension load

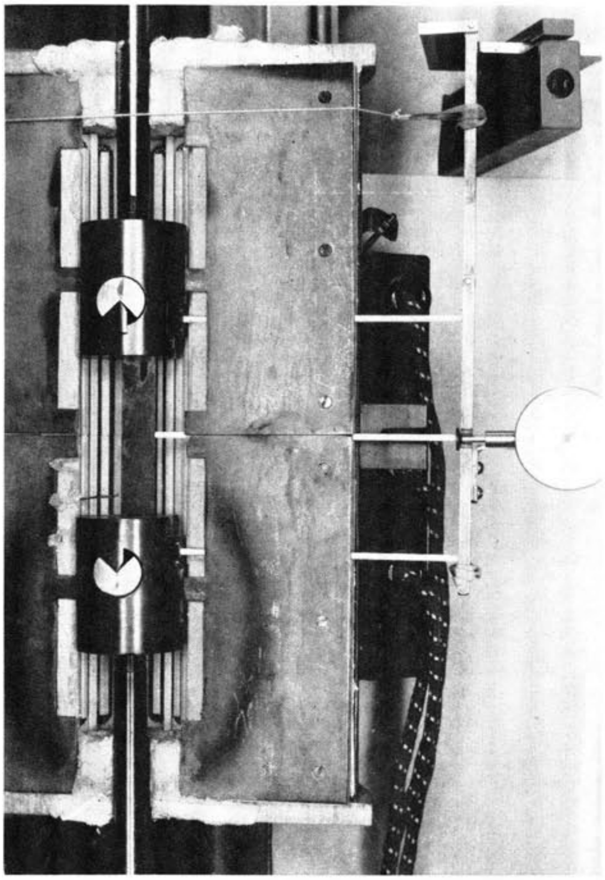

Figure 27. Eccentrically loaded tension member in the elevated temperature creep machine

loading the plastic and metal eccentrically loaded columns. A schematic diagram of the fixtures used in the elevated temperature tests is shown in Figure

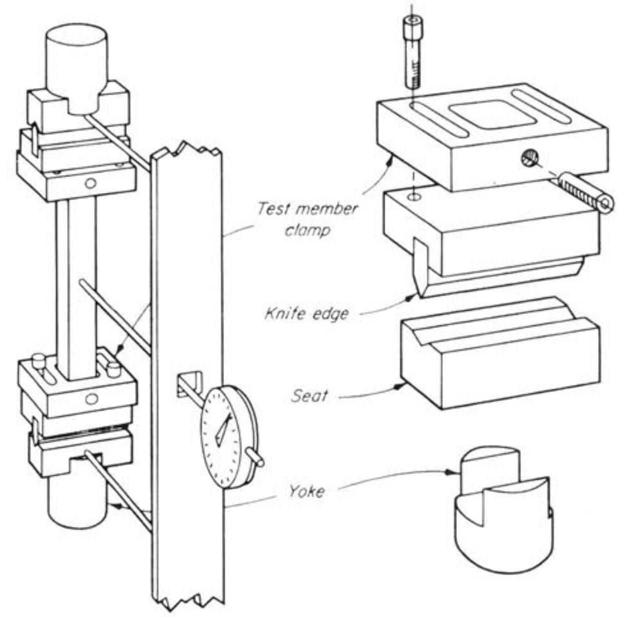

Figure 28. Fixture used in testing eccentrically loaded columns

28. The length of the knife edge was 2 in. The initial eccentricity could be easily adjusted, and the error in setting the initial eccentricity was believed to be less than ± 0.002 in. In order to offset the effect of initial crookedness of the column, the initial eccentricity was adjusted with respect to the center of the column. As indicated in Figure 28, the deflections of the columns were obtained by measuring the movement of the midpoint of the column with respect to the knife edge seats. A 1/1,000 in. dial was used in measuring the deflection.

IV. DISCUSSION OF RESULTS

A. BEAMS

1. Beams Subjected to Pure Bending

A total of 8 beams was subjected to pure bending in the fixture shown in Figure 25a. Four of the beams were made of high-pressure canvas laminate, and 4 were made of Zytel 101 nylon. The cross-sectional dimensions of the rectangular- and T-section beams are shown in Table 2.

The deflection of each beam was measured in the center of a 6 in. gage length (Fig. 25a). The creep curves for the 8 beams are shown in Figure 29. From these curves, moment-deflection data were obtained for zero time, 100 hours, and 1,000 hours; representative data for 4 of the beams are shown in Figures 30 and 31. The theoretical moment-deflection curves were constructed using the stress-strain properties listed in Table 1, the appropriate curve in Figure 4, and Equation 12. As indicated in Article IIA, the theoretical moment was decreased 5% to compensate for the fact that the stress distribution in the beams changes with time. The data, presented in Figures 30 and 31, indicate good agreement between theory and experiment. The ratios of the theoretical to experimental deflections for the beams are shown in Table 2. Since a given error in predicting the deflection results in a smaller percentage error for

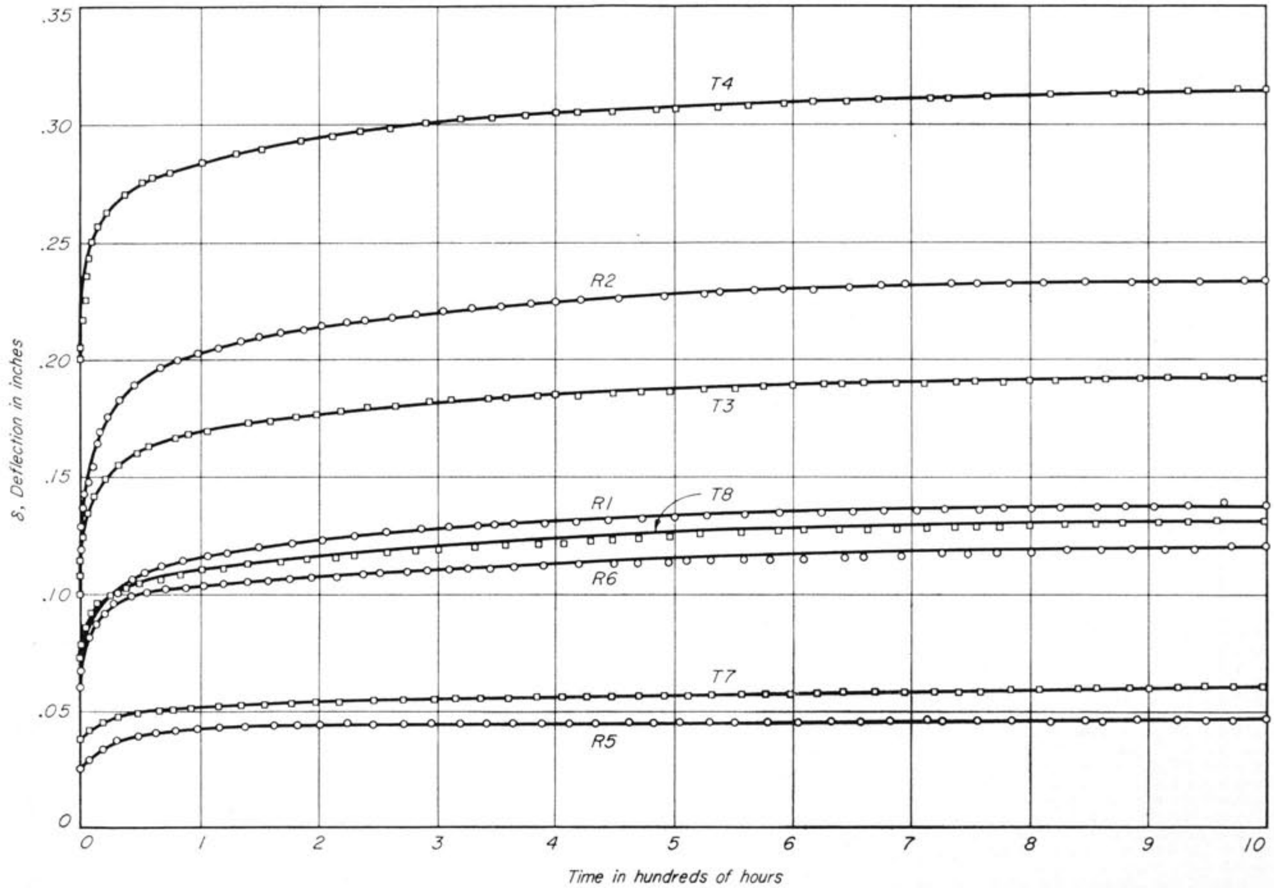

Figure 29. Creep curves for nylon and canvas laminate beams subjected to pure bending

Table 2

Data for Beams Made of Plastics

Beam Number	Width b inch	Depth h inch	Flange Thickness t_2 inch	Web Thickness t inch	Length l inches	Moment pound inches	Load P pounds	Zero Time $\delta_{experimental}$ inch	Zero Time $\frac{\delta_{theoretical}}{\delta_{experimental}}$	100 Hours $\delta_{experimental}$ inch	100 Hours $\frac{\delta_{theoretical}}{\delta_{experimental}}$	1,000 Hours $\delta_{experimental}$ inch	1,000 Hours $\frac{\delta_{theoretical}}{\delta_{experimental}}$
					Zytel 101 Nylon Beams — Pure Bending								
R1[a]	0.248	0.755	....	....	6	35	...	0.060[b]	1.15	0.116	1.15	0.140	1.04
R2	0.248	0.755	....	....	6	55	...	0.103	1.12	0.204	1.08	0.234	1.04
T3	0.496	0.744	0.186	0.124	6	35	...	0.090	0.98	0.170	1.02	0.190	0.99
T4	0.495	0.741	0.185	0.124	6	55	...	0.150	0.94	0.284	1.00	0.314	0.99
					Canvas Laminate Beams — Pure Bending								
R5	0.504	0.752	....	....	6	163	...	0.033	0.90	0.043	0.92	0.048	1.01
R6	0.503	0.752	....	....	6	343	...	0.070	1.01	0.103	1.03	0.120	1.07
T7	0.500	0.750	0.188	0.125	6	80	...	0.039	0.88	0.051	0.91	0.061	0.93
T8	0.500	0.750	0.188	0.125	6	140	...	0.072	0.94	0.109	0.90	0.133	0.94
					Canvas Laminate Beams — Both Ends Fixed								
R9	0.506	0.751	....	....	12	...	180	0.086	0.88	0.107	0.89	0.120	0.92
R10	0.504	0.752	....	....	12	...	233	0.111	0.92	0.141	0.97	0.160	1.00
T11	0.500	0.750	0.187	0.125	12	...	52	0.056	0.86	0.069	0.84	0.078	0.85
T12	0.500	0.750	0.187	0.125	12	...	74	0.083	0.84	0.108	0.82	0.126	0.82
					Canvas Laminate Beams — One End Fixed, Other End Simply Supported								
R13	0.504	0.752	....	....	12	...	120	0.095	0.95	0.117	0.99	0.132	0.98
R14	0.503	0.751	....	....	12	...	160	0.128	0.99	0.163	1.02	0.185	1.06
T15	0.500	0.750	0.187	0.125	12	...	35	0.063	0.95	0.075	0.93	0.085	0.94
T16	0.500	0.750	0.187	0.125	12	...	49	0.091	0.99	0.116	0.91	0.136	0.91

[a] R designates rectangular-section and T designates T-section.
[b] In case of beams subjected to pure bending, the deflection was measured in the center of a 6 inch gage length.

larger strains, the best agreement between theory and experiment was found at 1,000 hours. The theory was conservative by an average of 4% in predicting the deflection of the rectangular-section beams at 1,000 hours and nonconservative by an average of 4% in predicting the deflection of the T-section beams at 1,000 hours.

2. Statically Indeterminate Beams

The statically indeterminate beams were all made of high-pressure canvas laminate. Four beams had fixed ends and were tested in the fixtures shown in Figure 25b. Four beams were fixed at one end and simply supported on the other end by the fixtures shown in Figure 25c. The cross-sectional dimensions of the rectangular- and T-section beams are given in Table 2.

The deflections were measured at the center of the beam in Figure 25b and at a distance of $l/16$ from the center in Figure 25c. The creep curves for the 8 beams are shown in Figure 32. Moment-deflection data for zero time, 100 hours, and 1,000

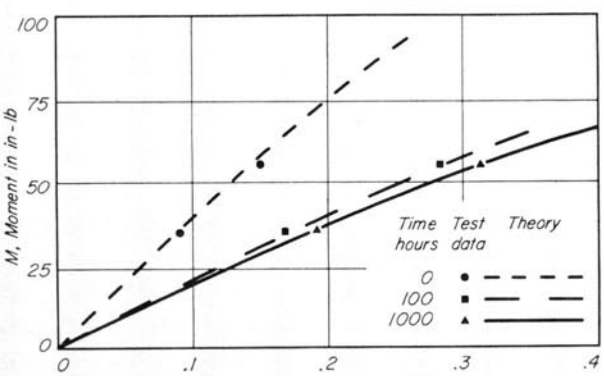

Figure 30. Moment-deflection curves for T-section Zytel 101 nylon beams subjected to pure bending

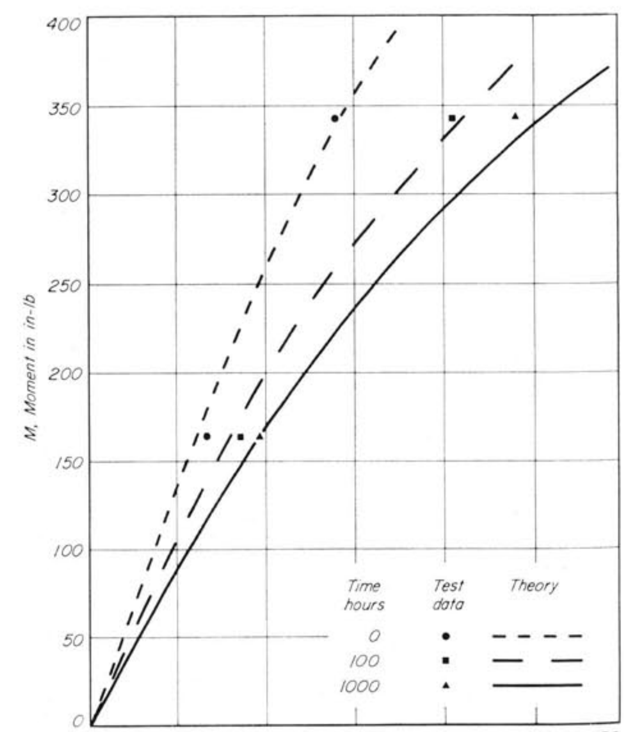

Figure 31. Moment-deflection curves for rectangular-section canvas laminate beams subjected to pure bending

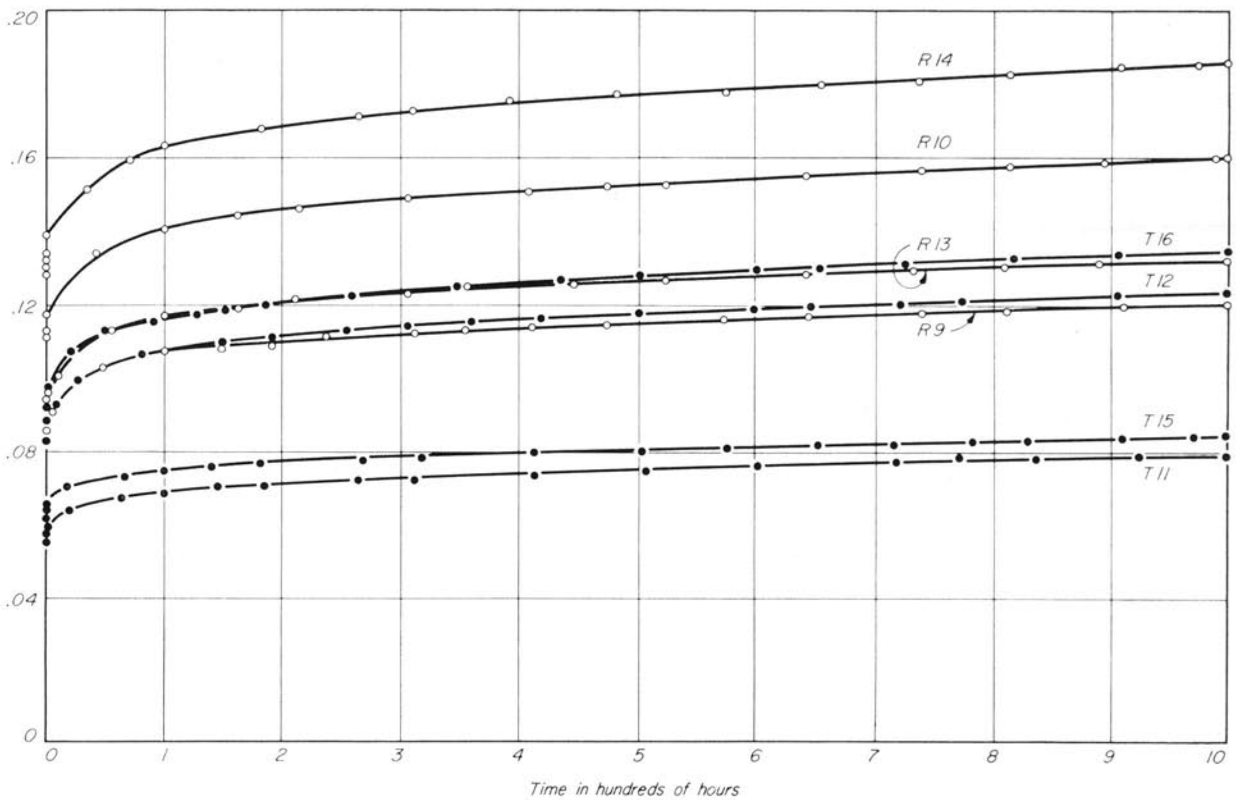

Figure 32. Creep curves for statically indeterminate canvas laminate beams

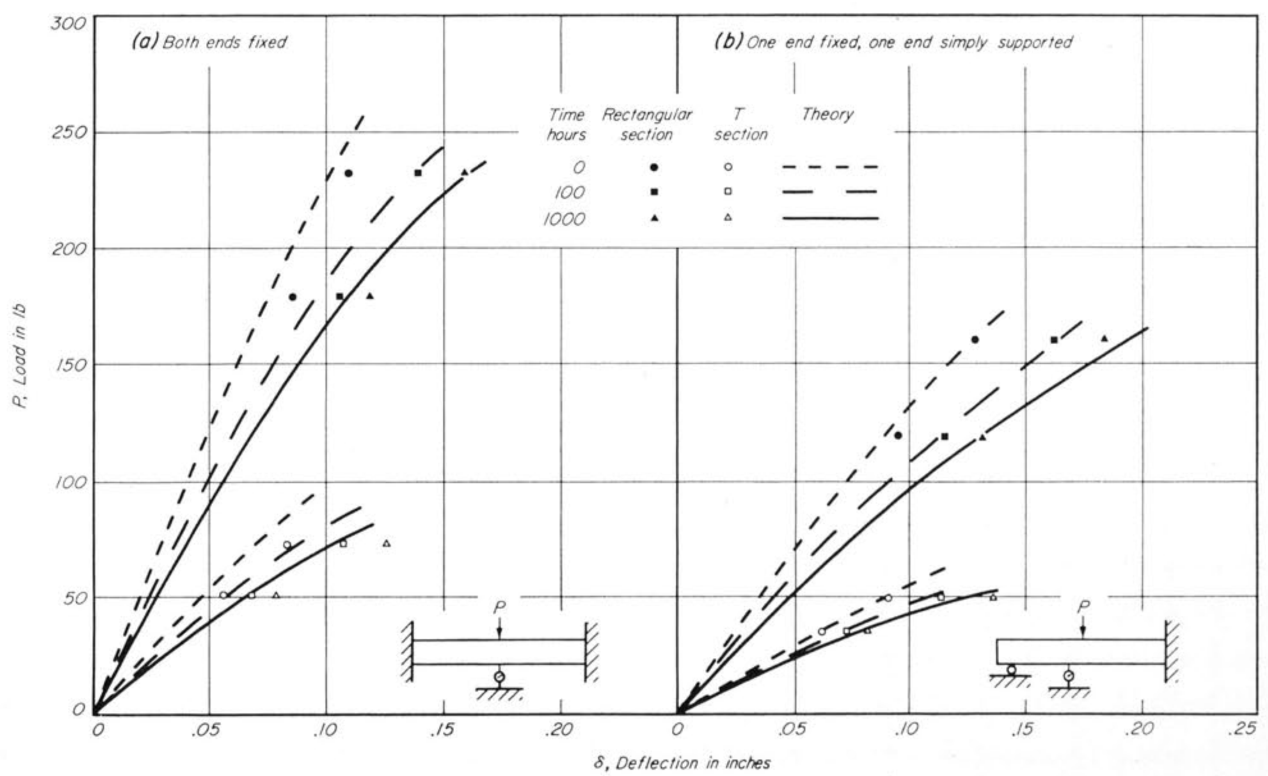

Figure 33. Load-deflection curves for statically indeterminate canvas laminate beams

Table 3

Data for Eccentrically Loaded Tension Members Made of Plastics

Member Number	Width b inch	Depth h inch	Flange Thickness t_2 inch	Web Thickness t inch	Length l inches	Eccentricity e/h %	Load P pound	Zero Time $\delta_{experimental}$ inch	Zero Time $\frac{\delta_{theoretical}}{\delta_{experimental}}$	100 Hours $\delta_{experimental}$ inch	100 Hours $\frac{\delta_{theoretical}}{\delta_{experimental}}$	1,000 Hours $\delta_{experimental}$ inch	1,000 Hours $\frac{\delta_{theoretical}}{\delta_{experimental}}$
							Zytel 101 Nylon						
R17[a]	0.251	0.754	....	....	6	38	80	0.051	0.95	0.084	1.04	0.098	0.95
R18	0.254	0.750	....	....	6	35	140	0.079	0.94	0.128	1.01	0.149	0.91
T19	0.496	0.745	0.186	0.124	6	32	100	0.044	1.04	0.071	1.04	0.082	0.97
T20	0.500	0.750	0.188	0.125	6	32	180	0.068	1.06	0.102	1.08	0.115	0.99
							Canvas Laminate						
R21	0.394	0.746	....	....	6	50	506	0.047	0.92	0.062	0.96	0.069	1.00
R22	0.394	0.745	....	....	6	50	675	0.061	0.98	0.081	1.02	0.094	1.03
T23	0.496	0.745	0.186	0.124	6	34	400	0.045	0.89	0.059	0.88	0.068	0.90
T24	0.496	0.745	0.186	0.124	6	34	575	0.061	0.94	0.084	0.90	0.095	0.95

[a] R designates rectangular-section and T designates T-section.

hours were taken from these curves and plotted in Figure 33. The theoretical moment-deflection curves were constructed using the stress-strain properties listed in Table 1, the appropriate curve in Figure 4, and the numerical integration procedure outlined by Newmark.[23] In the case of the beams fixed at one end and simply supported at the other, a trial and error solution was required since the magnitude of the reaction at the simple support necessary to give zero deflection at the support was not known. It was found that the reaction was only slightly different from that for elastic conditions since the reaction is 0.3125 P for elastic conditions and 0.3127 P for K equal to 2.5.

The theoretical loads in Figure 33 were decreased 5% to compensate for the fact that the stress distribution in the beams changes with time (see Art. IIA). As indicated in Figure 33 and Table 2, the agreement between theory and experiment is good in all cases except for the T-section beams fixed at both ends. In this case the theory was nonconservative by as much as 18%; however, most of this difference was due to the fact that the deflection for zero time was larger than predicted.

B. ECCENTRICALLY LOADED TENSION MEMBERS

1. Nylon and Canvas Laminate

A total of 8 eccentrically loaded tension members were subjected to dead loads in fixtures similar to that shown in Figure 26. The cross-sectional dimensions of the rectangular- and T-section members are given in Table 3. The initial eccentricity, e, of each member is also given in Table 3.

The deflection of each eccentrically loaded member was measured in the center of the 6 in. test length. Load-deflection data for zero time, 100 hours, and 1,000 hours are given in Table 3 for each member, and representative curves are shown in Figures 34 and 35.

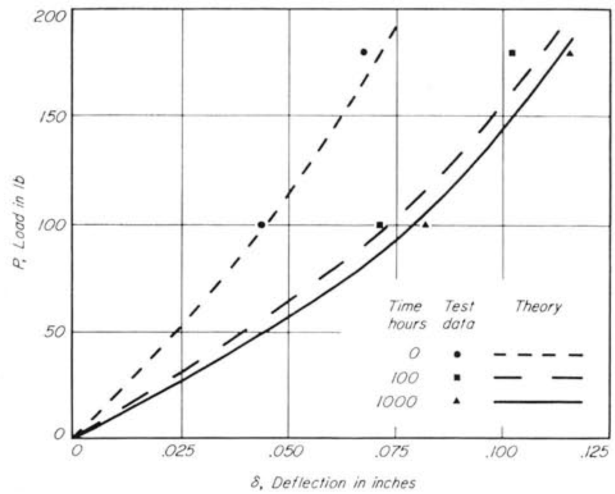

Figure 34. Load-deflection curves for eccentrically loaded tension members of Zytel 101 nylon

The theoretical load-deflection curves in Figures 34 and 35 were constructed using the stress-strain properties listed in Table 1, Equation 14, and Figures 5 through 8. Two different corrections were used in adjusting the theory which resulted in the theoretical curves in Figures 34 and 35 being lowered 5%. First, each theoretical load was decreased 10% to compensate for the fact that the stress distribution in the eccentrically loaded members changes with time (see Art. IIA). Second, each theoretical load was increased 5% to compensate for the fact that 0.75 in. at each end of the 6 in. test length was stiffened* (Figs. 11 and 12). A comparison between the theoretical and experimental deflections in Figures 34 and 35 and Table 3, indicates good agreement between theory and experiment.

* If the member is assumed to deflect into a segment of a circle, the deflection is reduced 6% if 0.75 in. at each end of a 6 in. length has infinite stiffness. The deflection is reduced 11% if 1 in. at each end has infinite stiffness (See Fig. 13 for 17-7PH stainless steel). Since the load-deflection curves were nearly linear, the correction was made on the load rather than on the deflection.

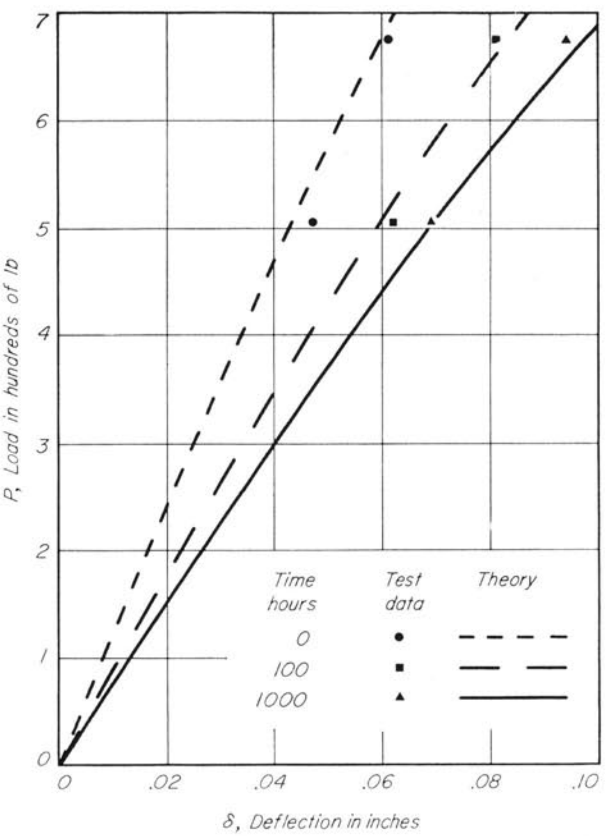

Figure 35. Load-deflection curves for eccentrically loaded rectangular-section tension members of canvas laminate

2. 17-7PH Stainless Steel at 972° F.

A total of 10 eccentrically loaded tension members were subjected to dead loads in the fixture shown in Figure 26. The cross-sectional dimensions of the rectangular- and T-section members are given in Table 4 along with the test length and initial eccentricity. Also given in Table 4 are the load and deflection data for zero time and for 30 minutes. The data for the T-section members are shown in Figure 36. The theoretical load-deflection curves in Figure 36 for zero time were obtained using the stress-strain properties listed in Figure 23 and Equation 19. The curves for 30 minutes were constructed using Equation 14 and Figures 6 and 8. Since the members were elastic at zero time, the theoretical load for zero time was increased 10% to account for the fact that 1 in. at each end of the 6 in. test length was enlarged. The theory was not corrected for 30 minutes since the 2 corrections balanced each other. A comparison between the theoretical and experimental deflections in Figure 26 and Table 4 indicates good agreement between theory and experiment.

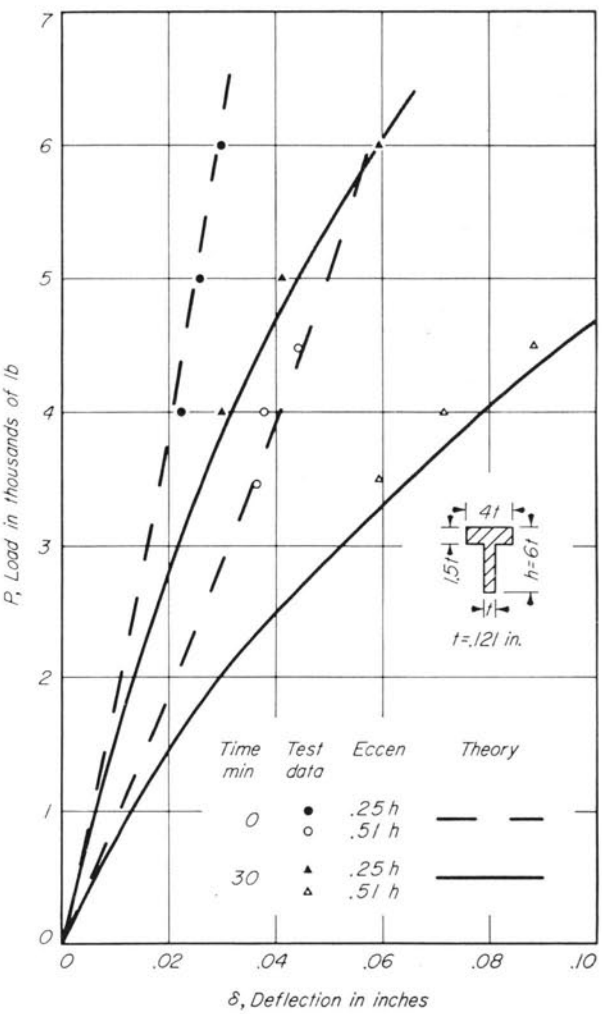

Figure 36. Load-deflection curves for eccentrically loaded tension members of 17-7PH stainless steel

3. Ti 155 Titanium Alloy at 772° F.

Tests were run on 3 eccentrically loaded tension members. The cross-sectional dimensions of the rectangular-section members are shown in Table 4. The members had a length of 6 in. and an initial eccentricity of 50% of their depths. The load-deflection data for these members are given in Table 4 for zero time and for 30 minutes. Since the stress-strain diagrams of this material were represented by 2 straight lines (Fig. 24a), the interaction curve — moment-load curve theory was used in the analysis of the test data as indicated in Figure 37.

The interaction curves shown in Figure 37 were constructed using the stress-strain properties listed in Figure 24a and Equations 21 and 22. The theoretical moment-load curves were constructed using Equation 25. The theoretical deflections used in

Table 4

Data for Eccentrically Loaded Tension Members Made of Metals

Member Number	Width b inch	Depth h inch	Flange Thickness t_2 inch	Web Thickness t inch	Length l inches	Eccentricity e/h %	Load P pounds	Zero Time $\delta_{experimental}$ inch	Zero Time $\frac{\delta_{theoretical}}{\delta_{experimental}}$	30 Minutes $\delta_{experimental}$ inch	30 Minutes $\frac{\delta_{theoretical}}{\delta_{experimental}}$
					17-7PH Stainless Steel						
R25[a]	0.255	0.754	....	....	6	47	5000	0.037	1.03	0.080	0.96
R26	0.255	0.754	....	....	6	47	4000	0.033	0.94	0.057	0.96
R27	0.254	0.755	....	....	6	47	3500	0.029	0.95	0.047	0.95
R28	0.255	0.754	....	....	6	47	3000	0.026	0.92	0.037	0.97
T29	0.484	0.726	0.181	0.121	6	25	6000	0.029	1.00	0.059	1.00
T30	0.484	0.726	0.181	0.121	6	25	5000	0.025	1.00	0.041	1.08
T31	0.484	0.726	0.181	0.121	6	25	4000	0.021	1.05	0.030	1.06
T32	0.487	0.730	0.182	0.122	6	51	4500	0.044	1.03	0.088	1.07
T33	0.487	0.730	0.182	0.122	6	51	4000	0.038	1.06	0.071	1.11
T34	0.487	0.730	0.182	0.122	6	51	3500	0.036	1.00	0.059	1.10
					Ti 155A Titanium Alloy						
R35	0.201	0.700	....	....	6	50	6006	0.138	0.96	0.151	0.93
R36	0.201	0.702	....	....	6	50	5541	0.118	0.93	0.128	0.90
R37	0.200	0.699	....	....	6	50	3984	0.076	0.91	0.080	0.91

[a] R designates rectangular-section and T designates T-section.

the calculations of Table 4 were obtained using Equation 27. The theory was nonconservative by about 9% in predicting the deflection.

C. ECCENTRICALLY LOADED COLUMNS

1. Columns Made of Canvas Laminate

A total of 27 eccentrically loaded columns were subjected to dead loads in fixtures similar to that shown in Figure 28. These columns are listed in Table 5. All but 4 of the columns had rectangular sections with a depth of 0.700 in. and a width of approximately ½ in. The T-section columns had a depth of 0.730 in., a width of 0.487 in., a flange thickness of 0.183 in. and a web thickness of 0.122 in. These columns had slenderness ratios of 30, 50, and 70 and had initial eccentricities of 2%, 5%, and 25% of their depths.

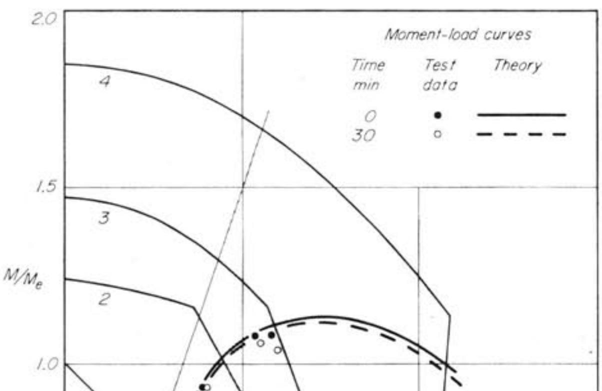

Figure 37. Moment-load curves for Ti 155A titanium alloy tension members having an initial eccentricity of 50% of the depth

The deflection-time creep curves are shown in Figures 38 and 39 for rectangular- and T-section columns, respectively. From these curves experimental P/A-deflection data were obtained for zero time, 100 hours, and 1,000 hours. Representative data are shown in Figure 40 for the rectangular-section columns having a slenderness ratio of 30 and initial eccentricities of 5% and 25% of their depths and in Figure 41 for the T-section columns. Three different theoretical P/A-deflection curves are shown in these figures. The curves based on the arc hyperbolic sine theory for column configurations of segment of circle and cosine curve were constructed using the properties listed in Table 1, Equations 14 and 15, and Figures 5 through 8. The curves based on the modified secant formula were constructed using Equation 20.

The theoretical collapse loads for the columns were obtained from the arc hyperbolic sine theory for cosine curve configuration of the deflected column. As indicated in Article IIA, the load for each point on these curves was increased 10% to compensate for the fact that the stress distribution in the columns changes with time. Comparison between the theoretical and experimental collapse loads can best be accomplished by means of the tabular form as indicated in Table 5. The experimental values of the average stress, P/A, in the

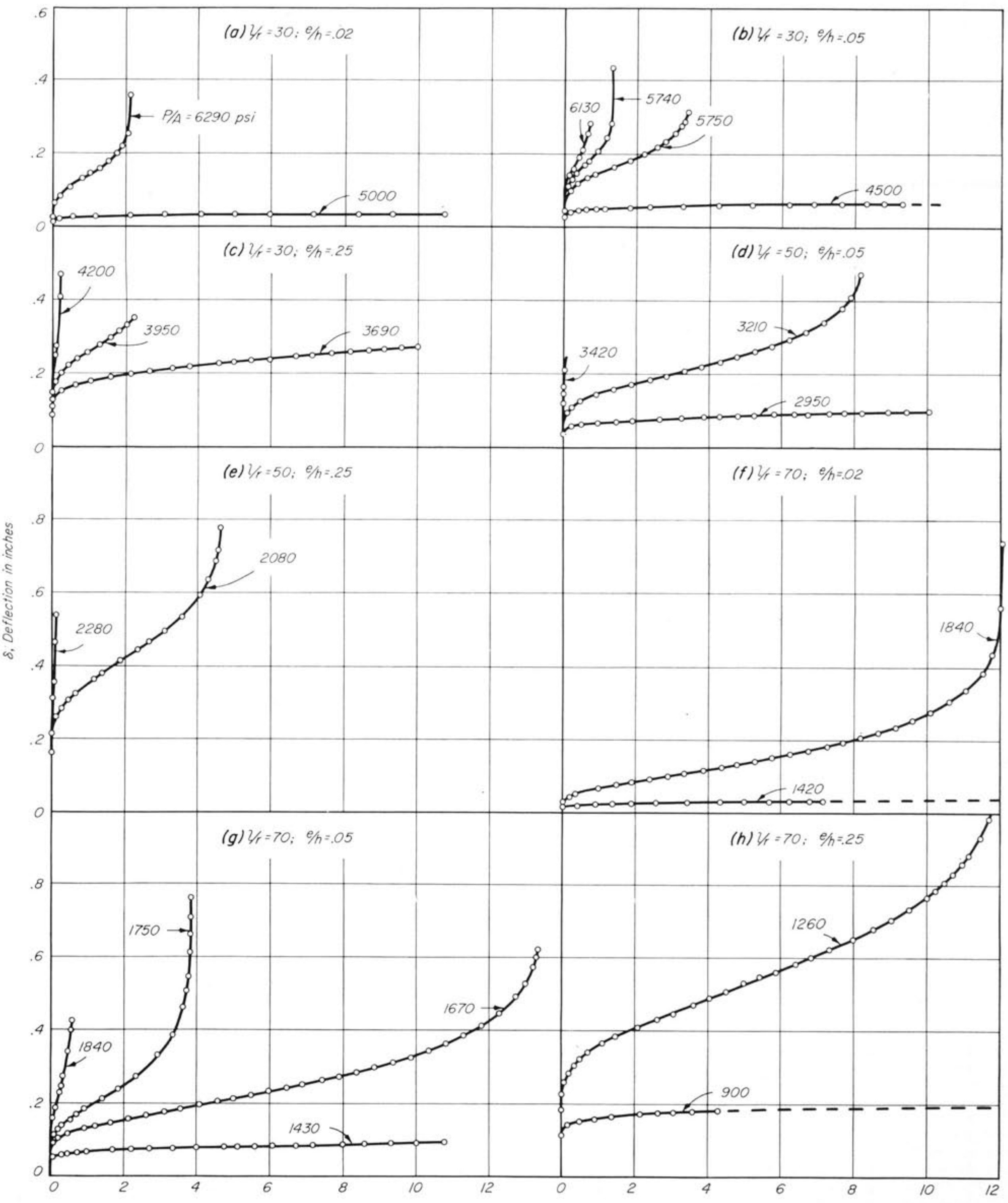

Figure 38. Deflection-time curves for rectangular-section columns of canvas laminate

Table 5

Collapse Load Data for Eccentrically Loaded Columns Made of Canvas Laminate

1 Column Number	2 Depth h inch	3 l/r	4 e/h %	5 Time Hours	6 Experimental P/A Actual psi	7 Experimental P/A Adjusted to 1,000 Hours psi	8 Theoretical P/A at 1,000 Hours Arc hyperbolic sine psi	9 Theoretical P/A at 1,000 Hours Adjusted tangent modulus psi	$\frac{7}{8}$	$\frac{7}{9}$
R38[b]	0.700	30.0	2	212	6290	5980	6270	6230	0.95	0.96
R39	0.700	30.0	2	1000[a]	5000	....	6270	6230	....	....
R40	0.700	50.0	2	38	3420	3140	3230	3300	0.97	0.95
R41	0.700	70.0	2	1208	1840	1860	1930	1900	0.97	0.98
R42	0.700	70.0	2	1000[a]	1420	....	1930	1900	....	....
R43	0.700	30.0	5	76	6130	5650	5780	5660	0.98	1.00
R44	0.701	30.0	5	136	5740	5400	5780	5660	0.94	0.95
R45	0.700	30.0	5	343	5750	5650	5780	5660	0.98	1.00
R46	0.700	30.0	5	1000[a]	4500	....	5780	5660	....	....
R47	0.699	50.0	5	18	3210	2900	2990	3000	0.97	0.97
R48	0.700	50.0	5	820	3010	3000	2990	3000	1.00	1.00
R49	0.700	50.0	5	1000[a]	2950	....	2990	3000	....	....
R50	0.700	70.0	5	60	1840	1710	1760	1720	0.97	0.99
R51	0.701	70.0	5	385	1750	1710	1760	1720	0.97	0.99
R52	0.700	70.0	5	1335	1670	1670	1760	1720	0.95	0.97
R53	0.700	70.0	5	1000[a]	1430	....	1760	1720	....	....
T54	0.730	50.2	5	6	3390	2950	3160	2970	0.93	0.99
T55	0.730	50.2	5	152	3090	2940	3160	2970	0.93	0.99
T56	0.730	50.2	5	790	2950	2920	3160	2970	0.92	0.98
T57	0.730	50.2	5	1000[a]	2150	....	3160	2970	....	....
R58	0.701	30.0	25	20	4200	3680	3870	3830	0.95	0.96
R59	0.701	30.0	25	240	3950	3760	3870	3830	0.97	0.98
R60	0.700	30.0	25	1000[a]	3690	....	3870	3830	....	....
R61	0.700	50.0	25	13	2280	2020	2150	2030	0.94	1.00
R62	0.700	50.0	25	465	2080	2050	2150	2030	0.96	1.01
R63	0.702	70.0	25	1185	1260	1270	1330	1170	0.95	1.09
R64	0.700	70.0	25	1000[a]	900	....	1330	1170	....	....

[a] Test was terminated at 1,000 hr. since the load was appreciably below the collapse load.
[b] R designates rectangular-section and T designates T-section.

columns resulted in 19 of the 27 columns buckling in time intervals ranging from 6 to 1,335 hours. The theoretical values of P/A necessary to produce buckling in 1,000 hours are listed in Table 5. Theoretical values of P/A necessary to produce buckling for other time intervals were also calculated in order to determine the effect of time to collapse on the collapse load. It was assumed that the effect of time to collapse was the same for the experimental as for the theoretical collapse load; in this way the experimental value of P/A necessary to cause each column to collapse in 1,000 hours was computed and is listed in Table 5.

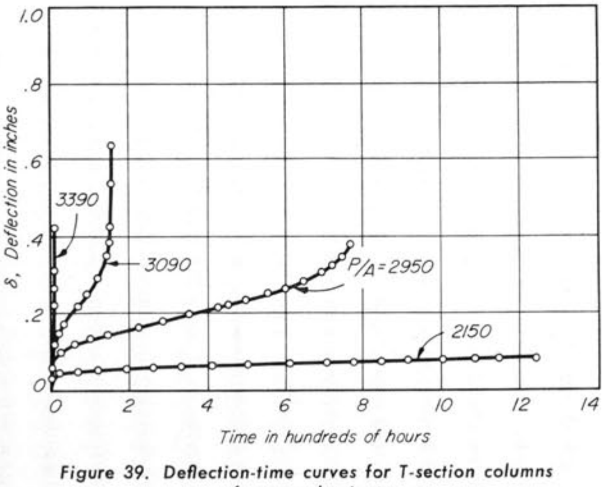

Figure 39. Deflection-time curves for T-section columns of canvas laminate

The ratios of the experimental to theoretical collapse load for 1,000 hours are listed in Table 5. The theory was nonconservative by an average of 4%. It should be noted that these data indicate little influence of either slenderness ratio, initial eccentricity, cross-sectional shape, or time to collapse. The agreement between theory and experiment is considered to be excellent; however, considerable work is required in making the theoretical analysis. To greatly reduce the number of computations, it was suggested in Article IIC that the modified secant formula (Eq. 20) be used in predicting the collapse load. Using Equation 20 and the correction coefficients in Figure 10, the theoretical collapse loads for 1,000 hours were computed, and the ratios of the experimental collapse loads to these loads are listed in Table 5. The theory based on the modified secant formula was nonconservative by an average of 2%. In case the tangent modulus load is obtained for ϵ_1/ϵ_0 less than 0.5, the column approaches an Euler column, and the collapse load is less influenced by the initial eccentricity of the column. This explains why the theory was conservative by 9% for column R63.

In addition to being able to calculate the collapse load for an eccentrically loaded column, it may also be desirable to calculate the deflection of the column for the design load. The creep deflection curves shown in Figures 38 and 39 indicate that small differences in load result in a large difference

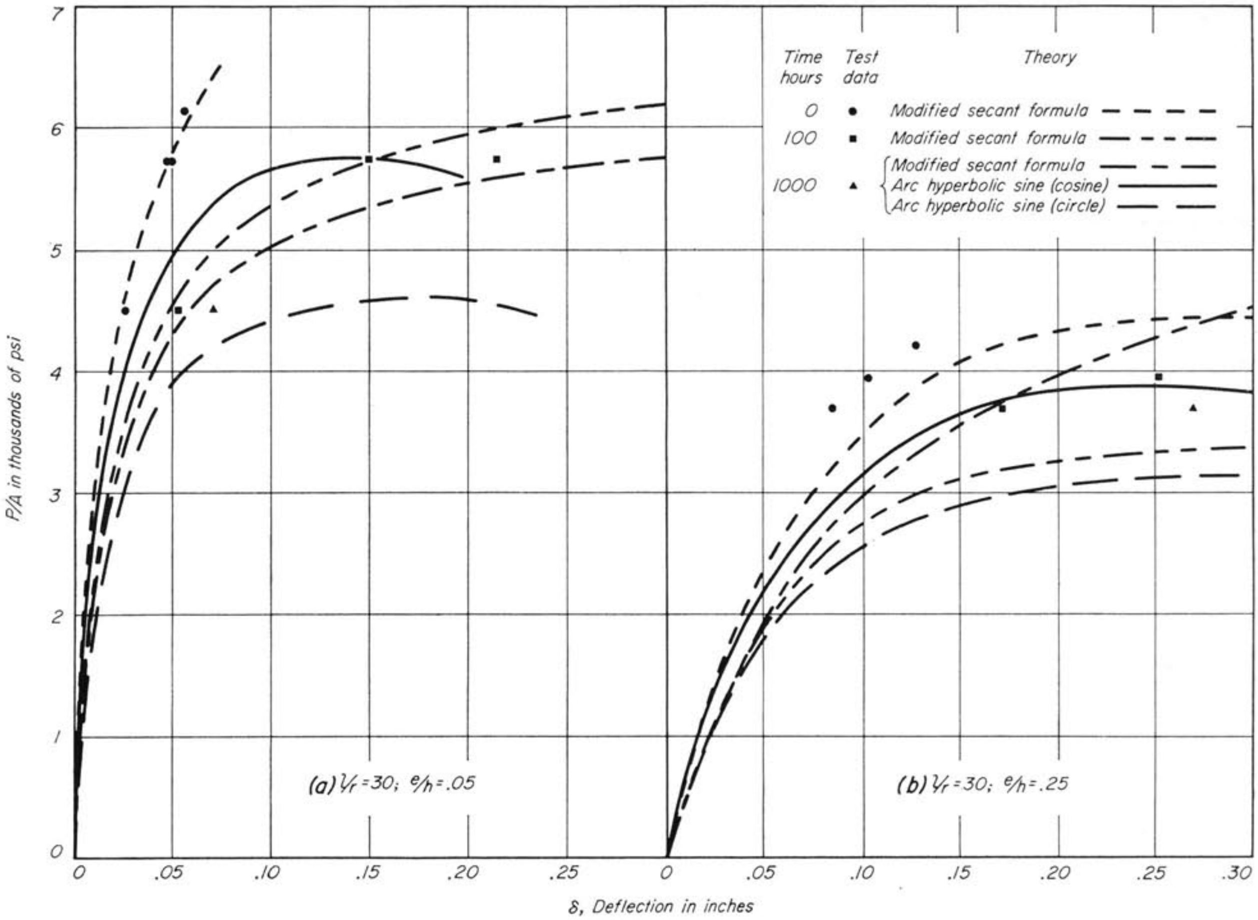

Figure 40. P/A-deflection curves for rectangular-section columns of canvas laminate

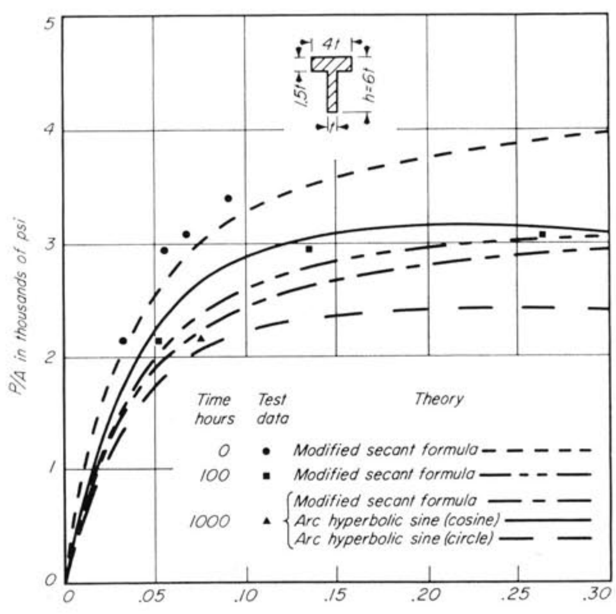

Figure 41. P/A-deflection curves for T-section columns of canvas laminate, l/r = 50.2

in deflection, particularly for loads in the neighborhood of the collapse load.

Although the arc hyperbolic sine theory for a cosine curve assumption of the deflected axis of the column was used in predicting the collapse load, this theory is not recommended for calculating the deflection, since the resulting deflection is non-conservative in most cases. The arc hyperbolic sine theory based on the assumption that the deflected axis of the column is a segment of a circle should give a conservative estimate of the deflection in all cases. P/A-deflection curves based on the latter theory are shown in Figures 40 and 41. This theory was used in predicting the deflection of columns subjected to initial eccentricities of 25% of their depths; however, the theory was too conservative for predicting the deflection of columns having initial eccentricities of 2% and 5% of their depths. The modified secant formula (Eq. 20) was used in predicting the deflection of columns subjected to the smaller eccentricities.

Table 6

Deflection Data for Eccentrically Loaded Columns Made of Canvas Laminate

Column Number	Depth h inch	l/r	e/h %	Experimental δ For zero time inch	Experimental δ For 100 hours inch	Experimental δ For 1,000 hours inch	$\delta_{experimental}/{}^{a}\delta_{theoretical}$ For zero time	$\delta_{experimental}/{}^{a}\delta_{theoretical}$ For 100 hours	$\delta_{experimental}/{}^{a}\delta_{theoretical}$ For 1,000 hours
R39	0.700	30.0	2	0.010	0.025	0.037	0.83	0.93	0.97
R42	0.700	70.0	2	0.011	0.024	0.029	0.50	0.63	0.62
R46	0.700	30.0	5	0.027	0.052	0.071	1.12	1.11	1.25
R49	0.700	50.0	5	0.034	0.065	0.096	0.94	1.02	1.43
R53	0.700	70.0	5	0.038	0.066	0.093	0.69	0.60	0.72
T57	0.730	50.2	5	0.031	0.053	0.077	0.89	0.95	1.17
R60	0.700	30.0	25	0.087	0.175	0.274	....	....	....
R64	0.700	70.0	25	0.111	0.160	0.215	0.82	0.78	0.90

[a] For e/h of 2 and 5%, the theoretical deflections were based on the modified secant formula. For e/h of 25%, the theoretical deflections were based on the arc hyperbolic sine theory for segment of circle configuration of deflected axis of column.

For comparative purposes, the actual deflection and the ratio of the actual to the theoretical deflection are presented in Table 6 for the columns whose loads were sufficiently low that they did not collapse. The agreement between the theoretical and experimental deflection was poor. It is believed that the large difference between theory and experiment was due to the fact that the test loads were approximately 0.8 of the collapse load. Better agreement would have been expected at lower loads.

2. Columns Made of 17-7PH Stainless Steel

A total of 29 eccentrically loaded columns was subjected to constant loads at 972° F. in the fixture shown in Figure 28. These columns are listed in Table 7. All but 4 of these columns had rectangular sections and slenderness ratios of 50, 75, and 100. The T-section columns had a slenderness ratio of 60, a depth of 0.604 in., a width of 0.403 in., a flange thickness of 0.152 in., and a web thickness of 0.101

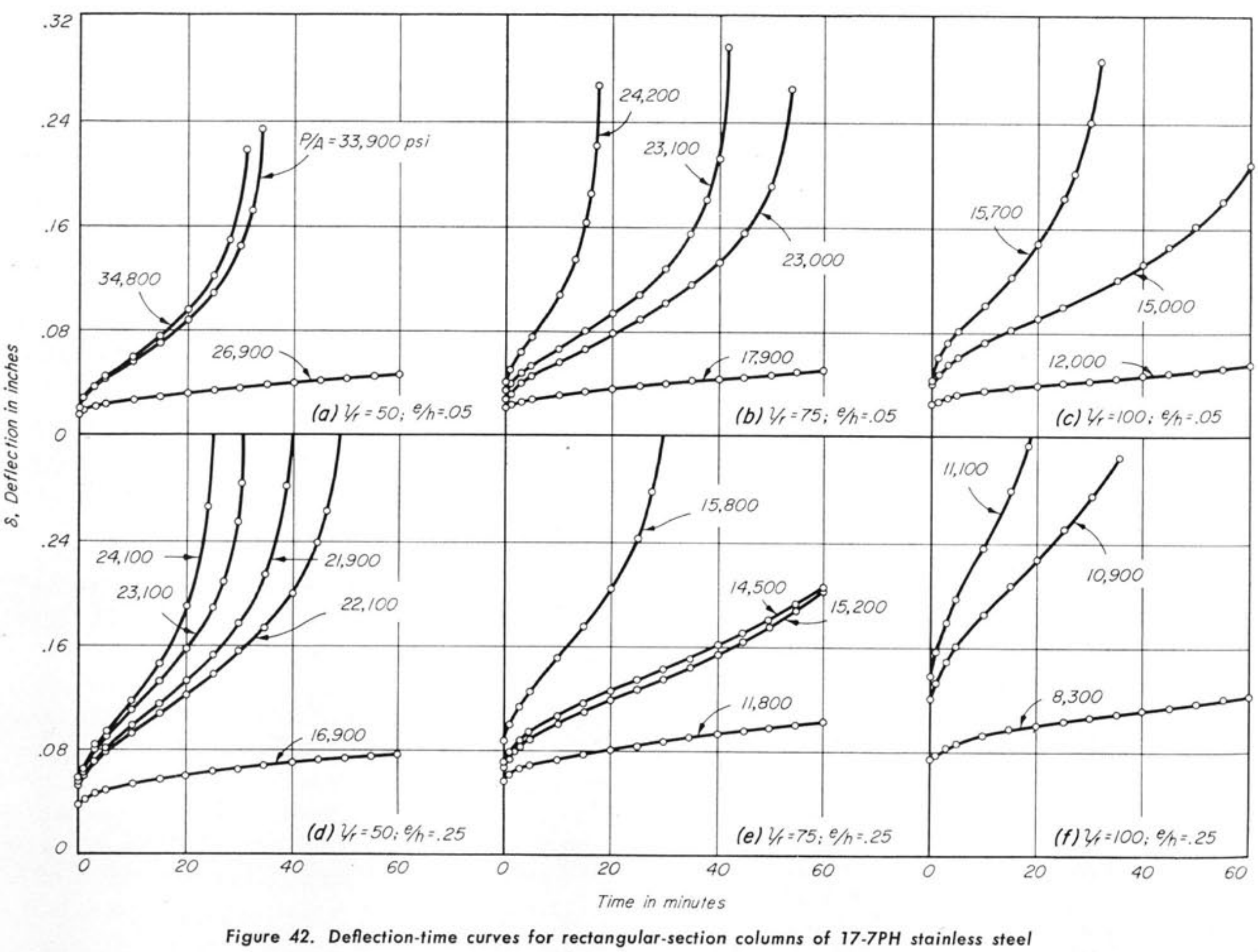

Figure 42. Deflection-time curves for rectangular-section columns of 17-7PH stainless steel

in. The initial eccentricities of these columns were either 5% or 25% of their depths.

The deflection-time creep curves are shown in Figure 42 for the rectangular-section columns and in Figure 43 for the T-section columns. From these curves experimental P/A-deflection data were obtained for zero time and 30 minutes. Representative data are shown in Figure 44 for the rectangular-section columns with a slenderness ratio of 75 and initial eccentricities of 5% and 25% of their depths and in Figure 45 for the T-section columns.

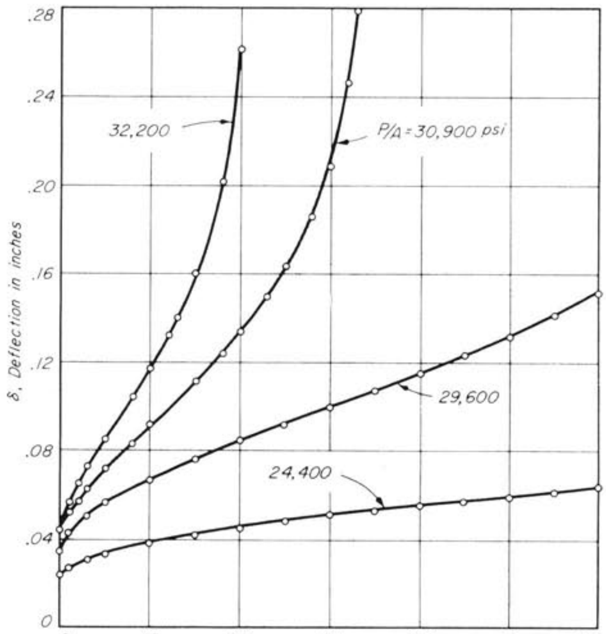

Figure 43. Deflection-time curves for T-section columns of 17-7PH stainless steel

As indicated in Table 7, the experimental values of the average stress in the columns resulted in 20 of the 29 columns buckling in time intervals ranging from 17 to 70 minutes. The magnitude of P/A necessary to cause each column to collapse in 30 minutes was computed and is listed in Table 7. The theoretical collapse load for 30 minutes was computed based on both the arc hyperbolic sine theory (corrected by 10% as indicated in Article IIA) for consine curve configuration of the deflected column and on the modified secant formula using the correction coefficients shown in Figure 10. As indicated in Table 7, the arc hyperbolic sine theory was conservative by an average of 2% in predicting the collapse loads, and the modified secant formula was conservative by an average of 5% in predicting the collapse loads. As in the case of the canvas laminate columns, the data indicate little influence of either slenderness ratio, initial eccentricity, cross-sectional shape, or time to collapse.

Nine of the columns listed in Table 7 did not buckle. The loads were kept low to compare the theoretical and experimental deflections. The experimental deflections for zero time and for 30 minutes are listed in Table 8 for each of the 9 columns. At zero time the material in each column was elastic so that the P/A-deflection curves for zero time were

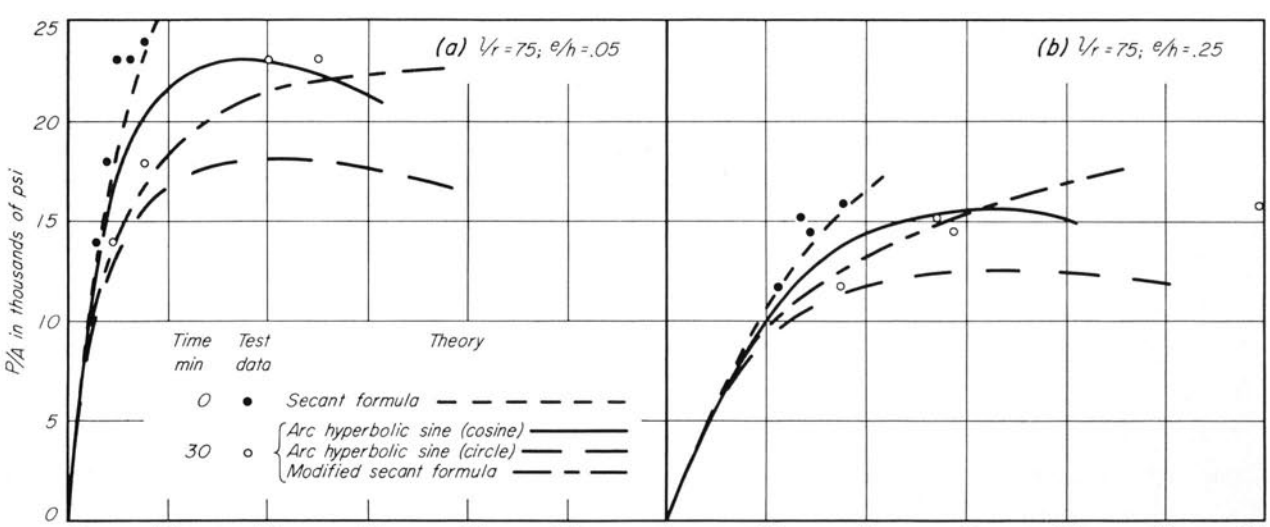

Figure 44. P/A-deflection curves for rectangular-section columns of 17-7PH stainless steel

Table 7

Collapse Load Data for Eccentrically Loaded Columns Made of 17-7PH Stainless Steel and Tested at 972° F.

1 Column Number	2 Depth inch	3 l/r	4 e/h %	5 Time minutes	6 Experimental P/A Actual psi	7 Experimental P/A Adjusted to 30 minutes psi	8 Theoretical P/A at 30 Minutes Arc hyperbolic sine psi	9 Theoretical P/A at 30 Minutes Adjusted tangent modulus psi	$\frac{7}{8}$	$\frac{7}{9}$
R65[b]	0.503	50	5	30[a]	26,900	....	34,210	33,050	....	....
R66	0.503	50	5	34	33,900	34,240	34,210	33,050	1.00	1.04
R67	0.503	50	5	32	34,800	34,970	34,210	33,050	1.02	1.06
R68	0.423	75	5	30[a]	14,000	......	23,100	22,400	....	....
R69	0.422	75	5	30[a]	17,900	......	23,100	22,400	....	....
R70	0.423	75	5	54	23,000	24,610	23,100	22,400	1.07	1.10
R71	0.422	75	5	42	23,100	23,920	23,100	22,400	1.04	1.07
R72	0.422	75	5	17	23,700	22,800	23,100	22,400	0.99	1.02
R73	0.422	75	5	23	23,700	23,100	23,100	22,400	1.00	1.03
R74	0.422	75	5	18	24,200	23,380	23,100	22,400	1.01	1.04
R75	0.424	100	5	30[a]	12,200	......	15,840	15,700	....	....
R76	0.424	100	5	70	15,000	16,300	15,840	15,700	1.03	1.04
R77	0.425	100	5	33	15,700	15,800	15,840	15,700	1.00	1.01
T78	0.604	60	5	30[a]	24,400	......	30,690	29,470	....	....
T79	0.604	60	5	30[a]	29,600	......	30,690	29,470	....	....
T80	0.604	60	5	34	30,900	31,220	30,690	29,470	1.02	1.02
T81	0.604	60	5	21	32,300	31,580	30,690	29,470	1.03	1.07
R82	0.503	50	25	30[a]	16,900	......	23,100	22,320	....	....
R83	0.503	50	25	40	21,900	22,500	23,100	22,320	0.97	1.01
R84	0.503	50	25	49	22,100	23,240	23,100	22,320	1.01	1.04
R85	0.503	50	25	31	23,100	23,160	23,100	22,320	1.00	1.04
R86	0.503	50	25	25	24,100	23,800	23,100	22,320	1.03	1.07
R87	0.421	75	25	30[a]	11,800	......	15,620	15,130	....	....
R88	0.422	75	25	70	14,500	16,290	15,620	15,130	1.04	1.08
R89	0.422	75	25	68	15,200	16,990	15,620	15,130	1.09	1.12
R90	0.423	75	25	31	15,800	15,850	15,620	15,130	1.01	1.05
R91	0.425	100	25	30[a]	8,300	......	11,000	10,600	....	....
R92	0.425	100	25	45	10,900	11,250	11,000	10,600	1.02	1.06
R93	0.424	100	25	21	11,100	10,800	11,000	10,600	0.98	1.02

[a] Test was terminated at 30 minutes since the load was appreciably below the collapse load.
[b] R designates rectangular-section and T designates T-section.

constructed using the secant formula (Eq. 16). Figures 44 and 45 show that some of the points did not fall on the curve for zero time.

Each of these columns was also loaded at room temperature. If the room temperature deflection was found to agree with the secant formula, the deflection for zero time at 972° F. agreed with the theory. The 30 minute theoretical deflection for the columns subjected to an initial eccentricity of 5% of their depths was obtained from the modified secant formula. For an initial eccentricity of 25% of their depths, the theoretical deflection was obtained from the arc hyperbolic sine theory based on the segment of circle configuration of the deflected column. As indicated in Table 8, the theoretical deflection for 30 minutes was conservative in all cases ranging from 4% to 27%. Even better agreement between theory and experiment would be expected at lower loads.

3. Columns Made of Ti 155A Titanium Alloy

A total of 24 eccentrically loaded columns was subjected to constant loads at 772° F. in the fixture shown in Figure 28. These columns are listed in Table 9. All but 4 of the columns were tested in the as-received condition. These columns were aged at 1085° F. following a water quench. The remaining 4 were aged at 1,000° F. following a water quench.

Since the inelastic deformation of this material at 772° F. was predominantly time independent, the interaction curve — moment-load curve theory was used in the analysis of the test data. The inter-

Table 8

Deflection Data for Eccentrically Loaded Columns Made of 17-7PH Stainless Steel and Tested at 972° F.

Column Number	Depth h inch	l/r	e/h %	Experimental δ For zero time inch	Experimental δ For 30 minutes inch	$\delta_{experimental}/\delta_{theoretical}$ For zero time	$\delta_{experimental}/\delta_{theoretical}$ For 30 minutes
R65[a]	0.503	50	5	0.016	0.035	1.14	0.95
R68	0.423	75	5	0.015	0.023	1.00	0.96
R69	0.422	75	5	0.020	0.040	0.87	0.86
R75	0.424	100	5	0.025	0.042	0.74	0.93
T78	0.604	60	5	0.024	0.052	0.92	0.79
T79	0.604	60	5	0.035	0.100	0.95	.....
R82	0.503	50	25	0.038	0.066	1.00	0.93
R87	0.421	75	25	0.056	0.087	0.98	0.73
R91	0.425	100	25	0.074	0.106	0.89	0.77

[a] R designates rectangular-section, T designates T-section.

action curves shown in Figure 46 were constructed using the stress-strain properties listed in Figure 24b and Equations 21 through 24. The theoretical moment-load curves were constructed using Equation 26. The solid points shown in Figure 46 are experimental points taken on the run as the columns were loaded; the open test points were obtained just preceding the collapse of the columns. As indicated in Figure 46 and Table 9, good agreement was found between the theoretical and experimental collapse loads.

Table 9

Collapse Load Data for Eccentrically Loaded Columns Made of Ti 155A Titanium Alloy and Tested at 772° F.

Column Number	Depth h inch	l/r	e/h %	Time minutes	P/A psi.	$\frac{P_{experimental}}{P_{theoretical}}$
		Material Aged at 1,085° F				
R94[a]	0.500	50	5	17	39,300	1.05
R95	0.501	50	5	26	39,300	1.05
R96	0.501	50	5	30	39,800	1.07
R97	0.421	75	5	13	21,400	0.98
R98	0.421	75	5	26	21,700	1.02
R99	0.420	75	5	27	21,900	1.01
R100	0.420	100	5	3	13,600	1.06
R101	0.421	100	5	14	13,600	1.03
R102	0.421	100	5	30	13,900	1.05
T103	0.600	60	5	1	31,000	0.91
T104	0.600	60	5	30	31,400	0.97
R105	0.501	50	25	30	26,100	1.07
R106	0.501	50	25	36	26,600	1.09
R107	0.501	50	25	32	25,400	1.04
R108	0.421	75	25	30	16,200	1.04
R109	0.421	75	25	28	16,400	1.06
R110	0.421	75	25	35	16,500	1.06
R111	0.421	100	25	9	11,000	1.03
R112	0.420	100	25	25	11,000	1.04
R113	0.420	100	25	29	11,000	1.04
		Material Aged at 1,000° F				
R114	0.420	75	5	15	22,500	1.00
R115	0.420	75	5	14	22,500	1.02
R116	0.420	75	25	28	17,100	1.00
R117	0.420	75	25	28	17,100	1.00

[a] R designates rectangular-section, T designates T-section.

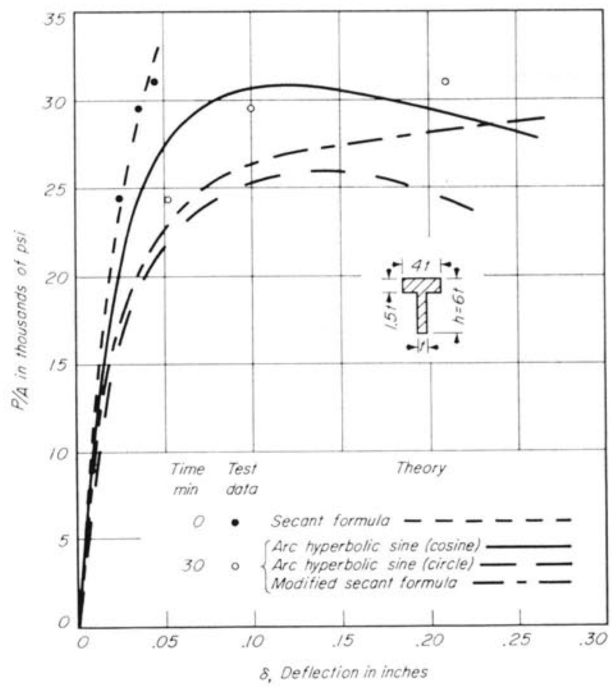

Figure 45. P/A-deflection curves for T-section columns of 17-7PH stainless steel, l/r = 60

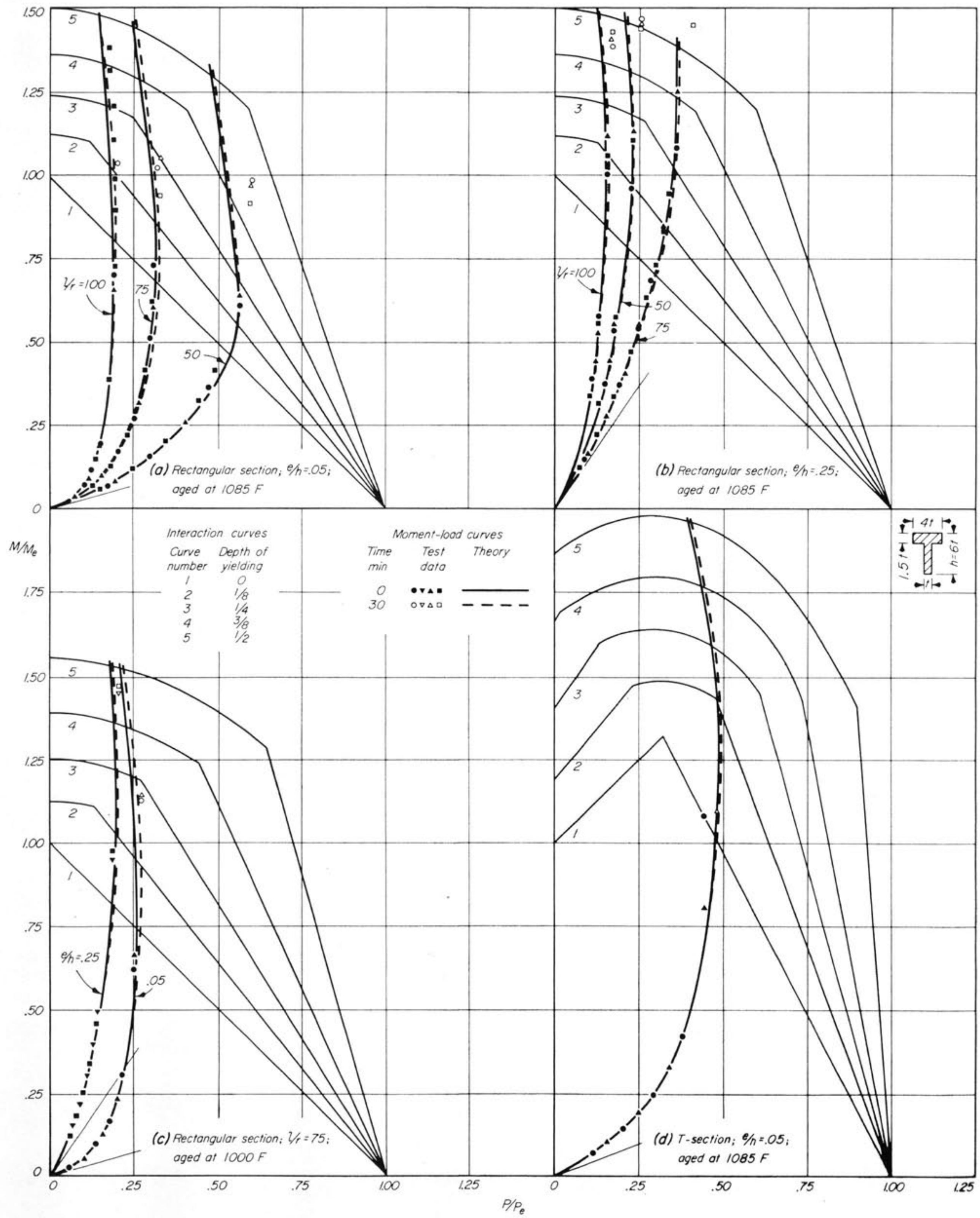

Figure 46. Moment-load curves for Ti 155A titanium alloy columns

V. SUMMARY AND CONCLUSIONS

A. SUMMARY

This investigation was undertaken to make a theoretical and experimental study of creep in beams and eccentrically loaded tension members and columns for which the action line of the loads was parallel to the axis of the members. A theory was developed to predict the load-deflection curves of members which had been subjected to a constant load for a specified time. The stress-strain-time relation for the material was obtained from constant-stress creep curves of the material by letting time be a constant to give an isochronous stress-strain diagram. It was found that this stress-strain diagram could be closely approximated by an arc hyperbolic sine curve as given by Equation 3.

Dimensionless design curves were developed to be used in constructing the load-deflection curves for beams and eccentrically loaded members. Except for the rectangular cross section, these design curves have to be developed for each cross section which has different relative dimensions. In the case of eccentrically loaded columns subjected to an initial eccentricity less than 5% of their depths, the load-deflection curves were closely approximated by a modified secant formula (Eq. 20) which is valid for any cross section and is independent of the properties of the material.

In the experimental part of the investigation, tests were run on 117 beams and eccentrically loaded members in addition to the tension and compression creep specimens. These members were made of high pressure canvas laminate and of Zytel 101 nylon tested in a controlled atmosphere room, of 17-7PH stainless steel tested at 972° F. and of Ti 155A titanium alloy tested at 772° F. The test duration was 1,000 hours for plastic test members and 30 minutes for metal test members.

B. CONCLUSIONS

1. The inelastic deformation was predominantly time-dependent creep for members made of high pressure canvas laminate and Zytel 101 nylon at room temperature and of 17-7PH stainless steel at 972° F. The isochronous stress-strain diagrams of these materials for any specified time could be approximated accurately by an arc hyperbolic sine curve (Eq. 3). In the case of the Ti 155A titanium alloy at 772° F., the inelastic deformation was predominantly time independent; the isochronous stress-strain diagrams were closely approximated by 2 straight lines.

2. Based on the arc hyperbolic sine theory, design curves (Fig. 4) were constructed for beams having various cross sections. Since the isochronous stress-strain relation for the material was obtained from constant stress-creep curves, the theoretical load for the beams was decreased 5% to compensate for the fact that the stress distribution changes with time.

3. Two rectangular-section and 2 T-section beams each of Zytel 101 nylon and high pressure canvas laminate were subjected to pure bending. At 1,000 hours the theory was conservative by an average of 4% in predicting the deflection of the rectangular-section beams and was nonconservative by an average of 4% in predicting the deflection of the T-section beams.

4. Two rectangular-section and 2 T-section beams of canvas laminate were fixed at each end and loaded in the center. The theory was nonconservative in predicting the deflection at 1,000 hours by an average of 4% for the rectangular-section beams and 17% for the T-section beams.

5. Two rectangular-section and 2 T-section beams of canvas laminate were fixed at one end, simply supported at the other end, and loaded in the center. The theory was conservative in predicting the deflection at 1,000 hours by an average of 2% for the rectangular-section beams and nonconservative by an average of 7% for the T-section beams.

6. Based on the arc hyperbolic sine theory, 2 families of curves were derived for rectangular-section and for the T-section eccentrically loaded members (Figs. 5 through 8) to be used along with

Equations 14 and 15 for constructing theoretical load-deflection curves for these members. Since the isochronous stress-strain relation for the material was obtained from constant-stress creep curves, the theoretical load for the eccentrically loaded tension members and columns was decreased and increased 10%, respectively, to compensate for the fact that the stress distribution in these members changes with time.

7. Two rectangular-section and 2 T-section eccentrically loaded tension members each of Zytel 101 nylon and high pressure canvas laminate were subjected to dead loads for 1,000 hours. The theory, based on the assumption that the member deflected into a segment of a circle, was nonconservative by an average of 4% in predicting the deflection at 1,000 hours.

8. Four rectangular-section and 6 T-section eccentrically loaded tension members made of 17-7PH stainless steel were subjected to constant load for 30 minutes at 972° F. The theory was nonconservative by an average of 4% in predicting the deflection of the rectangular-section members and conservative by an average of 7% in predicting the deflection of the T-section members.

9. Nineteen rectangular- and T-section canvas laminate columns were subjected to dead loads which resulted in the collapse of the columns in time intervals ranging from 6 hours to 1,335 hours. These columns had slenderness ratios of 30, 50, and 70 and initial eccentricities of 2%, 5%, and 25% of their depths. Twenty rectangular- and T-section 17-7PH stainless steel columns were subjected to constant loads which resulted in collapse of the columns in time intervals ranging from 13 minutes to 70 minutes. These columns had slenderness ratios of 50, 60, 75, and 100 and initial eccentricities of 5% and 25% of their depths. The arc hyperbolic sine theory based on cosine configuration of the deflected column was nonconservative by an average of 4% in predicting the collapse loads for the canvas laminate columns and conservative by 2% in predicting the collapse loads on the 17-7PH stainless steel columns. The theoretical collapse load based on modified secant formula (Eq. 20) using the correction coefficients given in Figure 10 was nonconservative by an average of 2% in predicting the collapse loads for the canvas laminate columns and conservative by 4% in predicting the collapse loads for the 17-7PH stainless steel columns. The difference between the theoretical and experimental collapse loads appeared to be independent of the column cross-sectional shape, slenderness ratio, initial eccentricity, or time to collapse.

10. The modified secant formula (Eq. 20) is independent of the column cross section and of the properties of the material as long as the isochronous stress-strain diagram can be represented by Equation 3. The formula can be used without correction for predicting the collapse load within ± 10% if the initial eccentricity is less than 5% of the column depth. The formula can also be used without correction for predicting the deflection of the same columns. For an initial eccentricity of 25% of the column depth, the formula can be used for predicting the column deflection for loads up to ½ the collapse load.

11. Three rectangular-section eccentrically loaded tension members and 24 rectangular- and T-section eccentrically loaded columns of Ti 155A titanium alloy were subjected to constant load at 772° F. The theoretical analysis of these members was based on the interaction curve-moment-load curve theory. The theory was nonconservative by an average of 9% in predicting the deflection of the eccentrically loaded tension members and conservative by an average of 3% in predicting the collapse load of columns.

VI. REFERENCES

1. J. Kempner, *Creep Bending and Buckling of Linearly Viscoelastic Columns,* N.A.C.A. Technical Note 3136 (1954).

2. J. Kempner, *Creep Bending and Buckling of Nonlinearly Viscoelastic Columns,* N.A.C.A. Technical Note 3137 (1954).

3. H. H. Hilton, "Creep Collapse of Viscoelastic Columns With Initial Curvature," *Journal of the Aeronautical Sciences,* vol. 19 (1952), page 844.

4. R. W. Bailey, "Utilization of Creep Test Data in Engineering Design," *Proceedings of the Institute of Mechanical Engineers,* vol. 131 (1935), p. 131.

5. H. J. Tapsell and A. E. Johnson, "An Investigation of the Nature of Creep Under Stress Produced by Pure Flexure," *Institute of Metals Journal,* vol. 57 (August 1935), p. 121.

6. C. C. Davenport, "Correlation of Creep and Relaxation Properties of Copper," *Journal of Applied Mechanics,* Trans. ASME, vol. 60 (1938), pp. A-55 — A-60.

7. I. Finnie and W. R. Heller, *Creep of Engineering Materials,* McGraw-Hill Book Company, 1959.

8. Y. H. Pao and J. Marin, "Deflections and Stresses in Beams Subjected to Bending and Creep," *Journal of Applied Mechanics,* Trans. ASME, vol. 74 (1952), pp. 478-484.

9. W. N. Findley and J. J. Poczatek, "Prediction of Creep-Deflection and Stress Distribution in Beams from Creep in Tension," *Journal of Applied Mechanics,* paper No. 54 — A-5.

10. W. N. Findley, J. J. Poczatek, and P. N. Mathur, "Prediction of Creep in Bending from Tension and Compression Creep Data When Creep Coefficients are Unequal," ASME Paper No. 57 — A-213.

11. W. Kauzmann, "Flow of Solid Metals from the Standpoint of the Chemical Rate Theory," *Trans. American Inst. of Mining and Metallurgical Engineering, Institute of Metals Division,* vol. 143 (1941), p. 57.

12. R. L. Carlson and G. K. Manning, *A Summary of Compressive-Creep Characteristics of Metal Columns at Elevated Temperatures,* WADC Technical Report 57-96 (1958).

13. S. Dharmarajan, "Prediction of Load and Creep Deflection for Specified Strain in Beams and Eccentrically-Loaded Members," unpublished master's thesis, University of Illinois, 1958.

14. O. M. Sidebottom and S. Dharmarajan, "Prediction of Load and Creep Deflection for Specified Strain in Beams and Eccentrically-Loaded Members," paper presented at the ASME annual meeting, December, 1958.

15. R. E. Carlson, "Primary and Secondary Creep Deflection of Two Types of Indeterminate Beams," unpublished master's thesis, University of Illinois, 1958.

16. G. A. Costello, "The Creep Buckling of Columns Made of Canvas Laminate," unpublished Ph.D. thesis, University of Illinois, 1959.

17. J. L. Gubser, "Theoretical and Experimental Analysis of Eccentrically-Loaded 17-7PH Stainless Steel Columns at 1000° F," unpublished master's thesis, University of Illinois, 1959.

18. O. M. Sidebottom, M. E. Clark, and S. Dharmarajan, *The Effects of Inelastic Action on the Resistance to Various Types of Loads of Ductile Members Made from Various Classes of Metals — Part VIII, Eccentrically-Loaded Tension Members Made of Two Stainless Steels Tested at Elevated Temperatures,* WADC Technical Report 56-330, April, 1958.

19. O. M. Sidebottom and S. Dharmarajan, *The Effects of Inelastic Action on the Resistance to Various Types of Loads of Ductile Members Made from Various Classes of Metals — Part IX, T-Section Eccentrically-Loaded Tension Members Made of Type 304 Stainless Steel and Tested at 1000° F,* WADC Technical Report 56-330, May, 1958.

20. O. M. Sidebottom and S. Dharmarajan, *The Effects of Inelastic Action on the Resistance to Various Types of Loads of Ductile Members Made from Various Classes of Metal — Part X, T-Section Eccentrically-Loaded Tension Members Made of 17-7PH Stainless Steel and Tested at 1000° F,* WADC Technical Report 56-330, November, 1958.

21. O. M. Sidebottom, S. Dharmarajan, J. L. Gubser, and J. D. Leasure, *The Effects of Inelastic Action on the Resistance to Various Types of Loads of Ductile Members Made from Various Classes of Metals — Part XII, Eccentrically-Loaded Tension Members and Columns Made of 17-7PH Stainless Steel and Ti 155A Titanium Alloy and Tested at Various Temperatures,* WADC Technical Report 56-330, October, 1959.

22. O. M. Sidebottom and M. E. Clark, *Theoretical and Experimental Analysis of Members Loaded Eccentrically and Inelastically,* University of Illinois Engineering Experiment Station Bulletin No. 477, March, 1958.

23. N. M. Newmark, "Numerical Procedure for Computing Deflection, Moments and Buckling Loads," *Proceedings of ASCE,* vol. 68 (1942), pp. 691-718.

VII. APPENDICES

APPENDIX A

Four-Place Tables of B_N

$$(B_N = N \log (N + \sqrt{N^2 + 1}) - \sqrt{N^2 + 1})$$

N	0	1	2	3	4	5	6	7	8	9
0	−1.0000	−0.9999	−0.9997	−0.9994	−0.9991	−0.9987	−0.9982	−0.9975	−0.9968	−0.9959
0.1	−0.9950	−0.9939	−0.9928	−0.9915	−0.9902	−0.9887	−0.9872	−0.9855	−0.9838	−0.9819
0.2	−0.9800	−0.9780	−0.9758	−0.9736	−0.9713	−0.9689	−0.9664	−0.9638	−0.9610	−0.9582
0.3	−0.9553	−0.9523	−0.9500	−0.9469	−0.9428	−0.9394	−0.9359	−0.9323	−0.9287	−0.9249
0.4	−0.9210	−0.9171	−0.9130	−0.9089	−0.9047	−0.9004	−0.8960	−0.8915	−0.8869	−0.8822
0.5	−0.8774	−0.8725	−0.8676	−0.8626	−0.8575	−0.8523	−0.8470	−0.8416	−0.8361	−0.8306
0.6	−0.8249	−0.8192	−0.8134	−0.8075	−0.8015	−0.7954	−0.7893	−0.7830	−0.7767	−0.7704
0.7	−0.7639	−0.7573	−0.7507	−0.7439	−0.7371	−0.7302	−0.7232	−0.7162	−0.7098	−0.7018
0.8	−0.6945	−0.6871	−0.6797	−0.6721	−0.6645	−0.6568	−0.6490	−0.6412	−0.6333	−0.6253
0.9	−0.6173	−0.6092	−0.6010	−0.5927	−0.5844	−0.5760	−0.5675	−0.5589	−0.5503	−0.5416
1.0	−0.5328	−0.5240	−0.5150	−0.5061	−0.4970	−0.4879	−0.4787	−0.4694	−0.4601	−0.4507
1.1	−0.4412	−0.4317	−0.4221	−0.4124	−0.4027	−0.3929	−0.3830	−0.3731	−0.3631	−0.3530
1.2	−0.3429	−0.3327	−0.3225	−0.3122	−0.3018	−0.2914	−0.2809	−0.2703	−0.2597	−0.2490
1.3	−0.2382	−0.2274	−0.2165	−0.2056	−0.1946	−0.1835	−0.1724	−0.1612	−0.1500	−0.1387
1.4	−0.1273	−0.1159	−0.1044	−0.0929	−0.0813	−0.0697	−0.0580	−0.0462	−0.0344	−0.0225
1.5	−0.0106	0.0014	0.0134	0.0255	0.0376	0.0498	0.0620	0.0744	0.0867	0.0991
1.6	0.1116	0.1241	0.1367	0.1493	0.1620	0.1747	0.1875	0.2003	0.2132	0.2261
1.7	0.2391	0.2521	0.2652	0.2783	0.2915	0.3047	0.3180	0.3313	0.3447	0.3581
1.8	0.3716	0.3851	0.3987	0.4124	0.4261	0.4398	0.4536	0.4674	0.4812	0.4952
1.9	0.5091	0.5231	0.5371	0.5512	0.5653	0.5795	0.5937	0.6080	0.6224	0.6368
2.0	0.6512	0.6657	0.6802	0.6947	0.7094	0.7240	0.7387	0.7534	0.7682	0.7830
2.1	0.7979	0.8128	0.8277	0.8427	0.8577	0.8728	0.8879	0.9030	0.9182	0.9334
2.2	0.9487	0.9640	0.9794	0.9948	1.0102	1.0257	1.0412	1.0568	1.0724	1.0880
2.3	1.1037	1.1194	1.1352	1.1510	1.1669	1.1827	1.1986	1.2146	1.2306	1.2466
2.4	1.2627	1.2788	1.2950	1.3111	1.3273	1.3436	1.3599	1.3762	1.3926	1.4090
2.5	1.4255	1.4420	1.4585	1.4751	1.4917	1.5083	1.5250	1.5417	1.5585	1.5753
2.6	1.5921	1.6090	1.6258	1.6428	1.6597	1.6767	1.6937	1.7108	1.7279	1.7450
2.7	1.7622	1.7794	1.7967	1.8139	1.8312	1.8486	1.8660	1.8834	1.9008	1.9183
2.8	1.9358	1.9533	1.9709	1.9886	2.0062	2.0239	2.0416	2.0594	2.0771	2.0950
2.9	2.1128	2.1307	2.1486	2.1666	2.1846	2.2026	2.2206	2.2387	2.2568	2.2749
3.0	2.2931	2.3113	2.3295	2.3478	2.3661	2.3844	2.4027	2.4211	2.4395	2.4580
3.1	2.4765	2.4950	2.5135	2.5321	2.5507	2.5693	2.5880	2.6067	2.6254	2.6442
3.2	2.6630	2.6818	2.7007	2.7196	2.7385	2.7574	2.7764	2.7954	2.8144	2.8334
3.3	2.8525	2.8716	2.8907	2.9099	2.9291	2.9483	2.9675	2.9868	3.0061	3.0254
3.4	3.0448	3.0642	3.0836	3.1030	3.1225	3.1420	3.1615	3.1811	3.2007	3.2203
3.5	3.2400	3.2597	3.2794	3.2991	3.3188	3.3386	3.3584	3.3782	3.3981	3.4180
3.6	3.4379	3.4578	3.4778	3.4978	3.5178	3.5379	3.5580	3.5781	3.5982	3.6183
3.7	3.6385	3.6587	3.6789	3.6992	3.7195	3.7398	3.7601	3.7805	3.8009	3.8213
3.8	3.8418	3.8623	3.8828	3.9033	3.9238	3.9443	3.9649	3.9855	4.0061	4.0268
3.9	4.0475	4.0682	4.0889	4.1097	4.1305	4.1513	4.1721	4.1930	4.2139	4.2348
4.0	4.2557	4.2767	4.2977	4.3187	4.3397	4.3608	4.3819	4.4030	4.4241	4.4452
4.1	4.4664	4.4876	4.5088	4.5300	4.5513	4.5726	4.5939	4.6153	4.6367	4.6581
4.2	4.6795	4.7009	4.7224	4.7439	4.7654	4.7869	4.8084	4.8300	4.8516	4.8732
4.3	4.8948	4.9164	4.9381	4.9598	4.9816	5.0033	5.0251	5.0469	5.0687	5.0905
4.4	5.1124	5.1343	5.1562	5.1781	5.2001	5.2221	5.2441	5.2661	5.2881	5.3102
4.5	5.3323	5.3544	5.3765	5.3986	5.4208	5.4430	5.4652	5.4874	5.5097	5.5320
4.6	5.5543	5.5766	5.5999	5.6213	5.6437	5.6661	5.6885	5.7109	5.7334	5.7559
4.7	5.7784	5.8009	5.8234	5.8460	5.8686	5.8912	5.9138	5.9365	5.9592	5.9819
4.8	6.0046	6.0273	6.0501	6.0729	6.0957	6.1185	6.1413	6.1642	6.1871	6.2100
4.9	6.2329	6.2558	6.2788	6.3018	6.3248	6.3478	6.3708	6.3939	6.4170	6.4401
5.0	6.4632	6.4863	6.5095	6.5327	6.5559	6.5791	6.6023	6.6255	6.6488	6.6721
5.1	6.6954	6.7187	6.7420	6.7654	6.7888	6.8122	6.8356	6.8591	6.8826	6.9061
5.2	6.9296	6.9531	6.9766	7.0002	7.0238	7.0474	7.0710	7.0946	7.1182	7.1419
5.3	7.1656	7.1893	7.2130	7.2367	7.2605	7.2843	7.3081	7.3319	7.3557	7.3796
5.4	7.4035	7.4274	7.4513	7.4752	7.4991	7.5231	7.5471	7.5711	7.5951	7.6191
5.5	7.6432	7.6673	7.6914	7.7155	7.7396	7.7637	7.7879	7.8121	7.8363	7.8605
5.6	7.8847	7.9089	7.9332	7.9575	7.9818	8.0061	8.0304	8.0547	8.0791	8.1035
5.7	8.1279	8.1523	8.1767	8.2012	8.2257	8.2502	8.2747	8.2992	8.3237	8.3483
5.8	8.3729	8.3975	8.4221	8.4467	8.4713	8.4960	8.5207	8.5454	8.5701	8.5948
5.9	8.6196	8.6444	8.6692	8.6940	8.7188	8.7436	8.7684	8.7933	8.8182	8.8431
6.0	8.8680	8.8929	8.9178	8.9428	8.9678	8.9928	9.0178	9.0428	9.0628	9.0929
6.1	9.1180	9.1431	9.1682	9.1933	9.2184	9.2436	9.2688	9.2940	9.3192	9.3444
6.2	9.3696	9.3948	9.4201	9.4454	9.4707	9.4960	9.5213	9.5466	9.5720	9.5974
6.3	9.6228	9.6482	9.6736	9.6990	9.7245	9.7500	9.7755	9.8010	9.8265	9.8520
6.4	9.8775	9.9031	9.9287	9.9543	9.9799	10.0055	10.0311	10.0568	10.0825	10.1082
6.5	10.1339	10.1596	10.1853	10.2110	10.2368	10.2626	10.2884	10.3142	10.3400	10.3658
6.6	10.3917	10.4175	10.4434	10.4693	10.4952	10.5211	10.5470	10.5730	10.5990	10.6520
6.7	10.6510	10.6770	10.7030	10.7290	10.7551	10.7812	10.8073	10.8334	10.8595	10.8856
6.8	10.9118	10.9379	10.9641	10.9903	11.0165	11.0427	11.0689	11.0952	11.1214	11.1477
6.9	11.1740	11.2003	11.2266	11.2529	11.2793	11.3057	11.3321	11.3585	11.3849	11.4113
7.0	11.4378	11.4643	11.4907	11.5172	11.5437	11.5702	11.5967	11.6232	11.6498	11.6763
7.1	11.7029	11.7295	11.7561	11.7827	11.8093	11.8360	11.8627	11.8893	11.9160	11.9427
7.2	11.9694	11.9961	12.0229	12.0496	12.0764	12.1032	12.1300	12.1568	12.1836	12.2105
7.3	12.2373	12.2642	12.2910	12.3179	12.3448	12.3717	12.3986	12.4256	12.4525	12.4795
7.4	12.5065	12.5335	12.5605	12.5875	12.6146	12.6416	12.6687	12.6958	12.7229	12.7500
7.5	12.7771	12.8042	12.8314	12.8585	12.8857	12.9129	12.9401	12.9673	12.9945	13.0218
7.6	13.0490	13.0763	13.1035	13.1308	13.1581	13.1854	13.2127	13.2401	13.2674	13.2948
7.7	13.3222	13.3496	13.3770	13.4044	13.4319	13.4593	13.4868	13.5142	13.5417	13.5692
7.8	13.5967	13.6242	13.6517	13.6793	13.7068	13.7344	13.7620	13.7896	13.8172	13.8448

Four-Place Tables of B_N (Concluded)

N	0	1	2	3	4	5	6	7	8	9
7.9	13.8725	13.9001	13.9278	13.9555	13.9831	14.0108	14.0385	14.0662	14.0940	14.1217
8.0	14.1495	14.1773	14.2051	14.2329	14.2607	14.2885	14.3163	14.3442	14.3720	14.3998
8.1	14.4277	14.4556	14.4835	14.5114	14.5393	14.5673	14.5953	14.6232	14.6512	14.6792
8.2	14.7072	14.7352	14.7632	14.7913	14.8193	14.8474	14.8755	14.9036	14.9317	14.9598
8.3	14.9879	15.0160	15.0442	15.0723	15.1005	15.1287	15.1569	15.1851	15.2133	15.2416
8.4	15.2698	15.2981	15.3264	15.3547	15.3830	15.4113	15.4396	15.4680	15.4963	15.5246
8.5	15.5530	15.5814	15.6098	15.6382	15.6666	15.6950	15.7234	15.7519	15.7803	15.8088
8.6	15.8373	15.8658	15.8943	15.9228	15.9513	15.9798	16.0083	16.0369	16.0655	16.0941
8.7	16.1227	16.1513	16.1799	16.2085	16.2372	16.2658	16.2945	16.3231	16.3518	16.3805
8.8	16.4092	16.4379	16.4666	16.4954	16.5241	16.5529	16.5817	16.6105	16.6393	16.6681
8.9	16.6969	16.7257	16.7546	16.7834	16.8123	16.8412	16.8701	16.8990	16.9279	16.9568
9.0	16.9857	17.0146	17.0436	17.0725	17.1015	17.1305	17.1595	17.1885	17.2175	17.2466
9.1	17.2756	17.3046	17.3337	17.3628	17.3918	17.4209	17.4500	17.4791	17.5082	17.5374
9.2	17.5665	17.5957	17.6248	17.6540	17.6832	17.7124	17.7416	17.7708	17.8001	17.8293
9.3	17.8586	17.8879	17.9171	17.9464	17.9757	18.0050	18.0343	18.0636	18.0930	18.1223
9.4	18.1517	18.1811	18.2105	18.2399	18.2693	18.2987	18.3281	18.3576	18.3870	18.4164
9.5	18.4459	18.4754	18.5049	18.5344	18.5639	18.5934	18.6229	18.6525	18.6820	18.7115
9.6	18.7411	18.7707	18.8003	18.8299	18.8595	18.8892	18.9188	18.9485	18.9782	19.0078
9.7	19.0375	19.0672	19.0969	19.1266	19.1563	19.1860	19.2157	19.2455	19.2752	19.3050
9.8	19.3348	19.3646	19.3944	19.4242	19.4540	19.4838	19.5136	19.5435	19.5733	19.6032
9.9	19.6331	19.6630	19.6929	19.7228	19.7527	19.7826	19.8125	19.8425	19.8724	19.9024

APPENDIX B

Four-Place Tables of C_N

$$\left(C_N = \frac{1}{4}\left[(2N^2 + 1)\log\left(N + \sqrt{N^2 + 1}\right) - N\sqrt{N^2 + 1}\right)\right]$$

N	0	1	2	3	4	5	6	7	8	9
0	0	0	0	0	0	0	0.0001	0.0001	0.0002	0.0003
0.1	0.0003	0.0005	0.0007	0.0009	0.0011	0.0013	0.0015	0.0018	0.0021	0.0024
0.2	0.0027	0.0031	0.0035	0.0040	0.0045	0.0052	0.0058	0.0064	0.0072	0.0080
0.3	0.0089	0.0098	0.0108	0.0118	0.0129	0.0141	0.0153	0.0167	0.0180	0.0195
0.4	0.0210	0.0226	0.0243	0.0261	0.0279	0.0298	0.0318	0.0339	0.0361	0.0384
0.5	0.0407	0.0432	0.0457	0.0483	0.0511	0.0539	0.0569	0.0599	0.0631	0.0663
0.6	0.0697	0.0732	0.0768	0.0804	0.0842	0.0881	0.0921	0.0963	0.1006	0.1050
0.7	0.1095	0.1141	0.1189	0.1238	0.1288	0.1339	0.1392	0.1446	0.1501	0.1557
0.8	0.1615	0.1674	0.1735	0.1797	0.1860	0.1925	0.1991	0.2059	0.2128	0.2199
0.9	0.2271	0.2345	0.2420	0.2496	0.2574	0.2654	0.2735	0.2818	0.2902	0.2988
1.0	0.3075	0.3164	0.3255	0.3347	0.3441	0.3536	0.3633	0.3732	0.3832	0.3934
1.1	0.4037	0.4142	0.4249	0.4358	0.4469	0.4581	0.4695	0.4811	0.4929	0.5048
1.2	0.5169	0.5292	0.5416	0.5542	0.5670	0.5800	0.5932	0.6066	0.6201	0.6339
1.3	0.6478	0.6619	0.6762	0.6907	0.7054	0.7203	0.7354	0.7506	0.7661	0.7818
1.4	0.7976	0.8136	0.8299	0.8463	0.8629	0.8797	0.8967	0.9139	0.9314	0.9490
1.5	0.9668	0.9848	1.0030	1.0215	1.0401	1.0589	1.0779	1.0972	1.1167	1.1363
1.6	1.1562	1.1763	1.1966	1.2171	1.2379	1.2588	1.2799	1.3013	1.3229	1.3446
1.7	1.3666	1.3888	1.4113	1.4339	1.4568	1.4799	1.5032	1.5268	1.5505	1.5745
1.8	1.5987	1.6231	1.6478	1.6727	1.6978	1.7231	1.7486	1.7744	1.8004	1.8266
1.9	1.8530	1.8797	1.9066	1.9337	1.9610	1.9886	2.0165	2.0445	2.0729	2.1015
2.0	2.1303	2.1593	2.1885	2.2180	2.2476	2.2775	2.3077	2.3381	2.3687	2.3996
2.1	2.4307	2.4621	2.4937	2.5255	2.5576	2.5899	2.6225	2.6553	2.6882	2.7216
2.2	2.7551	2.7889	2.8229	2.8572	2.8917	2.9264	2.9614	2.9966	3.0321	3.0678
2.3	3.1038	3.1400	3.1765	3.2133	3.2503	3.2875	3.3250	3.3627	3.4007	3.4390
2.4	3.4775	3.5163	3.5553	3.5945	3.6340	3.6738	3.7138	3.7541	3.7946	3.8354
2.5	3.8764	3.9177	3.9593	4.0011	4.0432	4.0855	4.1281	4.1710	4.2141	4.2575
2.6	4.3012	4.3451	4.3893	4.4338	4.4785	4.5235	4.5687	4.6142	4.6600	4.7060
2.7	4.7523	4.7989	4.8457	4.8927	4.9401	4.9877	5.0356	5.0837	5.1321	5.1808
2.8	5.2297	5.2789	5.3284	5.3782	5.4283	5.4786	5.5292	5.5800	5.6312	5.6826
2.9	5.7342	5.7861	5.8383	5.8908	5.9436	5.9966	6.0499	6.1035	6.1574	6.2115
3.0	6.2659	6.3157	6.3682	6.4235	6.4815	6.5423	6.5984	6.6548	6.7115	6.7684
3.1	6.8256	6.8831	6.9409	6.9990	7.0573	7.1159	7.1748	7.2339	7.2933	7.3530
3.2	7.4130	7.4733	7.5338	7.5947	7.6558	7.7172	7.7789	7.8409	7.9032	7.9657
3.3	8.0286	8.0918	8.1552	8.2190	8.2830	8.3474	8.4120	8.4769	8.5421	8.6076
3.4	8.6733	8.7393	8.8056	8.8722	8.9391	9.0063	9.0738	9.1415	9.2095	9.2778
3.5	9.3464	9.4153	9.4846	9.5542	9.6240	9.6942	9.7646	9.8354	9.9064	9.9778
3.6	10.0494	10.1213	10.1935	10.2660	10.3388	10.4118	10.4852	10.5588	10.6328	10.7070
3.7	10.7816	10.8564	10.9316	11.0070	11.0827	11.1587	11.2350	11.3117	11.3887	11.4660
3.8	11.5436	11.6215	11.6997	11.7782	11.8570	11.9361	12.0155	12.0952	12.1751	12.2554
3.9	12.3360	12.4169	12.4981	12.5795	12.6613	12.7434	12.8258	12.9085	12.9915	13.0748
4.0	13.1584	13.2423	13.3265	13.4111	13.4960	13.5812	13.6667	13.7525	13.8386	13.9250
4.1	14.0117	14.0987	14.1860	14.2737	14.3617	14.4500	14.5386	14.6274	14.7166	14.8061
4.2	14.8959	14.9860	15.0764	15.1671	15.2581	15.3495	15.4412	15.5332	15.6255	15.7181
4.3	15.8111	15.9044	15.9980	16.0919	16.1861	16.2806	16.3754	16.4705	16.5660	16.6618
4.4	16.7579	16.8543	16.9510	17.0480	17.1453	17.2430	17.3410	17.4393	17.5379	17.6368
4.5	17.7360	17.8356	17.9355	18.0357	18.1363	18.2372	18.3384	18.4399	18.5417	18.6439
4.6	18.7464	18.8492	18.9523	19.0557	19.1594	19.2635	19.3679	19.4726	19.5776	19.6829
4.7	19.7886	19.8946	20.0009	20.1075	20.2144	20.3217	20.4293	20.5372	20.6455	20.7541
4.8	20.8631	20.9724	21.0819	21.1918	21.3020	21.4126	21.5235	21.6347	21.7462	21.8580
4.9	21.9702	22.0827	22.1955	22.3087	22.4222	22.5360	22.6501	22.7646	22.8794	22.9945
5.0	23.1099	23.2257	23.3418	23.4582	23.5750	23.6921	23.8095	23.9273	24.0454	24.1639
5.1	24.2827	24.4018	24.5212	24.6410	24.7611	24.8815	25.0022	25.1233	25.2447	25.3664
5.2	25.4885	25.6109	25.7336	25.8567	25.9801	26.1038	26.2279	26.3523	26.4771	26.6022
5.3	26.7277	26.8535	26.9796	27.1060	27.2328	27.3599	27.4873	27.6151	27.7432	27.8717
5.4	28.0005	28.1296	28.2590	28.3888	28.5189	28.6494	28.7802	28.9113	29.0428	29.1746
5.5	29.3067	29.4392	29.5721	29.7053	29.8388	29.9727	30.1069	30.2415	30.3764	30.5116
5.6	30.6472	30.7831	30.9194	31.0560	31.1929	31.3302	31.4678	31.6050	31.7440	31.8826
5.7	32.0216	32.1609	32.3005	32.4405	32.5808	32.7215	32.8625	33.0039	33.1457	33.2878
5.8	33.4302	33.5730	33.7161	33.8595	34.0033	34.1475	34.2920	34.4368	34.5820	34.7275
5.9	34.8734	35.0196	35.1662	35.3131	35.4603	35.6079	35.7558	35.9041	36.0527	36.2016
6.0	36.3509	36.5006	36.6506	36.8010	36.9518	37.1029	37.2543	37.4061	37.5582	37.7107
6.1	37.8635	38.0167	38.1702	38.3241	38.4783	38.6329	38.7878	38.9431	39.0987	39.2546
6.2	39.4109	39.5676	39.7246	39.8819	40.0396	40.1977	40.3561	40.5149	40.6740	40.8335
6.3	40.9934	41.1536	41.3142	41.4751	41.6364	41.7980	41.9600	42.1223	42.2849	42.4479
6.4	42.6113	42.7750	42.9391	43.1035	43.2683	43.4335	43.5990	43.7648	43.9310	44.0976

Four-Place Tables of C_N (Concluded)

N	0	1	2	3	4	5	6	7	8	9
6.5	44.2645	44.4318	44.5994	44.7674	44.9358	45.1045	45.2736	45.4430	45.6128	45.7830
6.6	45.9535	46.1244	46.2956	46.4671	46.6390	46.8113	46.9839	47.1569	47.3303	47.5040
6.7	47.6781	47.8525	48.0273	48.2024	48.3779	48.5537	48.7299	48.9065	49.0835	49.2608
6.8	49.4385	49.6165	49.7949	49.9737	50.1528	50.3323	50.5121	50.6923	50.8729	51.0538
6.9	51.2351	51.4167	51.5987	51.7811	51.9638	52.1469	52.3303	52.5141	52.6983	52.8828
7.0	53.0677	53.2530	53.4386	53.6246	53.8110	53.9977	54.1848	54.3723	54.5601	54.7483
7.1	54.9369	55.1258	55.3151	55.5047	55.6947	55.8851	56.0758	56.2669	56.4583	56.6501
7.2	56.8423	57.0348	57.2278	57.4210	57.6147	57.8087	58.0031	58.1979	58.3931	58.5886
7.3	58.7845	58.9808	59.1774	59.3743	59.5717	59.7694	59.9675	60.1660	60.3648	60.5640
7.4	60.7636	60.9635	61.1638	61.3645	61.5655	61.7669	61.9687	62.1708	62.3733	62.5762
7.5	62.7794	62.9830	63.1870	63.3914	63.5962	63.8013	64.0068	64.2126	64.4189	64.6254
7.6	64.8324	65.0397	65.2474	65.4555	65.6640	65.8728	66.0820	66.2915	66.5015	66.7117
7.7	66.9224	67.1334	67.3448	67.5566	67.7688	67.9813	68.1942	68.4075	68.6212	68.8353
7.8	69.0497	69.2645	69.4797	69.6953	69.9112	70.1275	70.3442	70.5613	70.7787	70.9965
7.9	71.2147	71.4333	71.6522	71.8715	72.0912	72.3112	72.5316	72.7524	72.9736	73.1951
8.0	73.4170	73.6393	73.8620	74.0851	74.3086	74.5324	74.7566	74.9812	75.2062	75.4315
8.1	75.6572	75.8833	76.1098	76.3366	76.5638	76.7914	77.0194	77.2477	77.4764	77.7055
8.2	77.9350	78.1648	78.3951	78.6257	78.8566	79.0880	79.3198	79.5519	79.7845	80.0174
8.3	80.2507	80.4844	80.7184	80.9529	81.1877	81.4229	81.6585	81.8944	82.1308	82.3675
8.4	82.6046	82.8421	83.0799	83.3181	83.5567	83.7957	84.0351	84.2748	84.5150	84.7555
8.5	84.9964	85.2377	85.4794	85.7215	85.9640	86.2069	86.4502	86.6938	86.9378	87.1822
8.6	87.4270	87.6722	87.9177	88.1636	88.4099	88.6566	88.9037	89.1511	89.3990	89.6472
8.7	89.8958	90.1448	90.3941	90.6439	90.8940	91.1445	91.3954	91.6467	91.8984	92.1505
8.8	92.4030	92.6559	92.9091	93.1628	93.4168	93.6712	93.9260	94.1812	94.4367	94.6927
8.9	94.9490	95.2057	95.4628	95.7203	95.9782	96.2364	96.4950	96.7541	97.0135	97.2733
9.0	97.5335	97.7941	98.0551	98.3165	98.5782	98.8404	99.1030	99.3659	99.6292	99.8930
9.1	100.1571	100.4216	100.6865	100.9517	101.2174	101.4834	101.7498	102.0166	102.2838	102.5514
9.2	102.8194	103.0878	103.3565	103.6257	103.8953	104.1652	104.4356	104.7063	104.9775	105.2490
9.3	105.5210	105.7933	106.0660	106.3391	106.6126	106.8865	107.1608	107.4355	107.7106	107.9860
9.4	108.2619	108.5381	108.8148	109.0918	109.3692	109.6470	109.9252	110.2038	110.4828	110.7622
9.5	111.0420	111.3222	111.6028	111.8838	112.1651	112.4469	112.7291	113.0116	113.2946	113.5779
9.6	113.8617	114.1458	114.4304	114.7153	115.0007	115.2864	115.5725	115.8590	116.1459	116.4332
9.7	116.7209	117.0090	117.2975	117.5864	117.8756	118.1653	118.4554	118.7459	119.0367	119.3280
9.8	119.6197	119.9118	120.2042	120.4971	120.7903	121.0840	121.3780	121.6725	121.9673	122.2626
9.9	122.5582	122.8542	123.1507	123.4475	123.7448	124.0424	124.3404	124.6388	124.9376	125.2368